Universidade Federal do Rio Grande – FURG

Instituto de Oceanografia

Programa de Pós-Graduação em Oceanologia

Distribuição Geoquímica do mercúrio nos sedimentos do estuário da Lagoa dos Patos

Guilherme Castro da Rosa Quintana

Tese apresentada ao Programa de Pós-Graduação em Oceanologia, como parte dos requisitos para a obtenção do Título de Doutor.

Orientador: *Prof. Dr.* Nicolai Mirlean

Universidade Federal do Rio Grande (FURG), Brasil.

Rio Grande, RS, Brasil

Maio, 2020

Distribuição Geoquímica do mercúrio nos sedimentos do estuário da Lagoa dos Patos

Tese apresentada ao Programa de Pós-Graduação em Oceanologia, como parte dos requisitos para a obtenção do Título de Doutor.

Guilherme Castro da Rosa Quintana

Rio Grande, RS, Brasil

Maio, 2020

Quintana, Guilherme Castro da Rosa

Distribuição Geoquímica do Mercúrio nos Sedimentos do Estuário da Lagoa dos Patos / Guilherme Castro da Rosa Quintana. – Rio Grande: FURG, 2020.

Número de páginas p.88

Tese (Doutorado) – Universidade Federal do Rio Grande.

Doutorado em Oceanologia. Área de Concentração: Geoquímica

1. Mercúrio. 2. Estuário 3. Sedimentos

Agradecimentos

Primeiramente agradeço à minha família pelo apoio, encorajamento e paciência. Também agradeço aos meus colegas André Luís de Bem e Larissa Pinheiro Costa e à técnica Elisa Rosa Seus pelo suporte em todas as análises realizadas neste estudo. Dou também o devido crédito aos bolsistas de iniciação científica Alexandre Ferraz, Vinícius Dionysio, Bárbara Bernardes e Lucas Lins pela ajuda em tarefas cotidianas no laboratório. Mesmo à distância, também agradeço à professora Karen Johannesson, da Universidade de Tulane, EUA.

Meu agradecimento especial vai para o professor Nicolai Mirlean que me ensinou o pouco sobre ciência que sei e que ofereceu todas as condições e apoio para a realização deste trabalho ao longo dos últimos quatro anos. Também sou grato aos demais integrantes da banca avaliadora: Professores Doutores Carlos Andrade (FURG), Vinícius Tavares Kutter (UFPA) e Mônica Wallner-Kersanach (FURG), pelas sugestões valiosas que auxiliaram na melhoria do presente trabalho.

Por último agradeço ao historiador Professor Doutor Luiz Henrique Torres e aos trabalhadores de Rio Grande que me ofereceram ajuda na obtenção de informações sobre o histórico deste município, em especial ao meu primo Leonardo Bulcão e ao meu ex-colega de natação, jornalista e escritor Willy César, falecido em 2018.

Índice

Lista de Figuras

CAPITULO III

CAPÍTULO IV

Lista de Tabelas

Abstract

The Patos Lagoon Estuary is subject to an irregular hydrological regime and receives mercury (Hg) contaminated effluents from the city of Rio Grande, which is located on its right intertidal zone. The soil cover of Rio Grande is severely contaminated by Hg (up to 27 mg kg^{-1}) down to the water table level. Dissolved mercury concentration in groundwater was up to 13 times higher than that found in the *background* site. Despite the identification of Hg sources from Rio Grande to the estuary (soil cover and groundwater), there was no clear evidence of the antiquity of Hg contamination in Rio Grande. A joint assessment of the distribution of geochemical tracers (mercury, lead, copper and uranium) in the sediments of a shallow cove close to Rio Grande and the consultation to historical documents allowed us to discover that Hg contamination started in the colonial period in Southern Brazil (eighteenth century). The mercury distribution in sediments from shallow areas along the salinity gradient in the estuary is controlled by fine grain contents and probably by the formation of metal sulfide. Immobilization of Hg in sediments probably occurs via binding to organic matter coating on fine grain sediment particles, as well as by incorporation into and/or coprecipitation with iron sulfide. Mercury distribution in salt marsh sediments is chiefly controlled by fine grain sediment contents. The adsorption/incorporation of mercury into iron sulfide probably is a process of minor importance in salt marsh sediments because of the bioturbation caused mainly by burrow crabs and plants.

Keywords: mercury, iron sulfide, free dissolved sulfide, estuary, sediments.

Resumo

O estuário da Lagoa dos Patos está sujeito a um regime hidrológico irregular e recebe efluentes contaminados com mercúrio (Hg) da cidade de Rio Grande, localizada na zona intertidal direita. A cobertura do solo de Rio Grande está severamente contaminada por Hg (até 27 mg kg^{-1}) até o nível do lençol freático. A concentração de mercúrio dissolvido nas águas subterrâneas foi 13 vezes maior do que a encontrada no ponto controle. Apesar da identificação das fontes de Hg orinudas de Rio Grande para o estuário (cobertura do solo e águas subterrâneas), não havia evidências claras da antiguidade da contaminação por Hg em Rio Grande. Uma avaliação conjunta da distribuição de traçadores geoquímicos (mercúrio, chumbo, cobre e urânio) nos sedimentos de uma enseada rasa perto de Rio Grande e a consulta a documentos históricos nos permitiram descobrir que a contaminação por Hg começou no período colonial no sul do Brasil (século dezoito). A distribuição de mercúrio em sedimentos de áreas rasas ao longo do gradiente de salinidade no estuário é controlada pelo teor de grãos finos e provavelmente pela formação de sulfetos metálicos. A imobilização de Hg em sedimentos provavelmente ocorre através da ligação ao revestimento de matéria orgânica em partículas de sedimentos de granulometria fina, bem como pela incorporação e/ou co-precipitação com sulfeto de ferro. A distribuição de mercúrio em sedimentos de marismas é principalmente controlada pelo conteúdo de sedimentos de granulometria fina. A adsorção/incorporação de mercúrio em sulfetos de ferro provavelmente é um processo de menor importância em sedimentos de marismas devido à bioturbação causada principalmente por plantas e caranguejos.

Palavras-chave: mercúrio, sulfeto de ferro, sulfetos livres dissolvidos, estuário, sedimentos.

1. Introdução Geral

1.1. Anomalias de concentração de mercúrio e a importância do processo de redução do íon sulfato e de formação de sulfetos metálicos em sedimentos estuarinos

Altas concentrações de mercúrio em ambientes naturais são comumente associadas à contaminação gerada por pesticidas, amalgamação (usada para mineração de ouro) e indústrias de carvão e cloro-soda (Lacerda e Malm 2008). No entanto, processos geoquímicos naturais, tais como a redução do íon sulfato e a formação de oxihidróxidos compostos principalmente por ferro (Fe) e manganês (Mn), também podem favorecer o acúmulo de Hg em sedimentos estuarinos (Winfrey 1988).

A distribuição de mercúrio nos estuários é uma preocupação, pois esses ambientes fornecem habitats únicos para várias espécies, além de serem frequentemente usados para atividades comerciais, portuárias e recreativas. Esses ecossistemas costeiros geralmente ficam próximos das principais áreas urbanas, portanto podem ser fortemente afetados pelas atividades humanas. A distribuição de mercúrio em sedimentos marinhos e estuarinos é fortemente condicionada por processos de diagênese precoce, como a redução de sulfato, a formação de sulfetos metálicos (Forstner e Wittmann 1979; Forstner e Salomons 1984) e a formação de oxihidróxidos de ferro (Bonnissel-Gissinger et al. 1999). Tais processos foram destacados em ambientes estuarinos e têm sido considerados importantes mecanismos de acumulação de metais em sedimentos (Benoit et al. 1998; Han et al. 2008). Os estuários são conhecidos como ambientes de transição onde ocorre a mistura de águas marinhas e continentais (Windom et al. 1999), levando à abundância de metais, íon sulfato e matéria orgânica, o que facilita a redução do sulfato nos sedimentos e, consequentemente, a formação de sulfetos metálicos (Jørgensen e Kasten 2005).

A distribuição de sulfetos nos sedimentos é controlada principalmente pela atividade de bactérias redutoras de sulfato (Vairavamurthy et al. 1995; Bianchi 2007). A intensidade da atividade bacteriana é atribuída à variação na quantidade e qualidade da matéria orgânica, abundância de bactérias redutoras de sulfato, temperatura e disponibilidade de sulfato (Kristensen et al. 1992; Zhang et al. 2013). Em sedimentos marinhos, a taxa de redução de sulfato diminui conforme o aumento da profundidade das camadas sedimentares devido à menor disponibilidade de sulfato (Leloup et al. 2007). A

taxa de redução de sulfato em sedimentos de baixa salinidade (inclusive em sedimentos estuarinos) pode ser tão alta quanto em sedimentos de alta salinidade, apesar da menor disponibilidade de sulfato e de uma menor densidade de bactérias redutoras de sulfato, devido à maior disponibilidade de matéria orgânica lábil (Pallud e Van Cappellen 2006).

O processo de sulfato redução pode ser muito importante em sedimentos estuarinos, onde condições anóxicas favorecem a formação de sulfetos metálicos constituídos principalmente por Fe e outros elementos calcófilos (Perelman 1967). As transformações diagenéticas do enxofre (S) são de grande importância na química dos sedimentos, principalmente em ambientes costeiros e estuarinos (Huerta-Diaz e Reimer 2010), porque o ciclo do S está ligado aos ciclos de carbono (C), oxigênio (O), Fe e numerosos oligoelementos em tais ambientes (Brüchert et al. 2003; Otero et al. 2009; Hernández-Crespo e Martín 2013; Yang et al. 2014). Sabe-se que os minerais sulfetados são adsorventes efetivos de Hg e, por isso, foram identificados como o principal trapeador de Hg no ambiente em vários estudos (Brown et al. 1979; Hyland et al. 1990; Ehrhardt et al. 2000; Barnett et al. 2001). A formação de sulfetos metálicos nos sedimentos é limitada pela quantidade e pela natureza de matéria orgânica e pela disponibilidade de sulfato e de metais, principalmente Fe (Berner 1984). No entanto, nenhum desses fatores limitantes costuma ser observado em áreas estuarinas de alta produtividade, onde os processos hidrodinâmicos favorecem a mistura e a oxigenação da coluna d'água. Além disso, metais e sulfato são fornecidos ao ambiente estuarino pela bacia hidrográfica terrestre e pelo oceano adjacente, respectivamente (Bianchi 2007).

Nos estuários sujeitos a mudanças de longo prazo no regime de energia hidrodinâmica, ocorre sedimentação irregular e, como resultado, variações no tamanho dos grãos dos sedimentos estuarinos são comumente observadas. A sedimentação de grãos finos (siltes e argilas) ocorre em locais caracterizados por baixa energia hidrodinâmica, enquanto a sedimentação de grãos grosseiros (areias e cascalhos) é normalmente associada a locais de alta energia hidrodinâmica (Antiqueira e Calliari 2005). O tamanho do grão de sedimento é importante para a compreensão dos processos geoquímicos naturais (por exemplo, formação de sulfetos metálicos) relacionados à distribuição de matéria orgânica, S, O e metais (Winfrey 1988; Rojas e Silva 2005; Álvarez-Iglesias e Rubio 2012). Entretanto, atividades antropogênicas podem alterar o comportamento hidrodinâmico natural dos estuários (Forstner e Wittmann 1979; Forstner e Salomons 1984), modificando os processos de sedimentação a longo prazo e, consequentemente, a distribuição granulométrica vertical dos sedimentos. Nesses

estuários impactados, compreender os processos geoquímicos naturais nos sedimentos é de grande importância, pois o acúmulo natural de elementos químicos (o qual é influenciado pela distribuição granulométrica) pode ser erroneamente classificado como resultante de processos antropogênicos e/ou contaminação.

1.2. Toxicidade e legislações internacionais e nacionais específicas para o mercúrio

O mercúrio é apontado como um elemento capaz de infringir graves danos à saúde e que causou óbitos em humanos em razão de contaminação ambiental, particularmente via ingestão de organismos aquáticos contaminados (Barkay et al. 2003; Dorea et al. 2003). Atividades industriais tais como a fabricação de cloro – soda, fabricação de carvão vegetal e de mineração, entre outros, são apontadas como potencial fonte deste metal para o ambiente e, consequentemente como possíveis causadoras de problemas ambientais (Malm 1998). Características como a alta volatilidade e a baixa pressão de vapor de algumas espécies desse metal (Hg^0 e CH_3Hg^+) fazem do mercúrio um perigoso contaminante na atmosfera. Espécies organometálicas do mercúrio (CH_3Hg^+ e C_2H_6Hg) são solúveis em água e, portanto, facilmente transportados em ambientes aquáticos. Além disso, essas espécies são lipossolúveis e facilmente assimiladas pelos organismos, facilitando a absorção desse metal por parte da biota (Lacerda e Malm 2008). A não degradação do mercúrio dificulta a sua eliminação dos ecossistemas naturais, de maneira que os efeitos da contaminação por esse metal podem perdurar por décadas ou até mesmo séculos no meio ambiente. O mercúrio é, dentre os elementos metálicos, aquele que apresenta a maior toxicidade para seres humanos, além de ser o único metal capaz de sofrer biomagnificação em quase todas as cadeias alimentares (Unep 2002).

Na segunda metade do século XX diversas técnicas químico-industriais que utilizavam mercúrio ou geravam resíduos de mercúrio foram proibidas em todo o mundo, com destaque para o maior controle das emissões de mercúrio oriundas das indústrias de cloro-soda e das plantas produtoras de carvão e combustíveis (Lacerda e Malm 2008). Em 2001 a União Europeia (EU) extinguiu as atividades de mineração de mercúrio em seu território, embora alguns países integrantes tenham continuado como grandes fornecedores para exportação até 2008. Em 2011, a exportação de mercúrio foi encerrada pelos países da EU. Nos EUA, a "Environmental Protection Agency" (USEPA) criou diversas legislações e limites legais visando controlar as concentrações do mercúrio em

diferentes compartimentos ambientais (geosfera, atmosfera e hidrosfera) e nas emissões das principais atividades industriais que liberam o mercúrio para o ambiente (USEPA, 2020). Os limites legais para mercúrio nos Estados Unidos são definidos considerando a sua especiação e o compartimento ambiental estudado, é possível verifica-los diretamente no website da USEPA (https://www.epa.gov/mercury/resources-mercury-science-and-research). A organização mundial da saúde realizou diversos estudos que trataram da periculosidade das diferentes espécies de mercúrio para a saúde humana, principalmente no âmbito dos trabalhadores que poderiam estar em contato constante com este metal (WHO, 2020; Risher 2003).

No Brasil, as duas principais leis que tratam do despejo de resíduos de mercúrio são a 12.305/2010 e a 9.976/2000. A primeira trata da Política Nacional de Resíduos Sólidos e a segunda dispõe sobre a produção de cloro e dá outras providências. Existem ainda decretos e portarias específicos para o mercúrio, com destaque para o decreto 97.507/1989, o qual "Dispõe sobre licenciamento de atividade mineral, o uso do mercúrio metálico e do cianeto em áreas de extração de ouro, e dá outras providências".

O Conselho Nacional do Meio Ambiente (CONAMA) dá posição de destaque para o mercúrio em suas resoluções, definindo níveis de alerta para a concentração deste metal em solos, águas e sedimentos de acordo com o uso destinado a estes compartimentos ambientais (CONAMA, 2005; CONAMA 2008; CONAMA 2009; CONAMA 2012). Os níveis legais mais rigorosos foram estipulados para atividades de contato primário com a água e os solos (consumo e agricultura, por exemplo), para atividades de menor contato (água para dessedentação de animais e solos destinados a instalação de plantas industriais) foram definidos níveis de alerta menos rigorosos. Nas resoluções que tratam especificamente da qualidade das águas, o CONAMA discrimina a classificação de acordo com a salinidade dos corpos hídricos (águas doces, salobras e salinas). Dessa forma, existe uma ampla gama de níveis de alerta para mercúrio descritos nestas resoluções. Também existem leis estaduais e municipais que tratam da contaminação por mercúrio.

No Estado do Rio Grande do Sul, a Lei Estadual nº 11.187/1998 que trata dos resíduos de lâmpadas, pilhas e outros artefatos que contenham metais pesados está em vigor. Algumas cidades do mesmo estado, como Caxias do Sul, Rio Grande e Nova Prata possuem leis próprias que tratam da destinação de pilhas, baterias, lâmpadas e outros materiais que liberam metais pesados para o ambiente.

1.3. Estudos sobre a contaminação por mercúrio no Brasil e no estado do Rio Grande do Sul e o "carroting"

Casos de poluição ambiental por mercúrio já foram relacionados a processos industriais recentes (WHO 1989). No Brasil, os principais casos de contaminação por mercúrio foram estudados na Amazônia, onde a mineração teve o seu auge entre as décadas de 1970 e 1990. Os mineradores utilizaram a amalgamação como principal técnica para extrair o ouro, levando à larga contaminação dos solos, dos rios e da atmosfera na Amazônia (Malm 1998). A contaminação na região amazônica persiste até hoje, pois os solos contaminados funcionam como finte passiva de merúrio (Adler Miserendino et al. 2018), além disso o consumo de peixes contaminados trouxe problemas de saúde para populações indígenas locais (Anne et al. 2003). Nas regiões sudeste e sul do Brasil, as indústrias de cloro-soda e de carvão são apontadas como as principais fontes antrópicas de mercúrio para o meio ambiente (Lacerda e Malm 2008). Mais recentemente, foi revelada a contaminação de águas superficiais e subterrâneas na bacia do rio São Pedro, no estado do Paraná (região sul do Brasil) em função do uso de pesticidas que contem mercúrio em sua composição para atividades agrícolas (Justus et al. 2020). No estado de Minas gerais (região central do Brasil), a contaminação de solos de áreas ribeirinhas e rios por mercúrio ocorreu em função de atividades de mineração realizadas no século XIX em meio à primeira corrida do ouro. Nessa época, amalgamação foi amplamente utilizada na mineração de metais preciosos e os resíduos de mercúrio decorrentes dessa atividade persistem na região até os dias atuais (Miranda et al. 2020).

No Estado do Rio Grande do Sul, no extremo sul do Brasil, casos de contaminação por mercúrio foram relatados. A contaminação por mercúrio na bacia hidrográfica do Rio dos Sinos, por conta da crescente ocupação urbana e industrial na área foi comprovada (Nascimento et al. 2015). Trabalhos realizados numa antiga área de mineração no município de Lavras do Sul comprovam a contaminação dos solos e sedimentos de corrente em riachos na região (Pestana et al. 2000; Pestana and Formoso 2003). Técnicas químico-industriais também já foram apontadas como fonte de mercúrio no município de Rio Grande, onde o emprego do *carroting* foi apontado como provável causador da

contaminação de solos superficiais e sub-superficiais no centro histórico da cidade (Mirlean and Oliveira 2006; Fragomeni et al. 2010; Gripp 2012).

O *carroting* é uma antiga técnica químico-industrial que empregava nitrato de mercúrio para o tratamento químico de peles de animais para a produção de feltro e de carpetes e já foi apontado como a principal causa para casos de contaminação por mercúrio em cidades como Danbury, Brookfield e Norwalk nos EUA, famosas por possuírem um largo histórico na indústria do feltro (Varekamp et al. 2003). Nos EUA, o *carroting* foi proibido ainda na década de 1930, devido ao risco de contaminação dos trabalhadores envolvidos no manejo das substâncias empregadas em sua utilização. Entretanto, no Brasil, o *carroting* foi utilizado até o final década de 1950. Em Rio Grande, uma das cidades mais antigas do sul do Brasil fundada ainda no século XVIII e com fortes tendências ao desenvolvimento comercial, o tratamento de peles de animais pode ter iniciado ainda no século XVIII como atividade informal, realizada de maneira artesanal (Fragomeni et al. 2010). Durante o século XIX empresas ligadas ao setor têxtil surgiram em Rio Grande, com destaque para a Companhia Ítalo-brasileira de Tecelagem e para as Malhas Rheighantz (Pesavento 1985). É provável que essas fábricas tenham utilizado o processo de *carroting* para o tratamento de feltro visando a produção de chapéus e outros produtos até a metade do século XX.

1.4. Estudos precedentes sobre a contaminação por Hg em Rio Grande e no estuário da Lagoa dos Patos

A cidade de Rio Grande é umas das maiores cidades do extremo sul Brasil, fundada em 1737, com uma população atual de aproximadamente 200.000 habitantes. Ela encontra-se numa península na margem direita do estuário da Lagoa dos Patos, o maior estuário do tipo estrangulado do sul do Brasil. Essa cidade apresenta um largo histórico de estudos com relação ao mercúrio. Altas concentrações desse metal, de até 5 mg kg^{-1}, foram encontradas nos sedimentos da região estuarina próxima à Rio Grande (Mirlean et al. 2001) após o vazamento de 12.000 toneladas de ácido sulfúrico em 1998 devido a uma rachadura no casco do navio Bahamas. Problemas ligados à exposição de peixes ao mercúrio no estuário da Lagoa dos Patos foram diagnosticados (Niencheski et al. 2001). Anomalias de concentração de mercúrio nos solos superficiais de Rio Grande tiveram sua

distribuição caracterizada (Gripp 2012). O risco de contaminação de mamíferos por mercúrio através da geofagia foi constatado na região (Muccillo-Baisch et al. 2012). Elevadas concentrações de mercúrio foram encontradas em camadas profundas do solo do centro histórico da cidade que estão diretamente em contato com as águas do lençol freático (Mirlean e Oliveira 2006; Fragomeni et al. 2010). Esse fato sugere que altas concentrações de mercúrio podem ser encontradas nas águas subterrâneas de Rio Grande.

Também foi demonstrado que o movimento em larga escala de solo durante as reformas da infraestrutura urbana de Rio Grande causou um aumento do teor de Hg nos sedimentos do canal de navegação do porto local, como resultado da lavagem de material particulado das áreas urbanas para o estuário (Mirlean et al. 2009). No entanto, a fonte original de Hg, bem como o início da contaminação por este metal no estuário ainda é desconhecida. Os solos urbanos são contaminados por Hg até a profundidade das camadas culturais correspondentes ao período de fundação da cidade, no início da colonização do sul do Brasil (Mirlean e Oliveira 2006). No entanto, esse fato não pode servir como prova irrefutável da antiguidade da contaminação devido ao deslocamento constante da cobertura dos solos urbanos, bem como à possível migração de Hg da superfície do solo para os horizontes inferiores. Um estudo da distribuição de Hg em sedimentos não perturbados do estuário da Lagoa dos Patos, que recebe efluentes oriundos de Rio Grande desde a sua fundação, poderia fornecer novas informações sobre o histórico de contaminação por Hg na região. Entretanto a acumulação de Hg em sedimentos estuarinos também pode ocorrer por conta de processos geoquímicos relacionados à diagênese recente dos sedimentos, como a redução do íon sulfato e a subsequente formação de sulfetos metálicos.

Dessa forma é imprescindível investigar a distribuição do mercúrio nos sedimentos do estuário considerando não apenas possíveis eventos de contaminação, mas também a presença de anomalias de concentração naturais deste metal em decorrência de processos geoquímicos comumente observados durante a diagênese recente.

2. Hipótese

Anomalias de concentração de mercúrio em sedimentos estuarinos são originadas tanto pela acumulação deste metal em camadas impactadas por atividades industriais, quanto por processos geoquímicos naturais capazes de provocar a redistribuição deste elemento.

3. Objetivo geral

Compreender a distribuição do mercúrio nos sedimentos através de um estudo sobre a acumulação, a migração e a contaminação deste metal no estuário da Lagoa dos Patos

3.1. OBJETIVOS ESPECÍFICOS

1. Revelar as fontes de mercúrio oriundas da cidade de Rio Grande para o estuário.
2. Investigar a contaminação por mercúrio no contexto histórico, através do registro de anomalias deste metal em sedimentos impactados por atividades antrópicas no estuário, utilizando traçadores geoquímicos.
3. Investigar a os efeitos da redução do sulfato e da formação de sulfetos metálicos sobre a distribuição do mercúrio nos sedimentos estuarinos.
4. Revelar o efeito dos regimes hidrológicos de enchente e de vazante sobre a distribuição do mercúrio nos sedimentos do estuário tanto em áreas rasas não vegetadas quanto em marismas densamente vegetadas.

4. Área de estudo

4.1. O estuário da Lagoa dos Patos

O estuário da Lagoa dos Patos, localizado no extremo sul do Brasil, é um ambiente sujeito ao aporte de contaminantes desde o período colonial da região (século XVIII), com uma superfície de aproximadamente 900 km^2 (Kjerfve 1994). Este ambiente aquático recebe continuamente efluentes urbanos e industriais da cidade do Rio Grande, localizada em uma península ao longo de sua margem direita. Este estuário também abriga o segundo maior porto do Brasil (o Porto do Rio Grande) com relação à quantidade de carga movimentada. O estuário da Lagoa dos Patos é caracterizado como um sistema de micro maré (ou seja, maré < 0,5 m) que exibe variações sazonais de salinidade, nas quais baixas salinidades (< 5) dominam o sistema durante o inverno/primavera (estação chuvosa) e altas salinidades (20 – 30) dominam durante o verão/outono (estação seca; Moller et al. 1996; Marques et al. 2010). O regime hidrológico do estuário da Lagos dos Patos é controlado principalmente pelos ventos e pela vazão do rio (Moller et al. 2001). Os ventos de sudoeste promovem a entrada de águas marinhas no estuário, enquanto os ventos de nordeste aumentam a vazão do rio (Moller et al. 1996). Este regime hidrológico irregular promove tempos de permanência prolongados de água salobra durante o verão/outono e de água doce durante o inverno/primavera (Moller et al. 1996; Moller et al. 2001).

No estuário da Lagoa dos Patos, existem mais de 7.000 ha de marismas, onde *Spartina alterniflora* e *S. densiflora* constituem a vegetação nativa dominante (Costa et al. 2003). O caranguejo catanhão (Neohelice granulata) é a principal espécie animal que habita as marismas da ilha da Pólvora (uma pequena ilha no interior do estuário). As atividades desses crustáceos promovem alterações significativas nos aspectos físicos e químicos dos sedimentos (Costa et al. 2019). Os caranguejos escavam túneis semi-permanentes, removendo e redistribuindo quantidades consideráveis de sedimentos durante a alimentação e manutenção das tocas (Iribarne et al. 2000).

O nível de água do estuário da Lagoa dos Patos também é alterado pelo seu regime hidrológico irregular. O padrão hidrológico mostra variações acentuadas com níveis altos de água durante o período de água doce (estação chuvosa) para níveis baixos de água durante o período de água salobra (Costa et al. 2003; Vaz et al. 2006; Möller et al. 2009).

4.2. Baía da Coroa do Boi

Para os estudos de registros históricos de poluição nos sedimentos do estuário, a Baía de Coroa do Boi (BCB) localizada no extremo sul da península ocupada pela cidade de Rio Grande foi escolhida. A BCB representa a seção mais conveniente do estuário para este estudo, uma vez que os sedimentos da baía nunca foram dragados. Ao longo do resto das linhas costeiras da cidade, a dragagem de canais navegáveis é realizada periodicamente há mais de 100 anos e, como resultado, o perfil natural de sedimentos nos canais e áreas vizinhas foi severamente perturbado. Até o início do século XX, a BCB estava fora da zona de influência direta das emissões industriais e de atividades portuárias, que no século 19 estavam concentradas principalmente nas margens norte e leste da península ocupadas por edificações urbanas e por instalações industriais.

Em 1920, iniciou-se uma descarga centralizada de esgoto doméstico e industrial na BCB, que só foi interrompida em 2004 (Cesar 2015). No período de 1972 a 1990 (Assis e Veríssimo 1997), as fábricas de fertilizantes fosfatados operaram praticamente sem fiscalização na costa da BCB, poluindo fortemente a área adjacente com emissões atmosféricas e efluentes. Os marcadores geoquímicos dessas duas fontes de poluição serviram como ferramentas de datação adicionais para o estudo cronológico da coluna sedimentar.

4.3. O centro histórico de Rio Grande

A cidade de Rio Grande é uma das cidades mais antigas do sul do Brasil fundada ainda no século XVIII. Desde a sua fundação ela apresenta fortes tendências ao desenvolvimento comercial. Suspeita-se que a contaminação por Hg na cidade pode ter iniciado ainda no século XVIII, devido ao tratamento de peles de animais para a fabricação de roupas atividade informal, realizada de maneira artesanal com emprego do *carroting* (Fragomeni et al. 2010). Com a expansão do município, diversas áreas da cidade foram aterradas (Figura 1). Estes aterramentos foram feitos com diversos materiais possivelmente contaminados por resíduos do *carroting* desde o período colonial. Os

aterros alcançam profundidades superiores a um metro abaixo da cobertura de solos urbanos, representando um risco para o lençol freático da região.

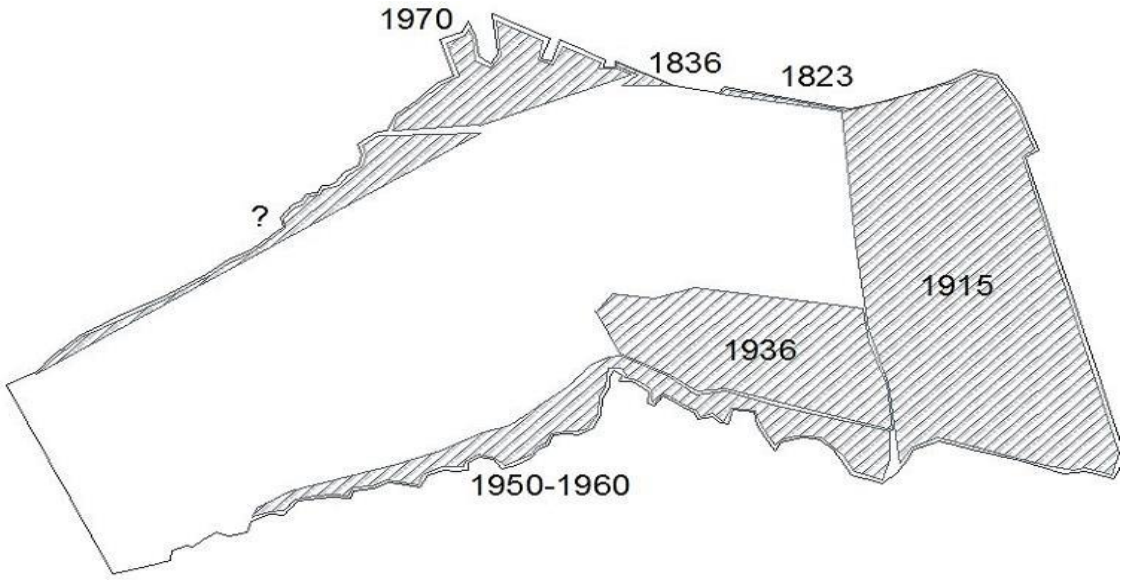

Figura 1. Principais aterros realizados na cidade de Rio Grande ao longo de sua história

5. Materiais e métodos

5.1. Amostragem e tratamento dos sedimentos estuarinos

5.1.1. Estuário da Lagoa dos Patos (áreas rasas e marismas)

Testemunhos foram coletados em três locais (SP, CP e NP; Figura 2) gradativamente mais distantes do Oceano Atlântico ao longo da margem esquerda do estuário para investigar a distribuição de Hg em perfis verticais dos sedimentos de fundo de áreas rasas (aproximadamente 1 m de profundidade). As condições hidrológicas em cada local variam em função da distância em relação ao Oceano Atlântico e devido ao regime hidrológico irregular do estuário. Os primeiros testemunhos foram coletados em setembro de 2016 (ou seja, primavera no hemisfério sul), caracterizada por forte descarga

fluvial (Moller et al. 1996; Marques et al. 2010). O ponto CP (também chamado de SA no capítulo 4) foi amostrado durante o período hidrológico dominado pela entrada de água salgada no estuário (abril de 2017, outono no hemisfério sul). Tubos de acrílico previamente limpos (8 cm de diâmetro; Figura 3 a) foram utilizados para a amostragem dos testemunhos. Visando comparar a distribuição de Hg em sedimentos de áreas rasas (ponto CP) com sedimentos de marismas, um ponto amostral localizado na Ilha da Pólvora também foi escolhido e identificado aqui como SM. Este ponto também foi amostrado durante os dois regimes hidrológicos do estuário (Figura 4).

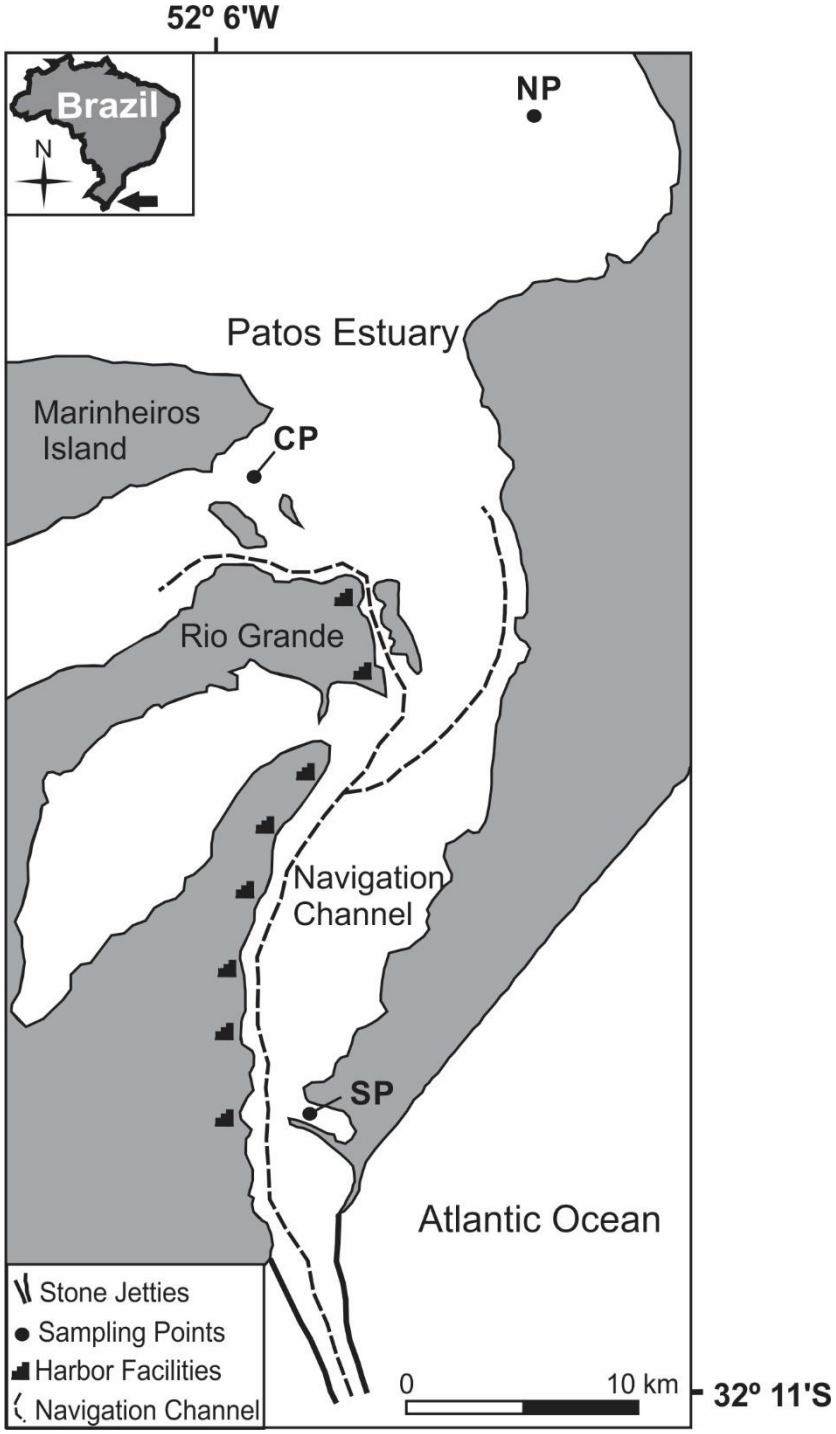

Figura 2. Estuário da Lagoa dos Patos e localização dos pontos SP, CP e NP.

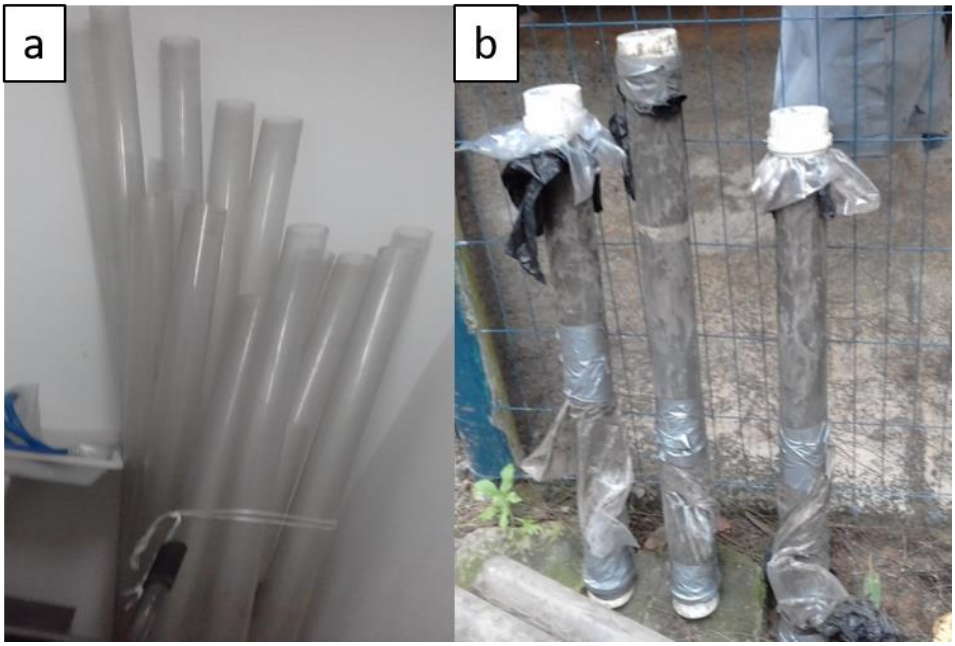

Figura 3. Tubos de acrílico utilizados na amostragem (a) e testemunhos de sedimentos coletados (b)

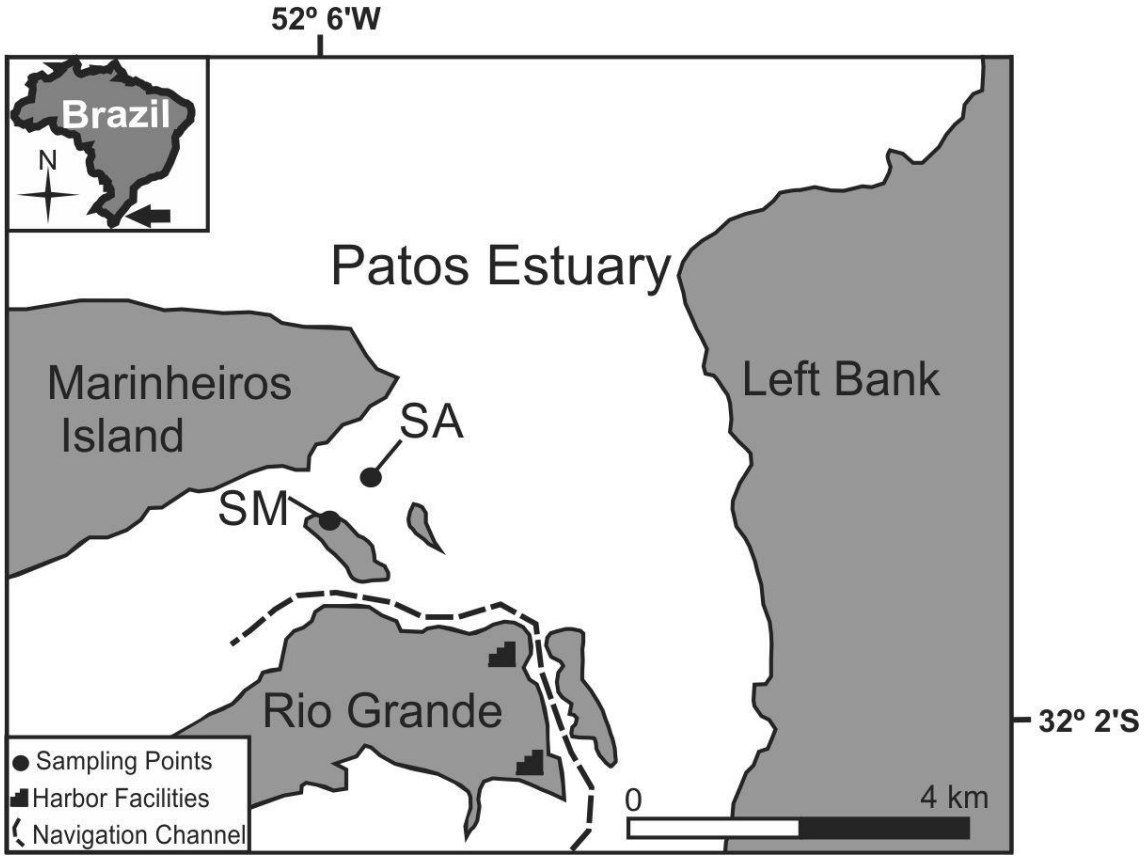

Figura 4. Localização dos pontos CP (também chamado SA no capítulo 4) e SM.

Após a amostragem, cada testemunho foi selado hermeticamente (Figura 3 b), transportado para o laboratório e armazenado a frio (4°C) por 12 horas antes das medições físico-químicas e separação das sub-amostras. Os testemunhos foram abertos e divididos longitudinalmente em duas metades em mesa de trabalho especial (Figura 5 a), em seguida sub-amostras foram coletadas em intervalos de 2 cm ao longo do comprimento de cada metade dos testemunhos (Figura 5 b). A seguir o potencial redox (Eh), pH e concentrações de sulfeto dissolvido livre (isto é, ΣS^{-II}) nas águas intersticiais foram determinados. Alíquotas separadas de cada sub-amostra de sedimentos de 2 cm foram destinadas à análise do conteúdo de Hg, ferro (Fe) e carbono orgânico (CO). A outra metade foi seccionada em intervalos de 2 cm e congelada para posterior análise do teor de enxofre inorgânico redutível total (EIT) e para análise granulométrica dos sedimentos.

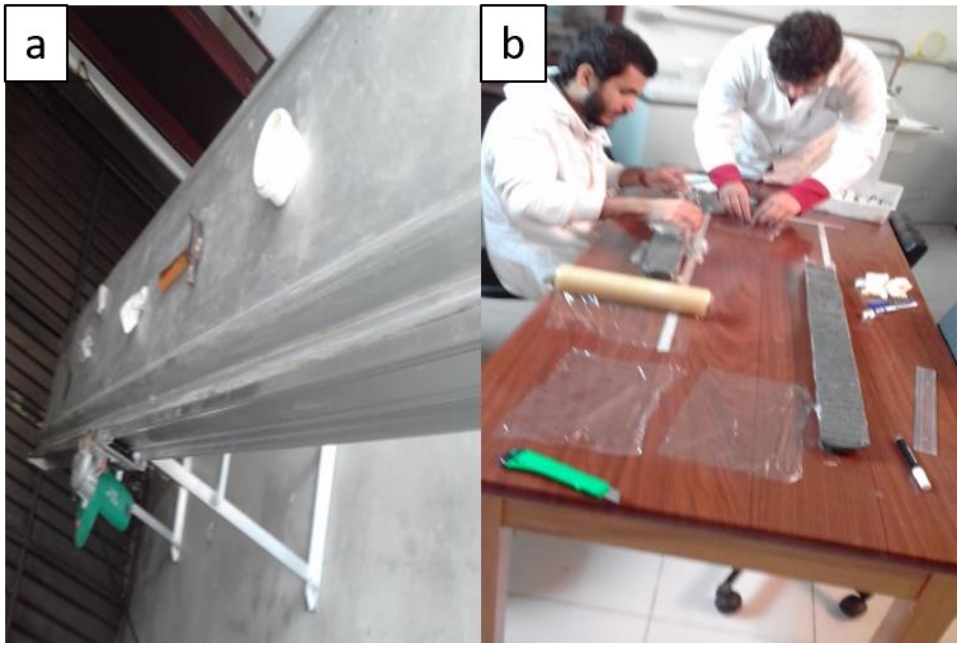

Figura 5. Mesa de trabalho especial para abertura de testemunhos (a) e separação das sub-amostras (b)

5.1.2. Área rasa da Baía da Coroa do Boi

O testemunho de sedimentos oriundos da BCB foi coletado em outubro de 2016, aproximadamente no centro da baía, a cerca de 300 m da costa, em uma área rasa (aproximadamente 1,0 m de profundidade; Figura 6). Um tubo de acrílico previamente limpo (8 cm de diâmetro; Figura 3 a) foi utilizado para a amostragem da coluna sedimentar até os 124 cm. A sub-amostragem foi realizada separando a coluna de sedimentos em fatias em intervalos de 2 cm para seção de 0–20 cm e em intervalos de 4 cm para seção de 20–124 cm. No total, foram selecionadas 36 sub-amostras de sedimentos. A fração granulométrica <63 μm (composto por silte e argila, de acordo com a classificação de Wentworth) foi recuperada das sub-amostras usando peneiração úmida. As amostras de sedimentos finos foram secas à temperatura ambiente e pulverizados em graal de ágata.

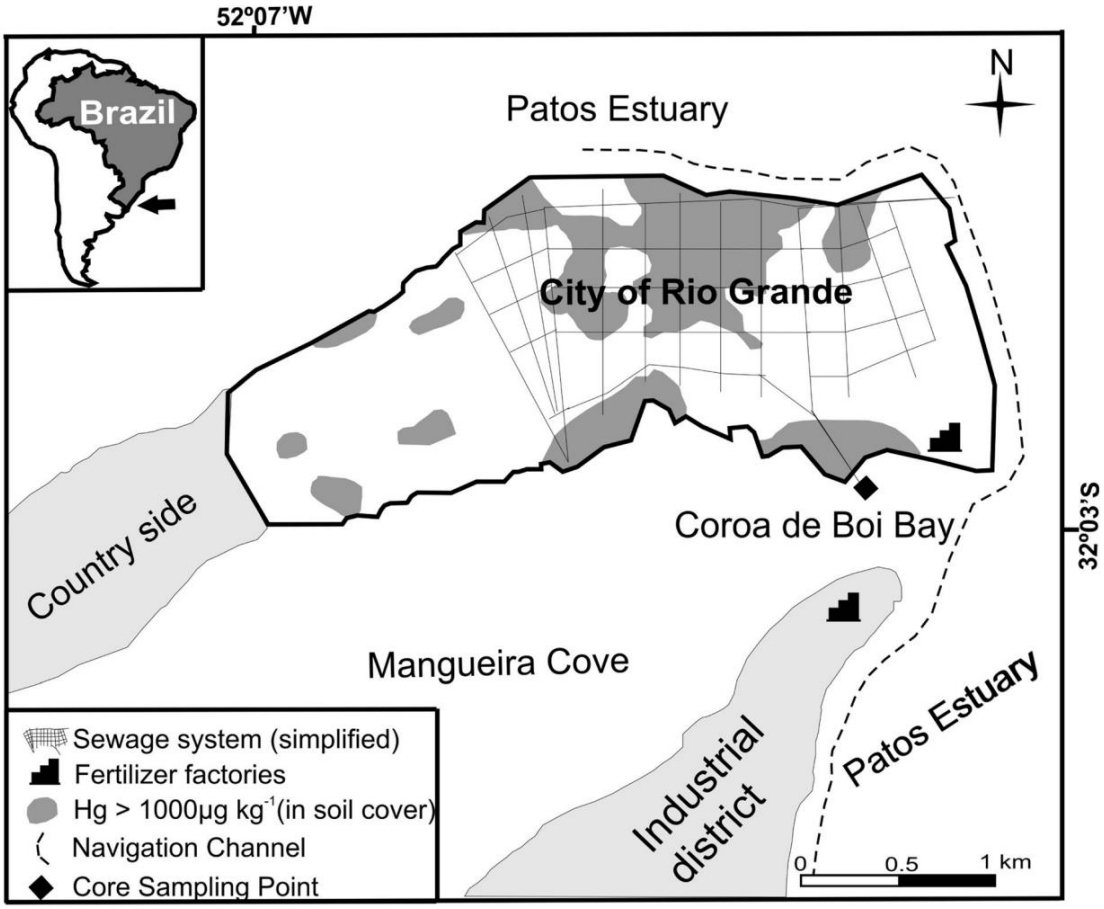

Figura 6. Localização do ponto amostral na BCB.

5.1.3. Solos urbanos e águas subterrâneas

Oito pontos amostrais localizados em regiões aterradas na área urbana de Rio Grande (Tabela 1; Figura 8), além de um ponto *background*, localizado numa região de paleodunas pristinas a 20 km da cidade, foram escolhidos para amostragem de solo e de água subterrânea. As amostras de solo foram coletadas com trado de aço inoxidável (Figura 7 a), da superfície até o nível do lençol freático, que variou de 60 a 150 cm de profundidade na área urbana e atingiu 50 cm no ponto background. As amostras foram coletadas em intervalos de 10 cm e foram armazenados em sacos plásticos. No laboratório, os solos foram secos a 25 °C, desgrumados e peneirados em malha de 63µm (Figura 7 b). A água subterrânea foi bombeada dos poços recém abertos e armazenada em garrafas de polietileno rigorosamente lavadas em ácido nítrico 1 %. No laboratório, as amostras de água foram filtradas através de uma membrana Milipore® de 0,45 µm. Sua condutividade e pH foram medidos logo após a filtração, as amostras filtradas foram armazenadas em ambiente refrigerado a 4 ° C até o momento das análises químicas.

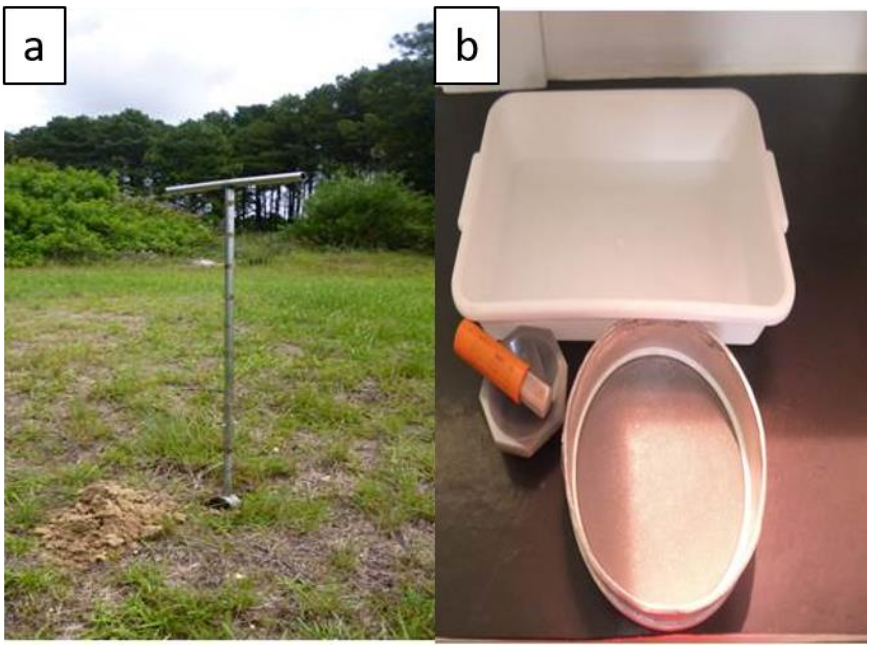

Figura 7. Trado de aço inoxidável (a) e material para desgrumação e peneiração

Tabela 1. Pontos amostrais localizados na área urbana de Rio Grande

Áreas aterradas	Materiais dos aterros	Época da construção dos aterros

1	Solo, entulhos, lixo e lama	Século XVIII (1º metade)
2	Solo, entulhos, lixo e lama	Século XIX (1º metade)
3	Solo, entulhos, lixo e lama	Século XIX (1º metade)
4	Solo, entulhos, lixo e lama	Século XIX (2º metade)
5	Solo, entulhos, lixo e lama	Século XIX (2º metade)
6	Solo, entulhos, lixo e lama	Século XX (2º metade)
7	Solo, entulhos, lixo e lama	Século XX (2º metade)
8	Solo, entulhos, lixo, lama e sedimentos estuarinos	Século XX (2º metade)

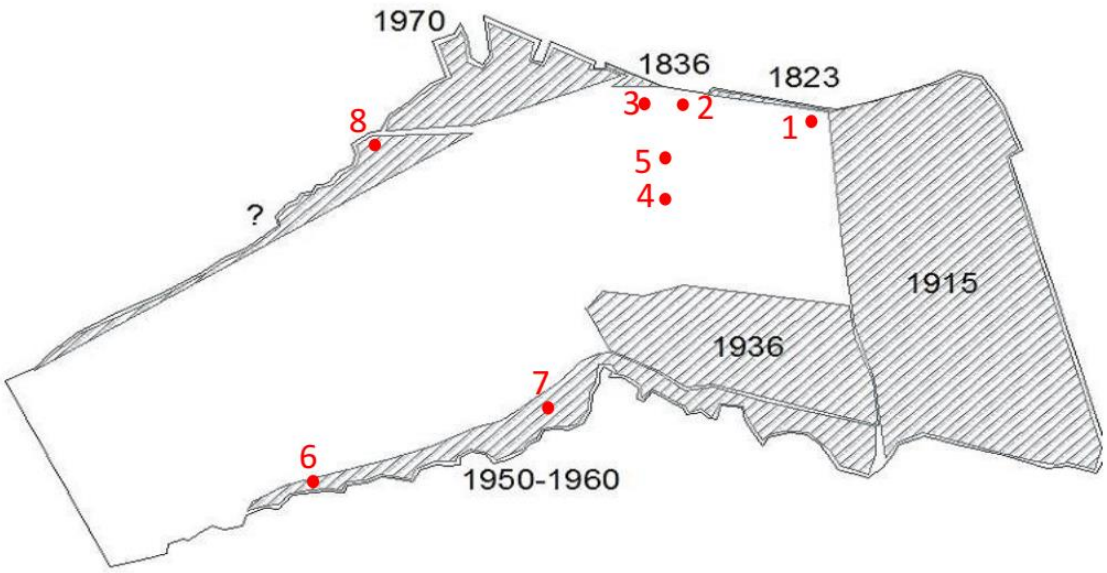

Figura 8. Pontos de coleta de solos urbanos e de águas subterrâneas.

5.2. Análises químicas

5.2.1. Determinação do potencial redox (Eh) nos sedimentos e de pH e sulfetos livres dissolvidos (ΣS^{-II}) nas águas intersticiais

O Eh foi medido na superfície recém-exposta dos sedimentos de marismas e de áreas rasas usando um eletrodo de platina (Analion®). O pH foi medido em águas intersticiais filtradas (membrana Milipore® de 0,45 µm) extraídas das sub-amostras de sedimentos por centrifugação (3000 rpm). A determinação de ΣS^{-II} nas águas intersticiais foi realizada usando um eletrodo seletivo de íons de combinação prata/sulfeto (modelo Hanna® 9616 BNC) acoplado a um medidor Orion™ ISE/pH/mV/Eh/temperatura (modelo 209a; Brooks 2001). Uma solução antioxidante básica para sulfetos (Sulfide Antioxidant Buffer - SAOB, Hanna Intruments®) e um padrão para sulfetos ($Na_2S.9H_2O$) foram previamente preparados e utilizados para calibração do eletrodo seletivo de íons. O eletrodo foi calibrado a cada 12 leituras a partir de uma curva de calibração de três pontos (100, 1000, 10000 µmol L^{-1}).

5.2.2Determinação de enxofre inorgânico redutível total (EIT) nos sedimentos estuarinos

O enxofre inorgânico redutível total (EIT) foram medidos usando sub-amostras integrais de sedimentos congelados seguindo o método descrito por (Fossing e Jørgensen 1989). Este procedimento consiste em submeter a amostra à digestão ácida com uma solução ácida (Cr^{+2} em HCl) sob uma purga de gás inerte (N_2), produzindo H_2S, que é então coletado em uma solução de retenção de sulfetos (Zn – acetato + NaOH). A quantificação do EIT foi feita por iodometria e o desvio padrão relativo (% RSD) para a medição foi ≤ 5%.

5.2.3. Determinação de matéria orgânica e de carbono orgânico (CO) nos sedimentos

A matéria orgânica dos sedimentos integrais (amostras integrais) foi determinada usando método de perda por ignição. Esta análise foi realizada exclusivamente para os sedimentos da BCB. O teor de CO dos sedimentos de áreas rasas e de marismas foi determinado em amostras integrais secas (30 mg), usando um TOC - VCPH, modelo SSM - 5000A, Shimadzu® (Figura 9) com detector de combustão. Os resultados do CO são

apresentados em porcentagem de carbono orgânico em sedimentos secos e o RSD foi <5% para análises em triplicata.

Figura 9. TOC - VCPH, modelo SSM - 5000A, Shimadzu®

5.2.4. Determinação de Fe nos sedimentos estuarinos

O Fe foi extraído das amostras integrais seguindo o método EPA 3050B (USEPA 1996). As soluções extraídas foram diluídas por um fator de 1:400 (v/v) e medidas por espectrofotometria UV/VIS utilizando um espectrofotômetro DR 2800 da Hach Company®, método 8008 - Método FerroVer® (Hach 2007). Amostras duplicadas (*spikes*) foram processadas rotineiramente com RSD <5%. O controle de qualidade da análise de Fe foi assegurado pela extração e quantificação de material de referência certificado MESS-4.

5.2.5. Determinação de Mercúrio total nos sedimentos estuarinos.

A digestão ácida de amostras peneiradas em malha 63µm (sedimentos da baía da Coroa do Boi) e integrais (áreas rasas e marismas) homogeneizadas foi realizada de acordo com o método EPA 7471 para a determinação de Hg (USEPA 1998). Um sistema de vapor frio, acoplado a um AAS GBS 932 (Figura 10), foi usado para a leitura das concentrações de Hg. Cada amostra foi analisada em triplicata; o desvio padrão relativo (RSD) dessas três medições de Hg não excederam 5%.

Figura 10. Sistema de vapor frio, acoplado a um AAS GBS 932

5.2.6. Determinação de Cobre (Cu), Chumbo (Pb) e Urânio (U) nos sedimentos estuarinos (somente na baía da Coroa do Boi)

A digestão das amostras foi feita de acordo com o método EPA 3050B (USEPA 1996) para analisar Cu e Pb. A determinação de Cu e Pb foi realizada em regime de chama utilizando o dispositivo AAS GBS 932 (Figura 10). A análise de urânio (U) nas amostras de sedimentos foi realizada por espectrometria de massa com plasma indutivamente acoplado utilizando o equipamento ICP MS X300 (Figura 11) com a adição de padrão interno de índio a todas os amostra para corrigir a estabilidade do sinal. Amostras de referência certificadas de sedimento MESS-3 (NRCC 2004) foram incluídas nas análises

como medida de controle de qualidade. A precisão das amostras de referência variou de 4 a 9% dos valores sugeridos para Cu, Pb e U.

Figura 11. ICP MS X300

5.2.7. Mercúrio total nos solos urbanos

As concentrações de Hg no solo (fração <63 μm) foram determinadas através da espectrofotometria de absorção atômica por vapor frio, método CVAAS (USEPA 1998), com limites instrumentais de detecção e de quantificação (LD e LQ) de 0,2 e 0,6 μg L^{-1}, respectivamente. As amostras foram analisadas em triplicata e o desvio padrão relativo (RSD) foi inferior a 4%. A precisão foi validada através da análise de amostras certificadas (MESS-3), de acordo com método padrão (NRCC 2004). A concentração certificada de Hg no MESS-3 é de 0,091 ± 0,009 mg kg^{-1} (neste estudo, -0,093 ± 0,003 mg kg^{-1} foram recuperados para dez réplicas).

5.2.8. Mercúrio, Carbono e íons principais dissolvidos nas águas subterrâneas

Concentrações de sódio (Na^{+}), cálcio (Ca^{2+}), cloreto (Cl^{-}) e sulfato (SO_4^{2-}) dissolvidos nas amostras de águas subterrâneas foram determinadas através do método de cromatografia iônica, utilizando equipamento Metrohm® (Figura 12 a). O mercúrio dissolvido (HgD) foi discriminado de duas formas: iônico (HgI) e complexado (HgC). As concentrações foram determinadas através da fluorescência atômica (USEPA 2002), utilizando equipamento Tekran® (Figura 12 b), com DL e QL de 0,3 e 0,9 ng L^{-1}, respectivamente. Todas as amostras foram analisadas em triplicata, com desvio padrão relativo abaixo de 5%. Carbono orgânico dissolvido (DOC) e carbono inorgânico dissolvido (DIC) também foram determinados usando equipamento Shimadzu® (Figura 9).

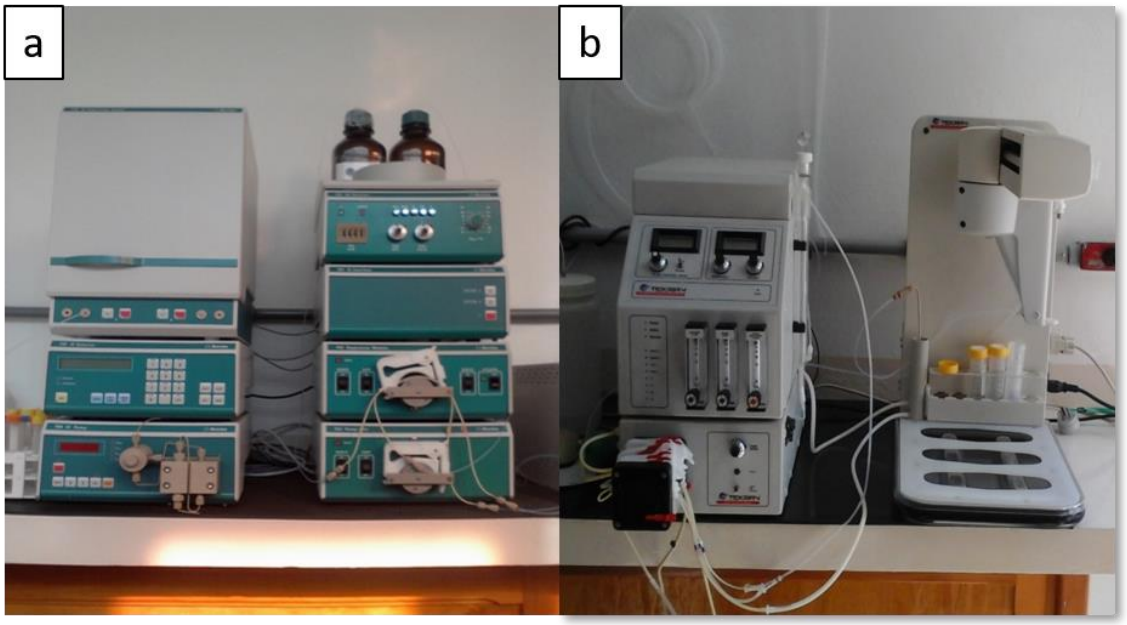

Figura 12. Cromatógrafo iônico Metrohm (a) e Tekran® modelo 2600, fluorescência atômica (b)

5.3. Análises granulométricas

Os sedimentos finos (<63 μm), compostos de silte e argila de acordo com a classificação de Wentworth, foram recuperados de sub-amostras usando métodos de peneiração padrão (ASTM C136 / C136M).

5.4. Cálculo de taxas de sedimentação (somente para os sedimentos da baía da Coroa do Boi)

As taxas de sedimentação (mm ano^{-1}) foram calculadas através da razão entre a espessura das seções de sedimentos que correspondem às anomalias de concentração de traçadores geoquímicos específicos e o tempo de duração das atividades antropogênicas responsáveis por gerar essas anomalias. Este cálculo foi realizado considerando períodos históricos documentados do desenvolvimento da cidade de Rio Grande, como lançamento de esgotos domésticos e industriais (1920–2004) e de emissões atmosféricas e de efluentes oriundos da produção de fertilizantes químicos (1972-1990) na BCB. Como resultado, quatro diferentes taxas de sedimentação foram calculadas (Tabela 2). Para a seção de sedimentos considerada com idade inferior a 1920, a taxa de sedimentação natural (3 mm ano^{-1}) previamente calculada (Niencheski et al. 2014) foi utilizada. Os intervalos de confiança temporal aplicados sobre as taxas de sedimentação foram calculados pela razão entre os intervalos de sub-amostragem (2 e 4 cm) e a taxa de sedimentação calculada para cada histórico período. O resultado desse cálculo foi dividido por dois, considerando que o início e o fim das anomalias de concentração ocorreram entre os intervalos de sub-amostragem.

Tabela 2. Informações usadas para o cálculo das taxas de sedimentação

Período Histórico (anos)	Atividades Antropogênicas	Tempo de duração (anos)	Seção dos sedimentos (mm)	Taxa de sedimentação (mm ano^{-1})
1920-1972	Descarga de esgoto	52	370–190	3,4
1972-1990	Descarga de esgotos e efluentes industriais	18	190-90	5,5
1990-2004	Descarga de esgoto recente	14	90-40	3,6

2004-2016	Descarga clandestina de esgoto	12	40-0	3,3

5.5. Consulta a documentos históricos

Para obter informações históricas a respeito do saneamento básico em Rio Grande, foram consultados relatórios redigidos pela intendência municipal durante o início do século XX, entre 1906 e 1908. Também foi consultado um relatório redigido pelo engenheiro Florisbello Leivas, responsável pela construção do primeiro sistema de esgotos da cidade, inaugurado em 1920 (Leivas 1922). Mudanças recentes no sistema sanitário da cidade foram investigados em relatórios da extinta Secretaria Riograndina de Água e Esgotos (SRGAE) e em documentos recentes da Companhia Riograndense de Saneamento (CORSAN), responsável pelo sistema de água e esgotos em Rio Grande atualmente. Tanto os relatórios de intendência quanto os livros acerca do saneamento básico da cidade foram consultados na biblioteca pública do município de Rio Grande (Biblioteca Riograndense) enquanto os documentos da SRGAE e da CORSAN foram obtidos diretamente em sedes da Companhia Riograndense de Saneamento.

Informações sobre o histórico das indústrias de fertilizantes que se instalaram em Rio Grande foram obtidas através de bibliografia fornecida de bom grado pela Companhia de Produtos de Petróleo Ipiranga S.A. (Assis e Veríssimo 1997) e através de consulta de jornais impressos preservados (jornal AGORA) na biblioteca Riograndense. Por fim, a obtenção de informações sobre o período de domínio espanhol em Rio Grande (1763 – 1777) foi realizada através de consulta da obra de Willy Cesar (Cesar 2015), um jornalista local especializado na história do município de Rio Grande.

ARTIGOS CIENTÍFICOS

Para a obtenção do título de Doutor pelo Programa de Pós-Graduação em Oceanologia, é requerido que o discente realize a submissão de pelo menos dois artigos científicos como primeiro autor em periódico indexado com corpo editorial. Dessa forma, os resultados da pesquisa desenvolvida durante a realização do projeto de doutorado e a discussão dos mesmos serão apresentados em forma de artigos nos capítulos subsequentes. O primeiro manuscrito, de autoria de Guilherme Castro da Rosa Quintana e Nicolai Mirlean, é intitulado "***Groundwater Contamination by Mercury from the Aforetime Carroting Practice***" e foi publicado no periódico *"**Bulletin of Environmental Contamination and Toxicology**"*. O segundo manuscrito, de autoria de Guilherme Castro da Rosa Quintana e Nicolai Mirlean, é intitulado "***Record of Hg pollution around outset of colonization in Southern Brazil*"** e foi publicado no periódico "***Environmental Monitoring and Assessment***". O terceiro manuscrito, de autoria Guilherme Quintana, Nicolai Mirlean, Larissa Costa e Karen Johannesson, é intitulado "***Mercury distributions in sediments of an estuary subject to anthropogenic hydrodynamic alterations (Patos Estuary, Southern Brazil*)**" e encontra-se sob revisão para publicação no periódico *"**Environmental Monitoring and Assessment**"*. Por fim, o quarto manuscrito de autoria de Guilherme Quintana, Nicolai Mirlean e Larissa Costa, intitulado "***Pattern of mercury distribution in sediments from an irregular hydrological regime estuary*"** também se encontra sob revisão para publicação no periódico "***Estuaries and Coasts***".

CAPÍTULO I: Groundwater Contamination by Mercury from the Aforetime Carroting Practice

Bulletin of Environmental Contamination and Toxicology
https://doi.org/10.1007/s00128-018-2333-5

Groundwater Contamination by Mercury from the Aforetime Carroting Practice

G. C. Quintana[1] · N. Mirlean[1]

Received: 14 November 2017 / Accepted: 24 March 2018

https://doi.org/10.1007/s00128-018-2333-5

Abstract

In the southernmost Brazilian city of Rio Grande, the chemical treatment of animal fur named carroting was performed between the eighteenth and twentieth century. This type of industry has led to contamination of urban soil with mercury down to the groundwater level. The present study has revealed that the dissolved mercury concentrations in groundwater in the mercury contaminated areas was up to 13 times higher than that found in the reference site. The association between SO_4^{2-}, Ca^{2+} and dissolved mercury indicate that urban man-made grounds composed by soil, construction and demolition waste, urban rubbish and mud contaminated by "carroting mercury" serve as a source of this metal to groundwater. Despite the high level of contamination, mercury concentrations found in groundwater were below the permissible level established for potable water. Most of the dissolved mercury was chemically combined, probably with organic matter.

Keywords Mercury · Groundwater · Contamination · Carroting

Introduction

Mercury (Hg) pollution reports have been related to many industrial processes (WHO 1989). Carroting is an ancient technique of chemical treatment of fur that employed mercury nitrate for felt manufacturing. The waste from this activity was indicated as the cause for Hg contamination in cities like Danbury, Brookfeld and Norwalk in the United States (Varekamp et al. 2003).

Carroting waste was mentioned as the most probable source for Hg contamination of soil in the city of Rio Grande, where concentrations up to 13.9 mg kg^{-1} were found (Mirlean and Oliveira 2006). There are some indirect indications testifying that carroting was employed for the artisanal production of felt in southern Brazil since the beginning of the colonial period, in the eighteenth century (Fragomeni et al. 2010).

The city of Rio Grande was founded in 1737 within the bounds of a peninsula inside the Patos' Lagoon estuary. Its territorial expansion was only possible through man-made grounds construction over shallow areas and wetlands along the nineteenth and twentieth centuries. Construction and demolition waste, soil, urban rubbish and mud were moved from the central area of the city to fill the man-made grounds in its periphery (Pimentel 1944). These materials probably were contaminated by carroting waste during the colonial period and favored the spreading of Hg contamination in the city (Mirlean et al. 2009).

Toxicological studies performed in Rio Grande revealed the risk of Hg contamination of humans (mainly children, through geophagy) due to the contaminated soils in squares and playgrounds (Muccillo-Baisch et al. 2012). The Hg contamination extended to deep layers of soil, up to 1.5 meters deep (Mirlean and Oliveira 2006; Fragomeni et al. 2010), reaching the level of the water table. This work aimed to study the Hg contamination both by industrial activities (carroting) and urban waste disposal along an urbanized region, in addition it was intended to evaluate the groundwater contamination by this metal taking in consideration its quality and potability.

Materials and methods

Eight sample points within the urban area of Rio Grande (Table 1) and one reference site located 20 km away from the city were chosen for soil and groundwater

sampling. Soil samples were collected by using stainless steel borer, from the surface to the groundwater level, which varied from 60 to 150 cm deep within the urban area and reached 50 cm at the reference site. Soil samples were divided into intervals of 10 cm and were stored in plastic bags. Groundwater was pumped from the boreholes and sampled in polyethylene bottles rigorously cleaned. In the laboratory, water samples were filtered through a 0.45 µm Milipore® membrane. Its conductivity and pH were measured right after filtration, then the samples were stored in a refrigerated environment, at 4°C.

Table 2. Sample points located in man-made grounds (MMG)

MMG	MMG materials	Time of construction
1*	Soil, construction and demolition waste, rubbish and mud	18th century (1st half)
2	Soil, construction and demolition waste, rubbish and mud	19th century (1st half)
3	Soil, construction and demolition waste, rubbish and mud	19th century (1st half)
4	Soil, construction and demolition waste, rubbish and mud	19th century (2th half)
5	Soil, construction and demolition waste, rubbish and mud	19th century (2th half)
6	Soil, construction and demolition waste, rubbish and mud	20th century (2th half)
7	Soil, construction and demolition waste, rubbish and mud	20th century (2th half)
8	Soil, construction and demolition waste, rubbish, mud and estuarine sediments	20th century (2th half)

*ancient felt manufacturing quarters

The total Hg concentrations in soil were determined through the cold vapor atomic absorption spectrophotometry – CVAAS method (USEPA 1998) with detection and quantification limits (DL and QL) of 0.2 and 0.6 µg L^{-1}, respectively. The samples were analyzed in triplicate and the relative standard deviation (RSD) was below 4%. The accuracy was validated through analysis of certified samples (MESS-3), by following the standard method (NRCC 2004). The certified concentration for Hg in MESS-3 is 0.091 ± 0.009 mg kg^{-1} (in this study, -0.093 ± 0.003 mg kg^{-1}; ten replicates have been recovered).

Concentrations of Na^{+}, Ca^{2+}, Cl^{-} and SO_4^{2-} dissolved in groundwater samples were determined through the ionic chromatography, by applying the Metrohm® instrument. Dissolved mercury (HgD) was discriminated in two forms: ionic (HgI) and complexed (HgC). The concentrations were determined through the atomic fluorescence (USEPA 2002), by applying the Tekran® device, with DL and QL equivalent to 0.3 and 0.9 ng L^{-1}, respectively. All samples were analyzed in triplicate, with a relative standard deviation below 5%. Dissolved organic carbon (DOC) and dissolved inorganic carbon (DIC) were also determined by using the Shimadzu® TOC device.

Results and Discussion

The distribution of Hg in soil cores was not uniform within the urban area (Table 2). This possibly occurred because the man-made grounds were arbitrarily filled, mixing rubbish, construction and demolition waste, mud and soil in different proportions. Despite the different degrees of contamination observed, concentrations up to 27 mg kg^{-1} (90 times higher than the reference site) were found in soils cores (Table 2).

Table 2. Hg concentrations in soil cores (triplicate average in mg kg^{-1}) and RSD (between parenthesis) in %.

Depth	Point								
	1[a]	2	3	4	5	6	7	8	9[b]
0 - 10	0,7 (3)	3,9 (2)	4,0 (3)	1,2 (3)	4,2 (2)	20,2 (1)	2,8 (3)	2,8 (3)	0,5 (3)

10 -20	0,9 (3)	3,5 (3)	2,4 (2)	4,4 (2)	3,3 (2)	24,9 (1)	6,1 (3)	21,5 (1)	0,4 (3)
20 -30	0,6 (3)	1,8 (3)	3,6 (3)	7,2 (2)	5,9 (2)	14,0 (1)	5,9 (2)	27,7 (1)	0,2 (3)
30 -40	0,5 (3)	1,6 (3)	4.2 (2)	9,5 (2)	3,1 (2)	12,0 (1)	4,9 (2)	26,0 (1)	0,3 (3)
40 -50	0,61 (3)	1,3 (3)	3,9 (3)	6,2 (2)	5,3 (2)	13,1 (1)	4,4 (3)	16,4 (1)	0,2 (3)
50 -60	0,3 (3)	1,6 (3)	3,0 (3)	6,3 (2)	4,7 (2)	13,7 (1)	6,9 (2)	11,0 (1)	
60 -70	0,5 (3)		2,2 (3)	6,4 (2)	4,2 (2)	16,8 (1)	7,7 (2)	24,5 (1)	
70 -80	0,3 (3)		2,5 (3)	3,6 (2)	5,4 (2)	12,4 (1)	3,8 (2)	14,6 (1)	
80 -90	0,2 (3)		1,1 (3)	2,0 (2)	2,6 (2)	18,2 (1)	4,0 (2)	5,2 (3)	
90 - 100	0,3 (3)		0,8 (3)	1,8 (2)	5,8 (2)	18,0 (1)	7,1 (2)	8,3 (3)	
100 -110			0,7 (3)	2,3 (2)	3,2 (3)	9,0 (1)	5,7 (2)	7,1 (3)	
110 -120			0,9 (3)		2,6 (2)	14,0 (1)	3,7 (3)		
120 -130			1,2 (2)		0,2 (3)	14,7 (1)	3,9 (3)		
130 -140						20,3 (1)	4,3 (2)		
140 - 150							4,2 (3)		

[a] Ancient felt manufacture quartes; [b] Reference site

Hg contamination in soils, due to the presence of landfills and man-made grounds in urban areas, was reported in southeast Brazil, in the region of the Guanabara Bay (Machado et al. 2002). Problems related to Hg contamination in soils and atmosphere were reported in the state of Florida, USA, due to the presence of dumps (Lindberg et al. 2001). These studies pointed to the presence of artifacts commonly found in landfills, like batteries and thermometers, as the main sources of Hg. It highlights the unique character of the present study, in which materials contaminated with residues generated by the production of felt were used to fill man-made grounds.

Groundwater collected in the city was neutral to slightly alkaline (pH between 7.8 and 8.8). The construction and demolition waste used to fill the man-made grounds were mainly composed by bricks and cement debris. These materials are rich in calcium carbonate and were responsible for the relatively elevated pH in urban area groundwaters. In the reference site, free from the influence of man-made grounds, groundwater was neutral (Table 3). The electric conductivity of city groundwaters considerably varied between 72 and 974 $\mu S\ cm^{-1}$, probably due to the influence of marine spray (Rio Grande is located close to the coastline) and arguably due to the leaking of domestic effluents

from the sewage system. Groundwaters located in the reference site demonstrated a low electric conductivity (130 µS cm^{-1}) in comparison to most of groundwaters collected in the urban area (Table 3).

Table 3. Hg concentrations in soil cores (average/min-max) and groundwater pH, electric conductivity (Cond), Hg concentrations (HgD / HgC - HgI), DOC, DIC and dissolved ions (Na^+, Ca^{2+}, Cl^- and SO_4^{2-})

Point	pH	Cond	Average (min-max)	Hg_D ($Hg_C - Hg_I$)	DOC	DIC	N^+	Ca^{+2}	Cl^-	SO_4^{-2}
		µS cm^{-1}	mg kg^{-1}	ng L^{-1}	mg L^{-1}					
1	8.7	193	3.9 (0.2 – 5.9)	92 (75 – 17)	17	32	28	46.3	24.1	16.4
2	8.8	384	15.8 (9 – 24.9)	119 (110 – 9)	13	67	50.5	133.2	183.3	40.3
3	8.7	216	5.0 (2.8 – 7.7)	148 (145 – 3)	18	56	40.9	71.8	41	30
4	8.7	455	2.3 (0.7 – 4.3)	253 (250 – 3)	16	61	139	93.9	250.2	122.4
5	7.8	72	4.6 (1.2 – 9.5)	34 (32 – 2)	18	14	10.8	18.7	21.5	1.4
6	8.7	247	0.5 (0.3 – 0.9)	65 (62 – 3)	32	49	42.8	45.2	56.2	0.9
7	8.6	258	2.3	43	20	57	20.5	61.4	22.6	4.6

			(1.3 – 3.9)	(40 – 3)						
8	8.2	974	15.0 (2.8 – 27.7)	75 (71 – 4)	20	73	429	46.5	1032	1.4
9*	6.8	130	0.3 (0.2 – 0.5)	19 (16 – 3)	48	7	9.3	6.3	11.8	7.1

*background point

At the reference site, groundwaters demonstrated relatively low concentrations of HgD (19 ng L^{-1}). Concentrations of HgD in urban area were up to 13 times higher than the ones found in the reference site, reaching up to 253 ng L^{-1} (Table 3). Despite the elevated concentrations of Hg found, the limits established in the Brazilian legislation (1 µg L^{-1}; Conama 2008) for potable water were not exceeded. Our results also revealed that most HgD in the city waters was not in free ionic state (Table 3). The organometallic species of Hg are the most stable ones in the aquatic ecosystems (Lacerda and Malm 2008), and hence, it is likely that most HgC is chemically bound to organic compounds. With the exception of methyl mercury, the organometallic species of Hg are less toxic to biota than HgI, which represented a small part of HgD and probably occurs as a product of HgC dissociation.

The multivariate statistic of principal component analysis (PCA) was used to better comprehend the relation between HgD and the others compounds dissolved within the groundwater. The PCA has enabled us to distinguish two groups of variables based on two principal components that, together, explained 85.1% of the total data variance. The principal component 1 represented 49.1% of the variance and was better represented by the variables HgD, Ca^{2+}, CID and SO_4^{2-} (Table 4). This principal component seemed to be related to dissolution of limestone and gypsum present in Hg contaminated construction and demolition waste and urban rubbish. These materials were moved from ancient areas of the city, occupied since the eighteenth century, and were used for man-made grounds construction over the nineteenth and twentieth centuries (Pimentel 1944).

The Principal component 2 explained 36% of the variance and was best represented by Na^+ and Cl^- (Table 4), whose most probable source were domestic

effluents from the city. Most domestic effluents in Rio Grande are not captured by the sewage network, so principal component 2 seemed to represent the influence of these effluents on the groundwaters sampled in the urban area. This hypothesis was reinforced by the low concentrations of these ions in reference site, which was not contaminated by domestic effluents (Table 3). The PCA plots (Fig. 1) illustrate the representation of the variables charges for the principal components 1 and 2.

Table 4 . Variable charges for the two first principal components (self-staggered data), using Hg_D, DIC and dissolved ions Na^+, Ca^{+2}, Cl^- and SO_4^{-2}.

Variable	DIC	SO_4^{-2}	Ca^{+2}	Hg_D	Cl^-	Na^+
Principal Component 1	-0.83	-0.74	-0.73	-0.8	-0.52	-0.53
Principal Component 2	-0.27	0.55	0.43	0.48	-0.84	-0.82

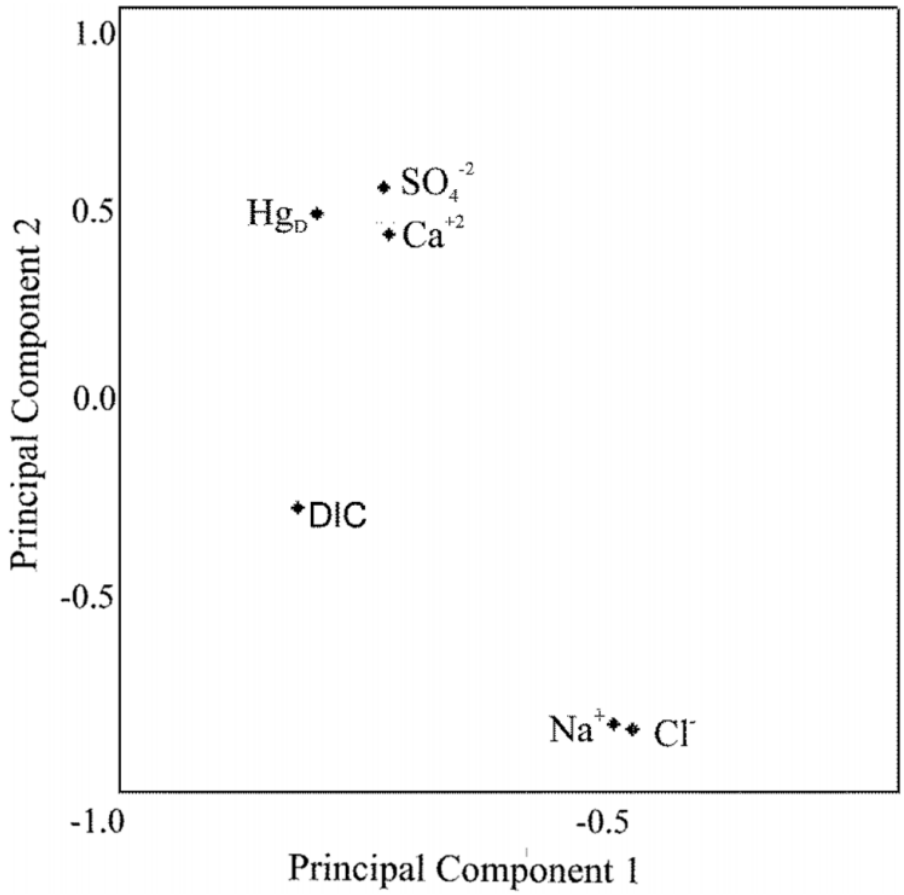

Fig. 1. (Table 4) – PCA plots for the two frst principal components (self-staggered data), using HgD, DIC and dissolved ions Na^{+}, Ca^{2+}, Cl^{-} and SO_4^{2-}

We concluded that the contamination of groundwaters by Hg had as its primary source the waste generated by felt manufacturing. Soil, construction and demolition waste, urban rubbish and mud were used to fill landfills during the nineteenth and twentieth centuries, spreading Hg contaminated materials all over the Rio Grande's urban area. Despite the elevated concentrations of HgD found in groundwaters, the legal limits of Hg for drinking water were not exceeded.

Acknowledgements

The research was founded by the Foundation for Research Support of the State of Rio Grande do Sul, Brazil (FAPERGS, Grant 12/0290-2).

CAPÍTULO II: Record of Hg pollution around outset of colonization in Southern Brazil

Environ Monit Assess (2019) 191:256
https://doi.org/10.1007/s10661-019-7404-5

Record of Hg pollution around outset of colonization in Southern Brazil

Guilherme Castro da Rosa Quintana ·
Nicolai Mirlean

https://doi.org/10.1007/s10661-019-7404-5

Abstract

This study presents results of a sediment core located in Coroa de Boi Bay, a not dredged cove within Patos Estuary, Southern Brazil. The distribution of metals (Hg, Cu, Pb) and U in the sediment profile records several contamination events since pre-colonial times to present days. A joint assessment of the distribution of these parameters and the consultation to historical documents allowed us to establish causal links between concentrations anomalies in the sediments and ancient anthropogenic contamination in the area. During the industrial period, sedimentation rates in the bay ranged from 3.4 to 5.5 mm $year^{-1}$. Applying a sedimentation rate previously calculated for undisturbed

sediments in the Patos Estuary, we trace the beginning of Hg contamination as having started in the colonial period in Southern Brazil, soon after a Hispanic–Lusitanian conflict situation in South America. The most probable source of Hg contamination during this period was carroting technology used in fur processing.

Keywords: Hg, Sediment core, Contamination events, Colonial period, Fur processing

Introduction

The mercury (Hg) content in estuarine sediments is monitored because of the high toxicity of this element to aquatic organisms and humans (WHO 1989; Machado et al. 2002; Wang et al. 2004; Lacerda and Malm 2008). The estuary of Patos Lagoon (32° 03′ S; 52° 04′ W) is one of the most dynamically developing industrial areas in the south of Brazil. Here, the second largest port of Brazil and the city of Rio Grande, founded at the beginning of the colonization period (in 1737), are located. Longstanding and intensive anthropogenic activity in the estuary area was recorded in the estuarine sediment showing elevated metal concentrations (Niencheski et al. 2014). The Hg pollution in sediments of Patos Estuary was first recorded in 1998 during a study of the consequences of 12,000 tons of sulfuric acid leaking in a tanker accident at Rio Grande port (Mirlean et al. 2001). High Hg content (up to 5 mg kg^{-1}) was detected in the sediments of the ports' navigation channel, but the source of the metal was not identified in that study. Later, high levels of Hg were also found in urban run-offs in the city of Rio Grande (Mirlean et al. 2003). It was also found that Rio Grande soils and groundwater are heavily polluted by Hg (Mirlean and Oliveira 2006; Fragomeni et al. 2010; Quintana and Mirlean 2018), and Hg contamination on fish that dwell in Patos Estuary was also revealed (Kütter et al. 2009). The geochemical mapping of the city revealed that a large portion of its soil cover is contaminated by Hg (Fig. 1).

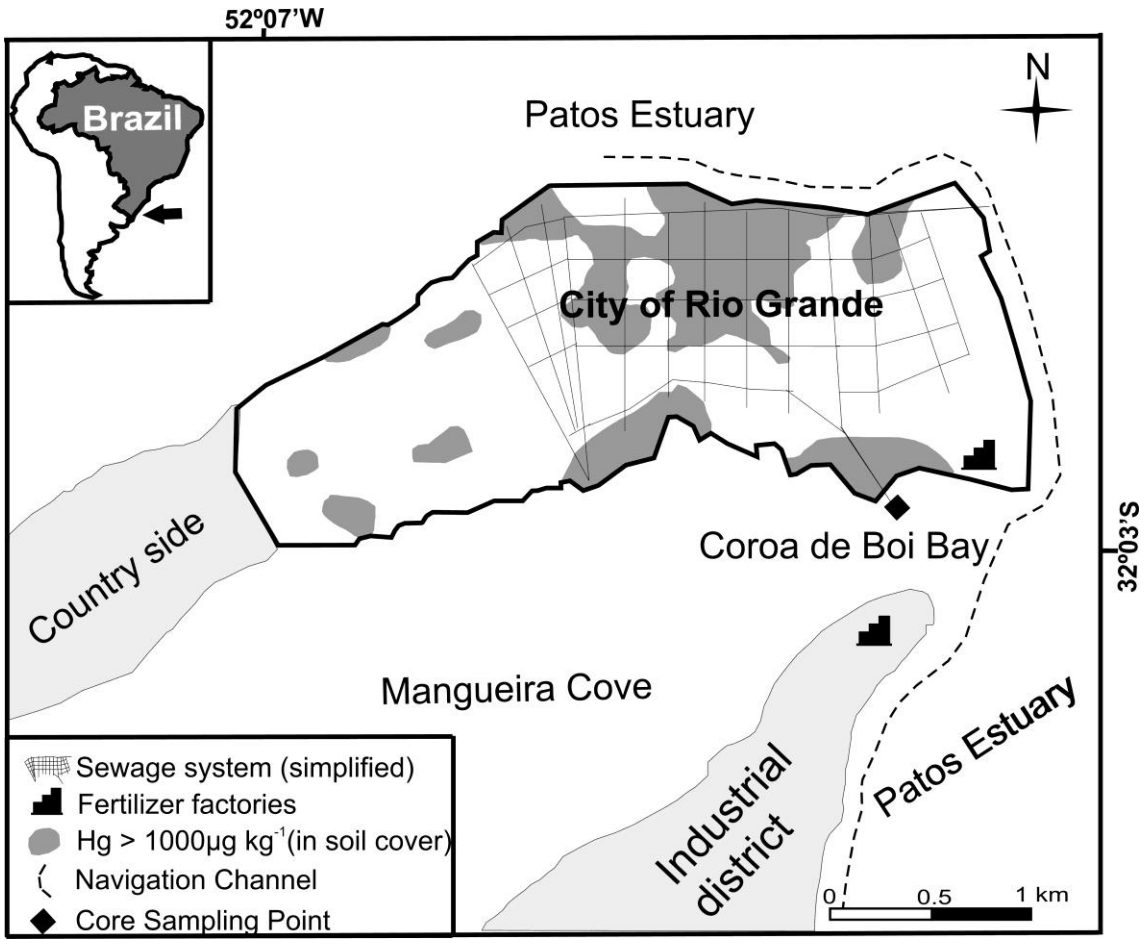

Fig. 1. Distribution of Hg in Rio Grande soil cover and sampling point location at CBB.

Large-scale movement of soil during urban infrastructure reforms and particulate material washout from urban areas caused an increase of Hg content in sediments of the port's navigation channel within the estuary (Mirlean et al. 2009). It was later proved that the principal source of Hg to the estuarine sediments is the Rio Grande's soil cover, in general. However, the original source of Hg, as well as the time of its appearance in the estuary, is still unknown. Recent studies point carroting, an ancient felt manufacture technique, as the most probable activity generating Hg-rich waste as the original source of Hg in the city based on the Hg contamination of urban soils to the depth of cultural layers corresponding to the beginning of the colonization of the South of Brazil (Mirlean and Oliveira 2006; Fragomeni et al. 2010). Carroting was widely used in North America during the colonial period and was pointed as the principal cause of environmental pollution by Hg in the Housatonic River in the USA (Varekamp et al. 2003). However, there is no evidence of the antiquity of Hg contamination in Rio Grande due to the

repeated displacement of the soil cover, as well as the possible migration of Hg from the soil surface to the lower horizons. A study of Hg distribution in the profile of not displaced estuarine sediments could provide new information on the history of Hg contamination in Southern Brazil.

For the studies of historical pollution records in the area, we chose Coroa de Boi Bay (CBB) in the southern tip of the peninsula occupied by the city of Rio Grande (Fig. 1). The CBB represents the most convenient section of the estuary for study, since the sediments in the bay were never dredged. Along the rest of the coastal lines of the city, dredging activities have been periodically conducted for more than 100 years. As a result, the natural profile of sediments in navigation channels and neighboring areas is severely disturbed. Until the early twentieth century, CBB was outside the zone of direct influence of industrial emissions and port activity, which in the nineteenth century were concentrated mainly along the northern and eastern shores of the peninsula occupied by urban buildings and commercial/industrial facilities.

In 1920, a centralized discharge of domestic and runoff sewage into CBB began (Leivas 1922) which was only discontinued in 2004. In the period from 1972 to 1990, phosphate fertilizer factories operated on the shore of CBB (Assis and Veríssimo 1997), heavily polluting the adjacent water area with aerial emissions and effluents. The geochemical markers of these two pollution sources could serve as additional dating points in the sediment profile. The purpose of this study was to determine the timing of Hg contamination in Patos Estuary area based on the study of one undisturbed sediment core.

Materials and methods

The sediment core was collected in October 2016 roughly in the center of CBB, about 300 m far from the coast and at approximately 1.0 m depth. One pre-cleaned acrylic tube (D = 8 cm) was used for core sampling down to the depth of 124 cm. Subsampling was performed by separating the sediment column in slices of 2 cm intervals for 0 –20 cm section and 4 cm intervals for 20 – 124 cm sediment section. In total, 36 sediment subsamples were picked out. The granulometric fraction <63 μm (composed by silt and clay, according to Wentworth's classification) was recovered from subsamples using wet

screening. The fine fraction samples were dried at room temperature and pulverized in agate mortar. The organic matter in sediments (whole samples) was determined by using loss on ignition procedure.

The acid digestion of homogenized samples was carried out according to EPA method 7471 for Hg determination (USEPA 1998). A cold vapor system, coupled with an AAS GBS 932, was used for Hg determinations. The AAS determination of copper (Cu) and lead (Pb) was performed in flame regime using the same device. Each sample was analyzed in triplicate; the relative standard deviation (RSD) of those three measurements of Hg did not exceeded 5%. The acid digestion according to EPA method 3050B was applied (USEPA 1996) to analyze Cu and Pb. Analysis of uranium (U) in sediment samples was performed by inductively coupled plasma-mass spectrometry ICP MS X300 with the addition of indium internal standard to every sample to correct the signal stability. Reference sediment MESS-3 sample (NRCC 2004) was included with the analyzed samples as quality control measures. The precision of reference samples ranged from 4 to 9% of the suggested values for Cu, Pb, U, and Hg.

Sedimentation rates were calculated through the ratio between the thickness of the sediment sections that correspond to the anomalies of concentration of Hg, Pb, Cu, and U and the time length of the anthropogenic activities responsible for generating such anomalies (mm $year^{-1}$). This calculation was carried considering documented historical periods of Rio Grande development such as the sewage (1920–2004) and fertilizer production effluent and emissions (1972–1990) discharge in CBB. As a result, four different sedimentation rates were calculated (Table 1). For the sediment section considered older than 1920, the natural sedimentation rate (3 mm year-1) previously calculated (Niencheski et al. 2014) was used.

Table 1. Information used for the calculation of the sedimentation rates

Historical Period (year)	Anthropogenic Activities	Time lengh (year)	Sediment section (mm)	Sedimentation rate (mm $year^{-1}$)
1920-1972	Sewage discharge	52	370–190	3.4

1972-1990	Sewage and industrial effluent discharge	18	190-90	5.5
1990-2004	Recent sewage discharge	14	90-40	3.6
2004-2016	Unknown and clandestine effluent discharge	12	40-0	3.3

Temporal confidence intervals were calculated by the ratio between the subsampling intervals (2 and 4 cm) and the sedimentation rate calculated for each historical period. The result of this calculation was divided by two, considering that the beginning and the end of the anomalies of concentration occurred in between the subsampling intervals.

Results and discussion

The content of the fine-sized sediment fraction (silt + clay) varied greatly (from 7 to 50%) along the sediment column, which attests a rather irregular hydrological regime in the estuary during the period of sediment accumulation (Fig. 2). However, a general trend of fine fraction content decrease towards the sediment surface can be observed. A sharp decrease of the fine fraction content occurs from a depth of 31 cm and reaches its minimum (7%) in the uppermost (0 – 2 cm) layer. Concentration of organic matter (OM) in the sediment profile varied from 0.46 to 3.57 % (average 1.32 %, n = 30). The distribution of OM along the sediment column was well correlated (r = 0.83) with the distribution of the fine fraction (Fig. 2). Usually, sediments mainly composed by silt and clay favor the accumulation of OM and heavy metals (Forstner and Wittmann 1979; Forstner and Salomons 1984); however, this tendency can be overthrown in severely contaminated sediments.

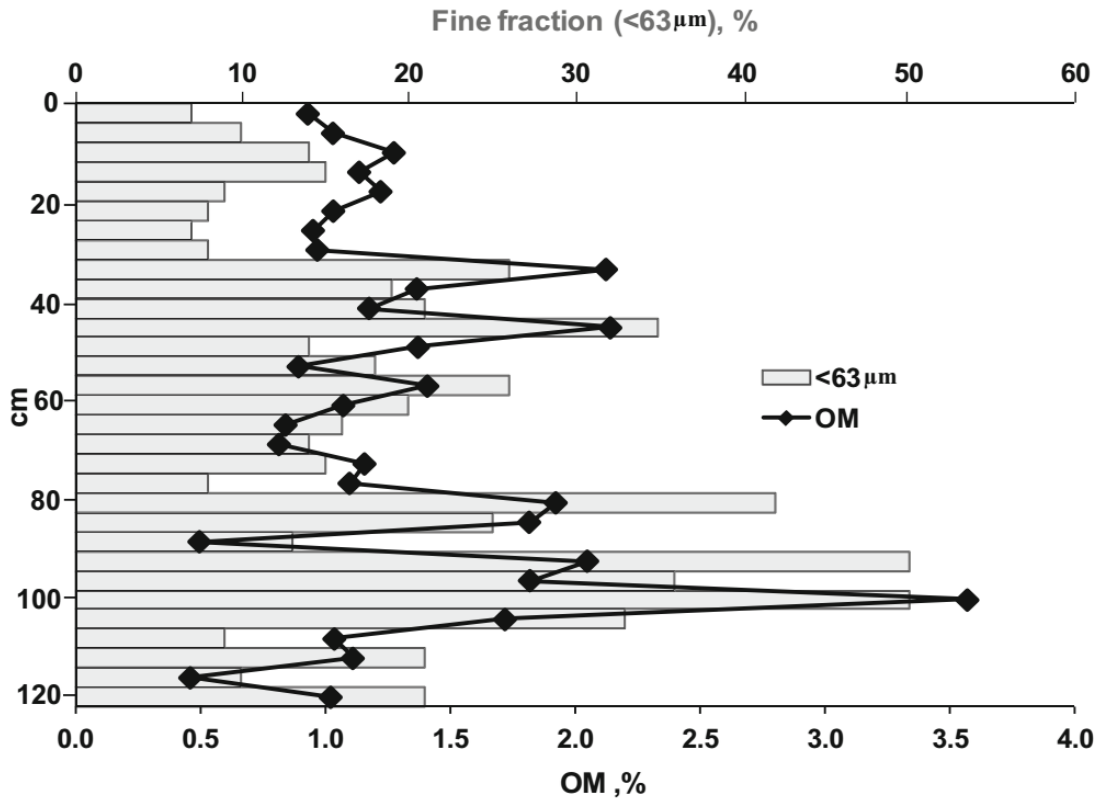

Fig. 2. Distribution of fine-sized fraction (< 63 μm) and organic matter down the sediment in CBB (made with Adobe Illustrator 2015)

The Hg content along the sediment core ranged from 7 to 668 μg kg^{-1}, demonstrating its non-uniform increase upward from the core bottom (Fig. 3). The highest Hg concentrations in the sediments were superior to effect range-low and very similar to effect range median, to benthic biota (150 and 710 μg kg^{-1}, respectively) according to the thresholds established by the National Oceanic and Atmospheric Administration of the USA for marine and estuarine sediments (Long et al. 1995). The Hg concentrations revealed at the present study also are superior to those proposed by the Canadian Council of Ministers of the Environment (CCME 2003) as threshold effect level (TEL) and probable effect level (PEL) for freshwater sediments (170 and 490 μg kg^{-1}, respectively) and marine sediments (130 and 700 μg kg^{-1}, respectively). Compared to the Brazilian Ministry of Environment limits for dredging purpose sediments (Conama 2012), the Hg content in CBB during the industrial period is between TEL (300 μg kg^{-1}) and PEL (1000 μg kg^{-1}) for brackish water sediments.

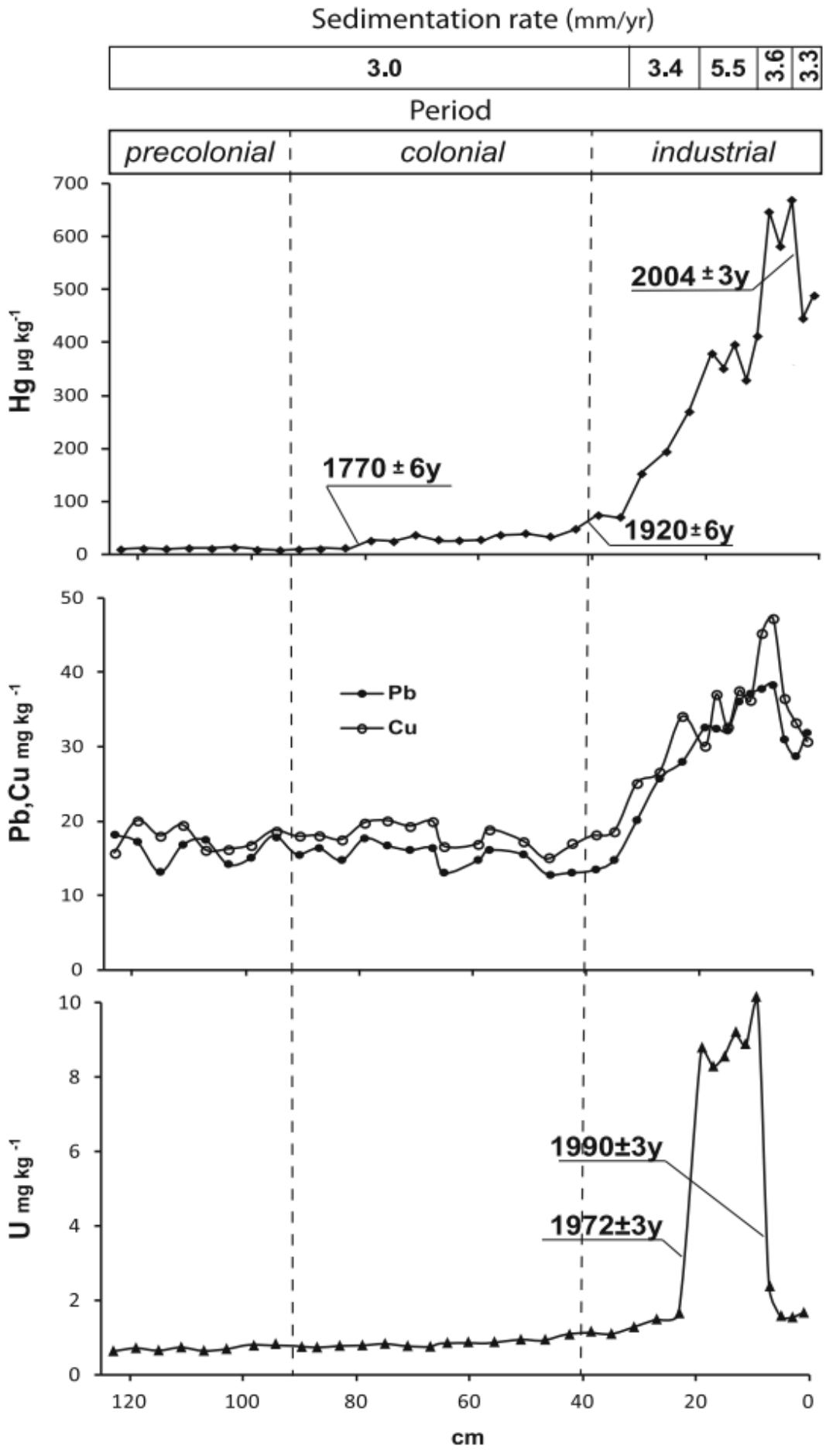
Sedimentation rate (mm/yr)
3.0
3.4
5.5
3.6
3.3
Period
precolonial
colonial
industrial
Hg µg kg-1
2004 ± 3y
1770 ± 6y
1920±6y
Pb,Cu mg kg-1
Pb
Cu
U mg kg-1
1990±3y
1972±3y
cm

Fig. 3. The dated distribution of Hg, Cu, Pb, and U along the sediment profile from Coroa de Boi Bay (made with Adobe Illustrator 2015)

In the lowermost interval of the core (124 – 81 cm), the average Hg content was 9.4 μg kg^{-1}, which corroborates the background concentrations of Hg in Brazilian coastal sediments (Marins et al. 2004). Above, in the 81 – 37 cm interval, the average Hg content considerably increased up to 40 μg kg^{-1}. Starting from 37 cm, an increase in Hg content was observed, with a maximum value of 668 μg kg^{-1} at the depth of 6 – 4 cm. In the uppermost sediment layer (0 – 4 cm), a sharp decrease in the metal concentration down to 445 μg kg^{-1} was observed. Pb and Cu in the sediments were analyzed as reliable geochemical tracers of urban emissions (Saet et al. 1990). The content of both metals varied slightly in the interval between the base of the core and the depth of 37 cm, but upwards it sharply increased by approximately two and a half times (Fig. 3). This increase in Pb and Cu concentrations, as well as its sharp decrease close to the surface of sediments, fully corresponds to the character of Hg distribution in this profile interval (Fig. 3). This simultaneous variation in the concentration of metals in the sediments indicates their common source as being the urban effluents, which, according to the documents of Rio Grande prefecture, were discharged into CBB from 1920 to 2004.

Another geochemical tracer in the sediments of CBB is U. It is known that U is present in high concentrations in wastes of phosphate fertilizer production (Schnug and Lottermoser 2013). In the studied profile, the concentration of U from the base of the core up to the depth of 19 cm varied slightly with an average of 0.9 mg kg^{-1}. Above the profile, the concentration in the sediments sharply increased by about 10 times and also sharply decreased at a depth of 9 cm from the surface of the sediments, most probably indicating the period of fertilizer production in the area (Fig. 3). The most intense period of activity of these factories in CBB was documented between 1972 and 1990 respectively (Assis and Veríssimo 1997).

The documentary registration of industrial and domestic discharges in the twentieth century in CBB made it possible for us to quite accurately calculate the sedimentation rate during the individual periods of industrial and urban activities (Table 1). In the period from the beginning of the discharge of sewage to the commencement of large-scale production of phosphorus fertilizers (1920–1972), the sedimentation rate was

3.4 mm $year^{-1}$. The sediments of this period are coarser than in the underlying core segments. The enrichment of sediments during discharges of urban effluents by sand fraction can be explained by the presence of storm sewage from city pavement in the outflow of material, in which the fraction of fine-grained sand predominates (Mirlean et al. 2009). In addition, the sewage system was built precariously, allowing fine-grained sand to enter in the pipes (Brito 1918; Leivas 1922).

During the period of activity of phosphate fertilizers factory (1972–1990), the sedimentation rate in the bay increased to 5.5 mm $year^{-1}$ and the grain size composition was enriched in fine sediments, probably due to the appearance of aerial emissions and dust that usually accompany the phosphate fertilizer production. In the period after the discontinuation of phosphate fertilizer production and before the termination of the centralized discharge of urban wastewaters (1990–2004), the sedimentation rate in CBB reduced to 3.6 mm $year^{-1}$, and after the termination of discharges in 2004, it was further reduced to 3.3 mm $year^{-1}$. This value is very similar tothe mean sedimentation rate for undisturbed sediments in Patos Estuary (3 mm $year^{-1}$) previously determined on the basis of ^{210}Pb dating of four sediment cores of 1 m deep in neighboring estuary areas not affected by direct anthropogenic impacts (Niencheski et al. 2014).

Assuming that in CBB the sedimentation rate before the direct discharge of industrial urban wastes was 3 mm $year^{-1}$, we can determine that an increase in the concentration of Hg in the sediments at a depth of 81 cm occurred approximately between 1764 and 1776. The certainty of the increase in Hg content in this period is confirmed by post hoc Tukey's test ($P < 0.001$), comparing Hg concentrations in sediments below 81 cm and in the sediment interval above this depth mark until the beginning of the discharge of wastes in 1920. This date of initial occurrence of Hg contamination of Patos Estuary is consistent with some historical details of the region's development.

The founding of the city of Rio Grande is officially dated as 1737, which can be considered as the beginning of the colonial period on the region (Pimentel 1944). The date of the founding of the city corresponds to the depth of about 90 cm in sediment core from CBB, where the concentration of Hg did not exceed 8 mg kg^{-1}. In the next two decades, the region had no noticeable economic development. Rio Grande was founded by Portuguese settlers, but in 1763, the city was invaded by Spanish military who occupied the place until 1776, the city was surrendered with no conflict. During this period, the Spanish rulers exempted the population from taxes, stimulating the emergence

of new business in the city (Queiroz 1987; Cesar 2015). Almost simultaneously with the appearance of the colonial economy, Hg content in the estuarine deposits increases almost threefold, indicating that Hg-rich waste was generated in the colonial period were felt manufacturing was a fully feasible business taking into account the increase of the purchasing power of the population, the high sale value of felt products, and the presence of animals like *Hydrochoerus hydrochaeris* and *Myocastor coypus bonariensis* in the region, whose fur is similar to that of the beaver (*Castor sp.*), commonly used in carroting technology. In the following 150 years, Hg content in the sediments slowly increases until the direct discharge of urban waste into the estuary with the onset of the industrial period, increasing the metal content in sediment by almost 20 times.

Conclusion

The current study confirmed the hypothesis of the beginning of Hg pollution in the area of Patos Estuary in the early colonial period (Mirlean and Oliveira 2006). However, the source of Hg contamination in the eighteenth century in the area has no documented evidence. Taking into account the leading branch of local production in the colonial period (processing of fur), we believe that the most likely source of Hg was the carroting waste.

In the eighteenth century, the manufacture of felt received this new technological process based on the processing of fur with solution of Hg nitrate. Carroting was reliably used in industrial production in Rio Grande in the nineteenth century and before its legislative prohibition in the 1960s of the twentieth century. However, the period of widespread contamination obviously occurred in the eighteenth century, when waste production was dispersed in an artisanal way. As a result, the soil cover of the city and manmade lands constructed from urban debris and street waste still serve as a source of Hg contamination in the Patos Estuary (Mirlean et al. 2009; Fragomeni et al. 2010).

It is possible that the carroting also has been consistently used in other settlements close to Rio Grande, with similar culture and colonization in the south of Brazil, Uruguay, and north of Argentina. In this way, many cities of this region may have been contaminated with Hg during the colonial period.

Acknowledgments

We are grateful to the Coordination of Improvement of Higher Level Personnel of Brazilian government (CAPES) by grant of scholarship. We are also grateful to the Public Library of Rio Grande, to the local Water and Sewer company (CORSAN), and to the Ipiranga fuel company for the help during the historical research.

CAPÍTULO III: Mercury distributions in sediments of an estuary subject to anthropogenic hydrodynamic alterations (Patos Estuary, Southern Brazil)

Environ Monit Assess (2020) 192:266
https://doi.org/10.1007/s10661-020-8232-3

Mercury distributions in sediments of an estuary subject to anthropogenic hydrodynamic alterations (Patos Estuary, Southern Brazil)

Guilherme Quintana · Nicolai Mirlean · Larissa Costa · Karen Johannesson

https://doi.org/10.1007/s10661-020-8232-3

Abstract

The city of Rio Grande, located on the right bank of the Patos Estuary, has been severely contaminated by mercury (Hg) due to anthropogenic activities that chiefly began in the eighteenth century. To investigate the natural mercury distribution along the salinity gradient in the estuary, three sediment cores were collected from a region of the estuary that has experienced less anthropogenic impacts, namely its left bank. Our study demonstrates that accumulation of Hg and formation of metal sulfide minerals takes place in fine grain sediment horizons within the sampled sediment cores. Mercury immobilization in these sediments occurs via binding to organic matter coatings on fine grain sediment particles, as well as by incorporation into and/or coprecipitation with iron sulfide minerals. The grain size controls over Hg accumulation and sulfide mineral formation were statistically demonstrated using Principal Component Analysis. Different fine particulate sediments deposition patterns occurred at each sampling location, which is attributed to the consequence of hydrological changes in the estuary resulting from navigation infra-structure reforms performed over the past 200 years in the local port (e.g., dredging) and its surroundings. We suggest that the port building and maintenance activities have influenced Hg distributions in the estuarine sediments.

Key-words: Mercury distribution, Sulfide formation, Estuary, Hydrological changes, Navigation infra-structure reforms

Introduction

Mercury (Hg) is a widely studied metal because of its high toxicity and its importance in public health issues (Forstner and Wittmann 1979; WHO 2003). High concentrations of mercury in natural environments are commonly associated with contamination generated by pesticides, amalgamation (i.e., used for gold mining), and the coal and chlorine-soda industries (Lacerda and Malm 2008). However, natural geochemical processes can also favor the accumulation of Hg in pristine environments (Winfrey 1988). Sulfidic "traps" can be very important in estuarine sediments, where anoxic conditions favor the formation of metal sulfide minerals mainly constituted by iron (Fe) and other chalcophile elements (Perelman 1967). In this context, polysulfide ions stand out because reactions between mackinawite (FeS) and polysulfides appear to be an important mechanism for pyrite formation (Bunsen 1847; Van Bemmelen 1886; Meysman and Middelburg 2005; Rickard and Luther 2007).

Diagenetic transformations of sulfur (S) are of great importance in sediment chemistry, mainly in coastal and estuarine environments (Huerta-Diaz and Reimer 2010) because the S cycle is linked to the cycles of carbon (C), oxygen (O), Fe, and numerous trace elements in such environments (Brüchert *et al*. 2003; Otero *et al*. 2009; Hernández-Crespo and Martín 2013; Yang *et al*. 2014). Sulfide minerals are known to be effective adsorbents of Hg and accordingly have been identified as the primary sink of Hg in the environment in several studies (Brown *et al*. 1979; Hyland *et al*. 1990; Ehrhardt *et al*. 2000; Barnett *et al.* 2001). The formation of metal sulfides in sediments is limited by the organic matter input and by the availability of sulfate and metals, mainly Fe (Berner 1984). However, none of these limiting factors tend to be observed in high-productivity estuarine areas, where hydrodynamic processes favor the mixing and the oxygenation of the water column. Furthermore, metals and sulfate are supplied to estuarine environment by the terrestrial catchment area and the adjacent ocean, respectively (Bianchi 2007).

In estuaries subject to long-term changes in the hydrodynamical energy regime, irregular sedimentation occurs, and as a result, grain size variations of the estuarine

sediments are a common feature (Winfrey 1988; Antiqueira and Calliari 2005). Fine grain sedimentation occurs in locations within estuaries characterized by low hydrodynamic energy, whereas coarse grain sedimentation is normally associated with high hydrodynamic energy locations (Winfrey 1988; Antiqueira and Calliari 2005). Sediment grain size is important for understanding natural geochemical processes (e.g., metal sulfide formation) related to the distribution of organic matter, S, O, and metals (Winfrey 1988; Rojas and Silva 2005; Álvarez-Iglesias and Rubio 2012). However, anthropogenic activities can change the natural hydrodynamical behavior of estuaries (Forstner and Wittmann 1979; Forstner and Salomons 1984), modifying sedimentation processes, and consequently, the vertical grain size distribution deposited in the sediments. In such anthropogenically impacted estuaries, understanding the natural geochemical processes is of great importance because natural accumulation of chemical elements could be erroneously classified as resulting from anthropogenic processes and/or contamination.

A recent study of bottom sediments from a shallow cove within Patos Estuary, the largest estuary of southern Brazil, demonstrated that the onset of Hg contamination in Rio Grande city can be dated to the eighteenth century (Quintana and Mirlean 2019). Despite the relatively well-documented anthropogenic Hg contamination of soils, waters, and sediments in the vicinity of Rio Grande city, there have been no investigations of Hg accumulation related to natural geochemical processes in the region. Understanding these natural processes may help to better discriminate anthropogenic contamination from natural accumulation of Hg in Patos Estuary sediments.

The aim of the present study is to establish the distribution of Hg in low impacted and undisturbed sediments of Patos Estuary and evaluate the Hg distributions with regards to natural, in-situ geochemical processes (i.e., sulfate-reduction and metal sulfide formation). Furthermore, we investigate the influence of fine grain sediment distributions, which is a consequence of the local estuarine hydrodynamic regime, on Hg contents and distributions in the estuarine sediments. The sediment Hg analyses are subsequently assessed with regards to possible impacts from anthropogenic activities within Rio Grande city and to the development of the Port of Rio Grande.

Study area

The Patos Estuary, located in the south of Brazil, is a long-term anthropogenically contaminated environment with a surface area of approximately 900 km^2 (Kjerfve 1994). The Patos Estuary receives continuous inputs of urban and industrial effluents from Rio Grande city, which is located on a peninsula along the right bank of the estuary. The estuary also harbors the second largest port in Brazil (i.e., the Port of Rio Grande) with regards to amounts of cargo handled (Fig. 1). The Patos Estuary is characterized as a microtidal system (i.e., < 0.5 m tidal range) that exhibits seasonal salinity variations whereby low salinities (0–5) dominate the system during the winter/spring (i.e., rainy season) and high salinities (20–30) dominate during the summer/fall (i.e., dry season; Moller *et al*., 1996; Marques *et al*., 2010). The hydrological regime of the Patos Estuary is mainly controlled by winds and by river discharge (Moller *et al*. 2001). Southwest winds promote the entrance of marine waters into the estuary, whereas northeast winds enhance the river discharge (Moller *et al.* 1996). This hydrodynamic seasonal cycle in the estuary promotes prolonged residence times of brackish water during summer/fall and fresh water during winter/spring (Moller *et al.* 1996; Moller *et al*. 2001).

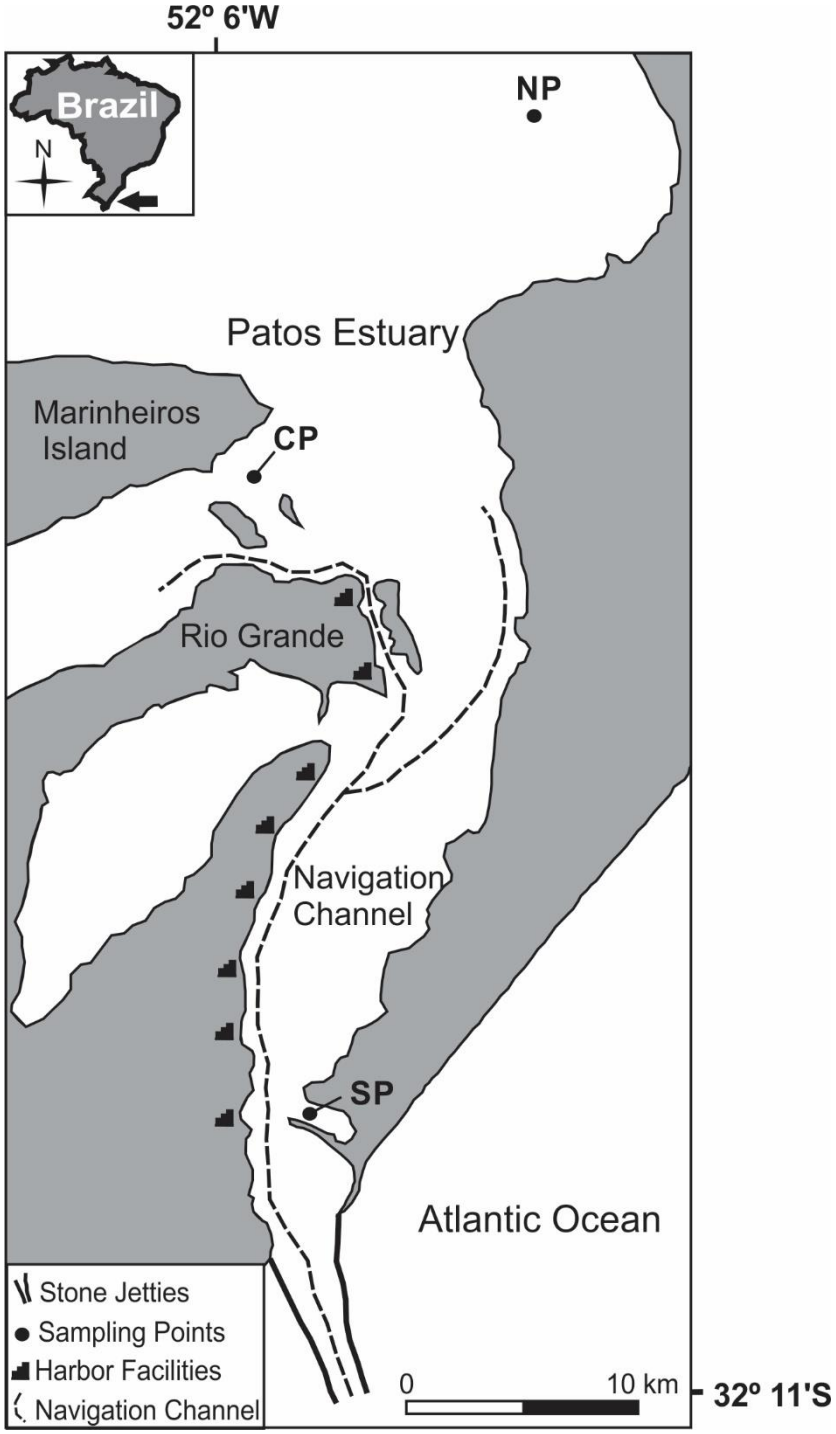

Figure 1. Patos Estuary and samples location (NP, CP and, SP).

Urban effluents from Rio Grande city contaminated with Hg are known to detrimentally impact the Patos Estuary (Mirlean *et al.* 2003). Furthermore, urban soils of the city as well as land fill used to build new land for the city growth and expansion are strongly contaminated by Hg (Mirlean and Oliveira 2006). Elevated concentrations of Hg (i.e., up to 13 mg kg^{-1}) occur in both the oldest part of the city, occupied since the eighteenth

century, and in more recently embanked areas, occupied since the nineteenth and twentieth centuries (Fragomeni *et al*. 2010). As a direct consequence of the soil Hg contamination, groundwater from the Rio Grande urban area is also contaminated by Hg (Quintana and Mirlean 2018).

Materials and methods

Sediment cores were collected from three locations along the left bank of the Patos Estuary to study Hg distribution in vertical profiles of the bottom sediments. The three sites are identified herein as the southern (SP), central (CP) and northern (NP) locations (Fig. 1). The hydrological conditions at each site vary as a function of distance from to the Atlantic Ocean and owing to the seasonal salinity cycle described above. The three sediment cores were collected in September 2016 (i.e., spring in the southern hemisphere), which is characterized by strong fluvial discharge (Moller *et al.*, 1996; Marques *et al.*, 2010). Pre-cleaned acrylic tubes (8 cm in diameter) were used for sediment core sampling. After sampling, each core was hermetically sealed, transported to the laboratory and stored cold (4°C) for 12 hours before physicochemical measurements and subsamples separation. The cores were opened and split longitudinally into two halves followed by sectioning at 2 cm intervals along the length of each half of the three cores. The various subsamples were subsequently measured for redox potential (Eh), pH and free dissolved sulfide (i.e., ΣS^{-II}) concentrations in the pore waters (e.g., Costa *et al.*, 2019). Separate aliquots of each 2 cm sediment subsample were then analyzed for Hg, Fe, and organic carbon (OC) contents. The other half was immediately sectioned in 2cm intervals and frozen for further insoluble sulfide content analysis in the sediments. Thirty-three specific sub-samples were chosen for chemical analysis along with the sediment profiles of the three sampling points.

Eh was measured on the freshly exposed surface of the sediment cores using a naked Pt-electrode (Analion®). The pH was measured in filtered (0.45 µm Milipore® membrane) interstitial pore waters extracted from the sediment subsamples by centrifugation (3000 rpm). The determination of ΣS^{-II} in the interstitial pore water was performed using a silver/sulfide combination ion selective electrode (model Hanna® 9616 BNC) coupled to an Orion™ ISE/pH/mV/Eh/temperature meter (model 209a; Brooks 2001). A basic antioxidant solution for sulfides (Sulfide Antioxidant Buffer -

SAOB, Hanna Intruments®) and a sulfide standard ($Na_2S.9H_2O$) were previously made and used for calibration of the ion selective electrode. The electrode was calibrated after every 12 readings from a three-point calibration curve (100, 1000, 10000 μmol L^{-1}).

The total reducible inorganic sulfides (TRIS) were measured using frozen sediment subsamples by chromium reducible sulfur (CRS) analysis following the method described by (Fossing and Jørgensen 1989). This procedure consists of subjecting the sample to acid digestion with an acid solution (Cr^{+2} in HCl) under an inert gas (N_2) purge, producing H_2S, which is then collected in a sulfide retention solution (Zn – Acetate + NaOH). The quantification of TRIS was made by iodometry and the relative standard deviation (% RSD) for the measurement was ≤ 5%. The organic carbon (OC) content of the sediment samples was determined on dried sediments samples (30 mg) by using a TOC - VCPH, model SSM - 5000A, Shimadzu® with combustion detector. The OC results are presented in percentage of organic carbon in dried sediment, and the RSD was < 5 % for triplicate analyses. The fine grain sediments (< 63 μm), composed of silt and clay according to Wentworth's classification, were recovered from subsamples using standard sieve methods (ASTM C136/C136M).

The acid digestion of homogenized sediment subsamples was carried out according to EPA method 7471 for Hg determination (USEPA 1998). A cold vapor system, coupled to an AAS GBS 932, was used for Hg measurements. Each sample was analyzed in triplicate; RSD of the three measurements of Hg did not exceed 5%. A certified reference material, MESS-3 sample (NRCC 2004), was included with the analyzed samples for quality control measurement. The recovery of reference samples were in the 91% confidence limits for the CRM. Iron was extracted from the samples following the EPA method 3050B (USEPA 1996). The extracted solutions were diluted by a factor of 1:400 (v/v) and measured by UV/VIS spectrophotometry using a DR 2800 Spectrophotometer from Hach Company®, method 8008 – FerroVer® Method (HACH, 2007). Spiked duplicate samples were processed on a routine basis (5% of each sampling point), with RSD < 5%. The quality control of Fe analysis was ensured by the extraction and quantification of certified reference material MESS-4. The precision of the reference samples was always within 5% of the suggested values for Fe. Reported concentrations for the samples were blank subtracted.

Results

For all three sediment core sampling locations the greatest changes in measured Eh values occurred within the superficial (i.e., 1-20 cm) sedimentary layer (-178.5 to -25.5 mV for the SP core; -350 to -50 mV for the CP core; -356 to -15 mV for the NP core). The Eh generally decreased with increasing depth in all three sediment cores, reaching values of -350 mV and -356 mV at depths of 51 cm and 45 cm in the CP and NP cores, respectively (Table 1; Fig. 2). The Eh in the SP core only decreased to -178 mV, attaining this minimum value as a depth of 37 cm (Table 1; Fig. 2). The mean Eh values were similar for the CP and NP cores (i.e., -189.3 ± 121.2 mV and -188.7 ± 128.6 mV, respectively, for the CP and NP cores). In contrast, for the SP core, which was collected from near the estuarine outlet to the Atlantic Ocean, the mean Eh was -107 ± 53 mV (Table 1; Fig.2). Conductivity of interstitial pore waters recovered from each core directly reflected the distance of the sediment core locations from the ocean, decreasing gradually from south to north (Table 1). The mean conductivity values were 42 ± 11.5 mS cm^{-1} for the SP core, 15.9 ± 4 mS cm^{-1} for the CP core and 9.3 ± 5.5 mS cm^{-1} for the NP core (Table 1). The pH of the interstitial waters varied little between each site such that the mean pH was 7.6 ± 0.3 for pore waters from the SP core, 7.7 ± 0.5 in pore waters from the CP core, and 7.7 ± 0.2 in pore waters from the NP core (Table 1).

Table 1. Geochemical parameters for samples location, SP, CP and NP. The upper numbers are the concentration range, and the mean ± SD for the entire core is presented within parentheses.

Parameter	SP	CP	NP
Eh (mV)	-178.5 – -25.5 (-107 ± 53)	- 350 – 50 (-189.3 ± 121.2)	- 356 – 15 (-188.7 ± 128.6)
Conductivity (mS cm^{-1})	29.7 – 56.5 (42 ± 11.5)	10.6 – 21.2 (15.9 ± 4)	2.9 – 17 (9.3 ± 5.5)
pH	7.07 – 7.98 (7.6 ± 0.3)	6.81 – 8.32 (7.7 ± 0.5)	7.33 – 8.1 (7.7 ± 0.2)
OC (%)	0.17 – 1.3	0.27 – 1.05	0.21 – 0.88

	(0.6 ± 0.3)	(0.5 ± 0.3)	(0.5 ± 0.3)
<63 µm (%)	7.83 – 86.4 (50.4 ± 24.8)	13.05 – 47.76 (28.1 ± 13.4)	9.02 – 60.93 (32.3 ± 20.8)
Hg (µg kg^{-1})	3.9 – 56.5 (27.2 ± 15.4)	7.6 – 35.4 (19.3 ± 10.4)	4.6 – 37.2 (18.6 ± 13.8)
Fe (%)	0.92 – 2.62 (1.96 ± 0.51)	1.35 – 2.82 (1.90 ± 0.46)	0.86 – 3.06 (1.94 ± 0.78)
TRIS (mg kg^{-1})	745.2 – 5474.4 (2427.4 ± 1554)	151.8 – 5474 (2881.6 ± 2162.6)	109.1 – 6745.1 (3348 ± 2904.7)
ΣS^{-II} (µmol L^{-1})	20.7 – 142.7 (51.2 ± 31.5)	11 – 690 (270.9 ± 267.5)	9 – 321 (96.3 ± 115.26)

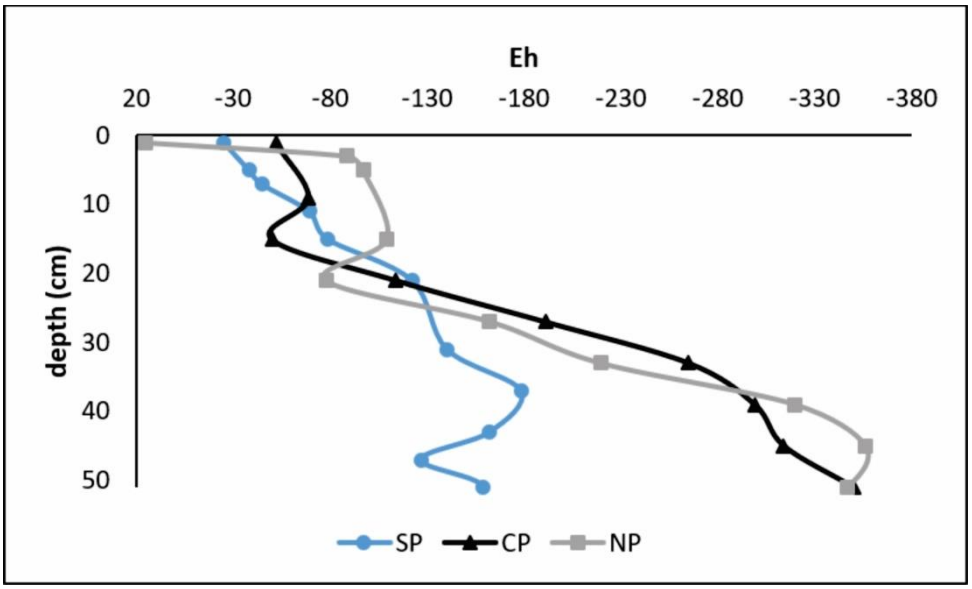

Figure 2. Eh vertical distribution, for sites SP, CP and NP.

In general, the sediment OC contents were relatively low (<1%) at all three sampling locations (Table 1), however there was a clear tendency of OC enrichment in the percentage of fine grain sediments from each core (Fig. 3). In the CP and NP cores there is a downward increase of OC and the percentage of fine grain sediments (Fig. 3). The SP profile showed a different distribution of OC and fine grain sediments compared to both the CP and NP cores. The percentage of fine grain sediments within the SP core

varies from 25 to 80 % in the first 21 cm, strongly decreases between 31 and 37 cm, and subsequently increases again at depths greater than 43 cm, reaching 80 – 90% in the deeper sediments of the profile (51 – 57 cm). These results indicate more variation of the hydrodynamic energy at the SP site within the time period when the cores were collected (Fig. 3). Nevertheless, OC content distribution, in general, appears to be largely controlled by the fine grain contents of the sediments at each sampling location (Fig. 3).

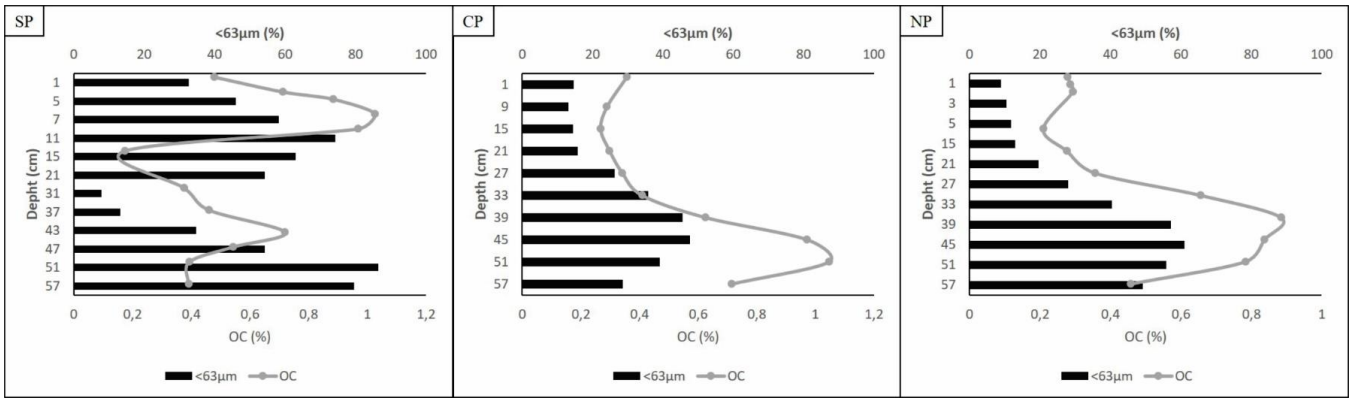

Figure 3. OC and fine grain (<63µm) vertical distribution in the sediment cores (SP, CP and NP locations).

The mean TRIS contents of the three sediment cores increase from south to north, such that the mean TRIS content is 2427.4 ± 1554 mg kg^{-1} in the SP core, 2881.6 ± 2162.6 mg kg^{-1} in the CP core, and 3348 ± 2904.7 mg kg^{-1} in the NP core. The vertical distribution of TRIS is similar to the vertical distribution of the OC contents, where the highest TRIS contents occur in the fine-grained sediments at all sampling locations (Table 1; Figs. 3, 4). In general, mean Hg contents were also higher in sediments enriched in silt and clay, such that the mean (± SD) Hg content was 27.2 ± 15.4 µg kg^{-1} for sediments from the SP core, 19.3 ± 10.4 µg kg^{-1} in sediments of the CP core, and 18.6 ± 13.8 µg kg^{-1} in sediments from the NP core. The mean Fe content did not vary between the three cores, exhibiting values of 1.96 ± 0.51% in sediment from the SP core, 1.90 ± 0.46 % in sediments of the CP core, and 1.94 ± 0.78 % in sediments from the NP core (Table 1). Nonetheless, the Fe content as well as the Hg content of sediments from each core exhibited similar variations with depth to both the OC and TRIS contents (Figs. 3, 4).

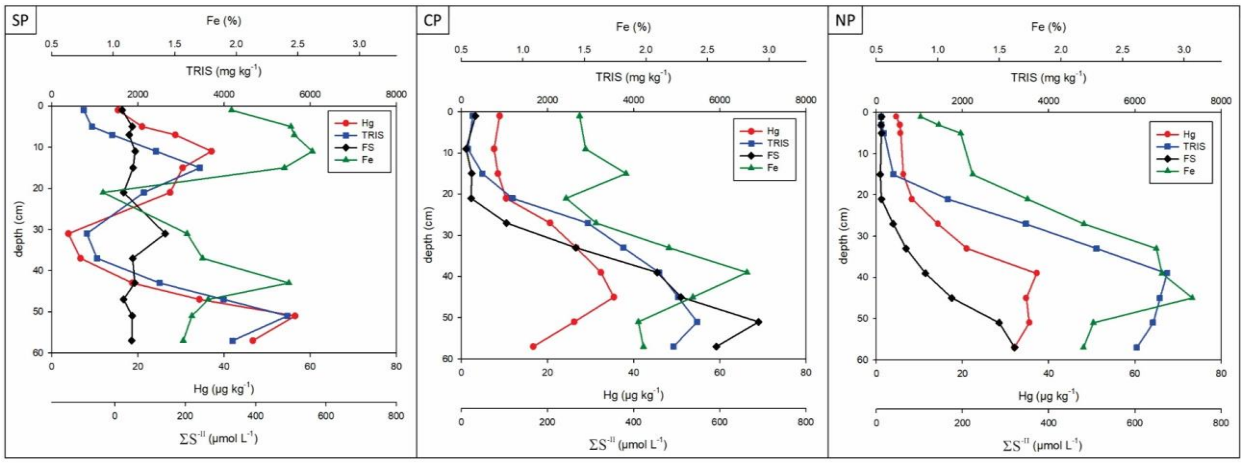

Figure 4. Hg, Fe, TRIS and ΣS^{-II} vertical distribution in sediment cores (SP, CP and NP).

In general, the ΣS^{-II} concentrations as a function of depth in pore waters from the CP and NP cores closely tracked the depth variations of the Hg and Fe contents of the sediments (Fig. 4). However, the mean ΣS^{-II} concentrations of pore waters differe between the cores, with the total dissolved sulfide concentration being 270.9 ± 267.5 µmol L^{-1} in pore waters from the CP core, and 96.3 ± 115.26 µmol L^{-1} in pore waters from the NP core. In contrast, pore water ΣS^{-II} concentrations were substantially lower for the SP core, exhibiting a mean (± SD) of 51.2 ± 31.5 µmol L^{-1}. In addition, the vertical distribution of dissolved sulfide in SP core pore waters differs from the other two cores by being comparatively invariant (Fig. 4). The one exception to the nearly constant pore water ΣS^{-II} concentrations with depth in the SP core is the subsurface maxima that occurs 30 cm depth. A possible explanation of the dissolved sulfide concentrations in the pore waters of the SP core could be the absence of substantial dissolved Fe concentration, because ΣS^{-II} is not a limitation for the formation of TRIS in estuarine sediments (Rojas and Silva 2005; Bianchi 2007). In the 30 - 40 cm interval of the SP core the contents of fine sediments decreases as does the TRIS and metals contents, before increasing at greater depths (Fig. 4).

Applying a previously calculated sedimentation rate (0.3 cm/y) for non-disturbed sediments of the Patos Estuary (Niencheski *et al.* 2014) it is possible to chronologically analyze the fine sediments distribution as a function of depth in each sediment core. As mentioned above, the percentages of fine grain sediments with depth are similar for the CP and NP cores, where higher contents of fine grain sediments occur at depth (27 - 57 cm, Fig. 3). This depth interval is chronologically dated to range between the years 1826

and 1926 (Niencheski *et al.*, 2014). During this historical period, bottom sediments were modified by anthropogenic activities such as dredging for improved navigation, and the construction of two large stone jetties at the inlet of the Patos Estuary in 1915 (Fig. 1). For shallower depths between 1 and 21 cm, the percentage of fine grain sediments strongly decreased upward (Fig. 3), suggesting a recent increase of the hydrodynamic energy at these sampling locations (i.e., cores CP and NP). We suggest that the changes in sediment grain size are a consequence of the massive engineering works realized in the port and in the construction and maintenance of the main navigation channel, which intensified beginning in 1915, and has continued to the present. At the SP core location the vertical distribution of fine grain sediments differs from that observed at the CP and NP cores. Unlike these others sampling locations, the SP core is located in a cove along the left bank of the estuary (Fig. 1), and is consequently protected to some degree from the anthropogenic activities that were undertaken to dredge the navigation channel and construct the port. Hence, the average contents of silt and clay that characterizes sediments from the SP core location (i.e., 50.4 %) exceeds the average silt and clay contents of the CP core sediment (28.1 %), and the NP core sediments (32.3 %).

Principal component analysis (PCA) and Pearson correlation coefficient (PCC) were used to better understand relationships between metals (Hg and Fe), TRIS, ΣS^{-II}, the distribution of fine grain sediments (<63µm), and OC contents of the sediment cores (Fig. 5). The PCA enabled us to distinguish two groups of variables based on two principal components that together, explained 82.9% of the total variance of the data. Principal component 1 contributes 66.9% of the data variance and was better represented by the variables Hg, Fe, TRIS, fine sediments and OC (Table 2; Fig. 5). This component is clearly related to the grain size control over the distribution of OC, TRIS, Hg and Fe. Pearson coefficient test ($p < 0.01$) showed positive linear correlation between these variables (Table 3). PCC also revealed statistical correlation (positive) between ΣS^{-II}, TRIS and OC (Table 3), a clear evidence that sulfate reduction and subsequent metal sulfide formation is dependent on OC contents in sediments. Principal component 2 explained only 16% of the data variance and probably represents secondary mechanisms of metals immobilization in the studied sediments (Table 2).

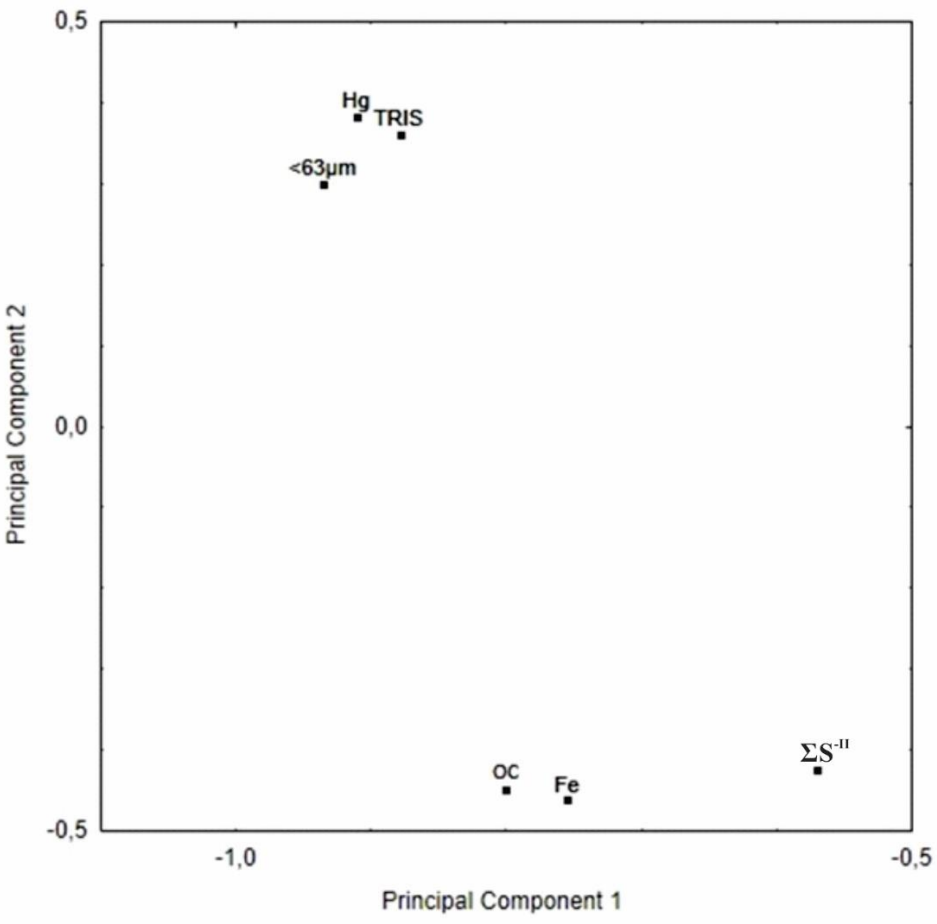

Figure 5. PCA plots for the two first principal components (self-staggered data), using Hg, Fe, TRIS, ΣS^{-II}, fine grain sediments (<63µm) and OC

Table 2. Variable charges for the two first principal components (self-staggered data), using OC, <63 µm, Hg, Fe, FS and TRIS results SP, CP and NP (n = 33).

Variable (variance of the data)	OC	<63 µm	Hg	Fe	ΣS^{-II}	TRIS
Principal Component 1 (66.9 %)	-0,80	-0,94	-0,91	-0,76	-0,57	-0,88
Principal Component 2 (16 %)	-0,45	0,30	0,38	-0,46	-0,42	0,36

Analysis of Variance (ANOVA) and Post hoc test (Fisher LSD, $p < 0.05$) were applied to reveal statistical difference between mean concentrations of Hg, Fe, TRIS, ΣS^{-II}, fine grain sediment (< 63µm) and OC contents spatially (Table 4). No significant difference is observed for most of parameters (Hg, Fe, TRIS and OC), nevertheless

ANOVA analysis showed that ΣS^{-II} and < 63µm mean contents are considerably different along the sampling points (Table 4). 4

Table 3. Pearson correlation coefficient values (significant correlations in red for p < 0.01), using Hg, Fe, TRIS, ΣS^{-II}, OC and < 63µm results from SP, CP and NP (n = 33).

Variable	Fe	TRIS	ΣS^{-II}	OC	< 63µm
Hg	0,49	0,77	0,28	0,52	0,96
Fe		0,62	0,34	0,77	0,52
TRIS			0,59	0,56	0,67
ΣS^{-II}				0,51	0,14
OC					0,56

Table 4. ANOVA analysis and Fisher LSD post-hoc test (p < 0.05) using Hg, Fe, TRIS, ΣS^{-II}, OC and < 63µm results from SP, CP and NP (n = 33).

Hg	SP = CP = NP
Fe	SP = CP = NP
TRIS	SP = CP = NP
ΣS^{-II}	(SP = NP) < CP
OC	SP = CP = NP
< 63µm	SP > (CP = NP)

Discussion

Windom *et al*. (1999) demonstrated that dissolved oxygen in the Patos Estuary water column varies from saturated conditions at low salinity to supersaturated at high salinity, which is consistent with marine waters being richer in dissolved oxygen compared to the continental fluvial waters entering the estuary. Therefore, it is probable that the difference in Eh measurements between the SP, CP, and NP sediment core locations is related to the distance of the sampling points from the ocean (Fig. 1). Furthermore Eh conditions are also affected by OC distributions of each sediment core,

especially considering that organic matter is the main substrate for oxygen respiring bacteria (Berner 1984; Jørgensen and Kasten 2005; Bianchi 2007). In general, the lowest Eh values were measured in the sediments that exhibited the highest OC contents (Figs. 2, 3). Pore water pH varied from neutral to slightly alkaline in the three sediment core profiles (Table 1). These conditions, together with the low oxidation potential observed at depth in the sediment cores, especially in the CP and NP cores (Table 1; Fig. 2), are favorable for formation of metal sulfide precipitates, as well as polysulfide generation, which together also favor the accumulation of Hg and other metals in these deeper sediment layers (Rickard and Luther 2007).

Principal component analysis and Pearson correlation coefficient reveals a strong correlation between the OC contents and the percentage of fine grain sediment fractions of the three cores (Tables 2 and 3; Fig. 5), which is corroborated with the general trend that the fine sediments have higher contents of organic compounds than coarser grained sediments (Fig. 3). Silt and clay size particles have larger specific surface areas compared to sandy sediments because the area/volume ratio of fine grain sediments is much larger than that of these coarser grain materials (Rojas and Silva 2005; Álvarez-Iglesias and Rubio 2012). Moreover, the surfaces of fine grain sediment particles tend to be coated by a layer of organic material (Winfrey 1988). Therefore, fine grained sediments commonly have larger contents of associated organic matter than coarser grained sediments like sands (Winfrey 1988; Rojas and Silva 2005; Álvarez-Iglesias and Rubio 2012). In turn, the organic matter in such sediments serves as a substrate for bacterial activity, promoting oxygen and sulfate ion consumption, lowering the redox potential, and the concomitant production of dissolved sulfide ions (Berner 1984; Jørgensen and Kasten 2005; Bianchi 2007).

The Hg content of Patos Lagoon sediments reported herein are comparable to background concentrations revealed in earlier investigations (Kütter *et al*. 2009; Mirlean *et al*. 2009; Quintana and Mirlean 2019), suggesting that these sediments are not contaminated by anthropogenic-sourced Hg. Instead, the distribution of Hg and Fe in the studied sediments is controlled by the presence of fine grain sediments and TRIS (Fig. 5). In fine grained estuarine sediments subjected to reducing conditions the dissolved Fe present in pore waters will react with dissolved S(-II), ultimately forming pyrite (FeS_2), a highly stable metallic sulfide. Other Fe sulfides of lower stability such as greigite (Fe_3S_4) and mackinawite (FeS) are also likely to occur, especially prior to stabilization of pyrite in the sediments. Pyrite also can be formed by reaction between mackinawite and

polysulfides ion and is, by far, the most abundant metal sulfide in estuarine sediments (Winfrey 1988; Jørgensen and Kasten 2005; Rickard and Luther 2007). Thus, it is likely that the TRIS compounds observed in the Patos Estuary sediments chiefly consist of FeS_2 and other dissolved polysulfides ions that are stable at neutral to slightly alkaline conditions such as HS_2^-, HS_3^-, HS_4^- , HS_5^- and H_2S_2 (Rickard and Luther 2007). Mercuric ion can be immobilized by iron sulfide (FeS) particles through adsorption or co-precipitation (Morse and Luther 1999; Jeong *et al*. 2007). Iron sulfide has also been shown to exchange its Fe^{+2} with Hg^{+2} to form HgS (Morse and Luther 1999; Svensson *et al*. 2006), which is extremely stable in the environment (Barnett *et al.* 2001). Furthermore, Hg can strongly complex with reduced sulfur groups in sediment organic matter, and the high affinity of Hg for S predominates even in oxic environments (Wolfenden *et al*. 2005; Skyllberg *et al*. 2006). Thus, in estuarine sediments where metal sulfides like mackinawite and pyrite are actively forming, such as appears to be the case in the studied Patos Lagoon sediments, similar spatial distributions of Hg and Fe as a function of depth within the sediment profile are expected (Fig. 4).

Total reducible inorganic sulfide contents of the Patos Lagoon sediment cores are also controlled by the sediment grain size in a similar fashion to both OC and metal (i.e., Hg and Fe) contents (Figs. 3 and 4, Tables 2 and 3). As noted above, the silt and clay sized fractions of the Patos Lagoon sediments are enriched in OC and metals in comparison to coarser sediments owing to the greater specific surface areas of the fine grained sediments (Rojas and Silva 2005; Álvarez-Iglesias and Rubio 2012). Accordingly, the OC associated with the fine-grained sediments serves as the substrate for bacterial respiration of oxygen and sulfate ions, which increases the concentrations and availability of ΣS^{-II} in the pore waters. The simultaneous availability of ΣS^{-II} and dissolved metals in these pore waters is subsequently responsible for the formation of TRIS in the fine grain sediments of Patos Estuary (Fig. 4). The PCA demonstrates associations between Hg, Fe, OC, TRIS, ΣS^{-II}, and fine grain sediments (< 63 μm) in the Patos Lagoon sediments, supporting the notion that sediment grain size exerts important controls over the distribution of these parameters in Patos Lagoon sediments (Fig. 5; Table 2). The PCA also suggests that other processes not necessarily related to metal sulfide mineral precipitation or sorption by organic matter coatings on fine grained sediments may also be of importance in controlling the contents of Hg in Patos Lagoon sediments. We suggest that these other processes may include adsorption of Hg onto Fe(III)/Mn(IV) oxides/oxyhydroxides which precipitate under oxidizing conditions, and

are common in the shallower estuarine sediments (Forstner and Wittmann 1979; Forstner and Salomons 1984; Winfrey 1988; Bonnissel-Gissinger et al. 1999; L. Costa et al. 2019). Nevertheless, taking into consideration that the studied sediments are chiefly subjected to reducing conditions (Fig. 2), adsorption of Hg onto Fe(III)/Mn(IV) oxides/oxyhydroxides is likely to be of relatively minor importance in the Patos Lagoon sediment cores, especially at depths in these cores.

The three sample coring locations were specifically chosen because they are located within non-dredged areas along the left bank of the estuary (Fig. 1). Consequently, the sediment grain size distributions within each core are likely the result of natural hydrodynamic variations that occurred within the estuary. Again, the natural hydrodynamics of Patos Estuary is controlled by seasonal changes of the wind direction and by river discharge intensity (Moller *et al.* 1996; Moller *et al*. 2001). That said, anthropogenic activities over the past 200 years have clearly impacted the estuary. For example, dredging machines were used in 1815 to deepen and subsequently maintain the first artificial navigation channels within the estuary (Saint-Hilaire 1820; Dreys 1827). The dredging activities were increased since 1832, and in 1849 the infrastructure for the port was begun, which included deepening the navigation channels.

In 1915 a massive naval engineering work was carried with the aim of stabilizing the main navigation channel of the port (Fig. 1) through the construction of two large stone jetties at the inlet of the estuary (Pimentel 1944; Cesar 2015). The construction of these jetties forever changed the morphology of the bottom sediments at the mouth of the lagoon (Antiqueira and Calliari 2005). Channel deepening and maintenance dredging activities became more frequent in the second half of the twentieth century with the further development and modernizing of the port (Cesar 2015). It is highly likely that effects of these anthropogenic alterations of the estuary, especially the dredging of the main navigation channel (Fig.1), has increased the natural estuarine hydrodynamic regime, leading to the deposition of coarser sediments in the most recent (superficial) layers of the CP and NP cores (Fig. 3). In contrast, the “protected” nature of the SP core sampling location within a shallow cove off the chief navigation channel in the Patos Estuary (Fig. 1), can explain the differences in grain size, TRIS, OC, and metal contents compared to the CP and NP cores. The SP core appears to be largely isolated from the anthropogenic hydrodynamic changes in the estuary that have affected the shallower sediments from the CP and NP core locations. This is because the hydrodynamic energy tends to be lower in coves and bays (Forstner and Wittmann 1979; Winfrey 1988;

Antiqueira and Calliari 2005), favoring the sedimentation of fine grained particles such as observed in the shallower sediments at the SP location (Table 1; Fig. 3).

The ANOVA test revealed that < 63μm particles mean content in SP sediment is superior to those found in CP and NP (Table 4), reinforcing the importance of the low hydrodynamic energy at the southern sampling point. Moreover, the proximity of SP to the ocean stimulates the flocculation of silt and clay in suspension within the water column to the bottom sediment due high concentration of dissolved salts in the water (Postma 1967; Aston and Chester 1976; Burton 1976). CP and NP sediments, however, are exposed to anthropogenic alterations that probably increased the natural hydrodynamic energy of the estuary, also, contrarily to SP, these sites are further from the ocean (Fig. 1).

ANOVA test also showed that CP mean concentrations of ΣS^{-II} were much superior to those found in SP and NP (Table 4), most probably due Eh of sediment and availability of sulfate in pore water. Theoretically, SP is able to receive large apports of sulfate due its proximity to the ocean, however, brackish water from Patos Estuary tends to be supersaturated in oxygen (Windom *et al.* 1999), provoking more oxidizing conditions in SP sediment in comparison to CP and NP (Table 1). These redox conditions are not favorable for sulfate reduction, causing the decrease of ΣS^{-II} in SP. Otherwise, NP is the sampling point furthest from the ocean, which collaborate to a lower sulfate apport at this site, limiting the sulfate reduction process. CP sediment profile presents more reducing conditions in comparison to SP, specially below 15 cm of depth (Fig. 2), and probably receives considerable apport of sulfate due its proximity to the ocean (Fig. 1), favoring the intensification of sulfate reduction process and subsequent increase in ΣS^{-II} concentration.

Conclusion

The current study revealed that Hg immobilization in sediments of the Patos Estuary occurs as a consequence of the synergic effect of geochemical processes mainly controlled by fine grain sediments distribution. Mercury, Fe, organic carbon (OC), and total reducible inorganic sulfide (TRIS) were statistically correlated to the silt and clay contents (i.e., < 63 μm) of local estuarine sediments. Fine grain sediments exhibited elevated contents of OC, Fe, and Hg in comparison to coarser sediments, which likely

reflects the predominance of organic coatings on the reactive surfaces of the fine grained sediments. The organic matter also served as the substrate for oxygen and sulfate respiring bacteria that consequently led to an increase in the availability of dissolved sulfide in the associated sediment pore waters, and the formation of metal sulfides like pyrite. The immobilization of Hg in the Patos Estuary sediments likely reflects the combination of adsorption on fine particles coated with organic matter as well as incorporation in precipitating metal sulfide minerals such as pyrite. Despite the presence of port-industrial facilities along the right bank of the estuary, we observed no obvious evidence that related anthropogenic activities have impacted the Hg content of sediments from the left back of the estuary. We suggest that our data and observations are consistent with the artificial navigation channel of the local port acting as a hydrodynamic barrier, limiting the transport of contaminated sediments from Rio Grande city on the right bank of the estuary to the more "pristine" left bank of Patos Estuary.

Acknowledgments

We are grateful to the Coordination of Improvement of Higher Level Personnel of Brazilian government (CAPES) by grant of scholarship.

CAPÍTULO IV: Pattern of mercury distribution in sediments from an irregular hydrological regime estuary

Abstract

Patos Estuary, in southern Brazil, is subject to an irregular hydrological regime (i.e., fresh water dominated and brackish water dominated) and receives mercury (Hg) contaminated effluents from the city of Rio Grande since the colonial period of southern Brazil. Four sediment cores were collected during two distinct hydrological regimes (i.e., fresh water dominated and salt water dominated), two at a shallow area (SA) and two at a salt marsh (SM). For shallow area sediments, redox conditions are relatively stable during both sampling periods. Mercury distribution in shallow area sediments is statistically correlated with fine grain particles (i.e., <63 μm) and free dissolved sulfide (ΣS^{-II}). For salt marsh sediments, bioturbation caused by burrow crabs and native vegetation promotes oxygen penetration and subsequent acidification of pore water associated with superficial sediment layers. Such oxidizing conditions hampers sulfate reduction and, thereafter, formation of metal sulfide. Mercury distribution in salt marsh sediments is statistically correlated only to fine grain sediment contents, indicating that adsorption/incorporation of mercury into iron sulfide is of minor importance in salt marsh sediments.

Key-words: Mercury distribution, Sediments, Irregular hydrological regime, Sulfate reduction, Bioturbation

Introduction

Mercury distribution within estuaries is a concern because those environments provide unique habitats for a number of species, and they are also frequently used for commercial and recreational fishing and harbor activities. These coastal ecosystems often lie in close proximity to major urban areas, so they may be strongly affected by human activities. Mercury is considered a hazardous metal, due its toxicity and lethality (Who 2003). Its distribution in marine and estuarine sediments is strongly conditioned by early diagenesis processes such as sulfate reduction, metal sulfide formation (Forstner and Wittmann 1979; Forstner and Salomons 1984; Winfrey 1988) and iron oxyhydroxides formation (Bonnissel-Gissinger et al. 1999). Such processes were highlighted in estuarine environments and have been considered important mechanisms for metal accumulation in sediments (Benoit et al. 1998; Han et al. 2008). Estuaries are known as transitional environments where mixing of marine and continental waters occurs (Windom et al. 1999), leading to abundance of metals, sulfate ion, and organic matter, which facilitates sulfate reduction and, consequently, metal sulfide formation in bottom sediments (Jørgensen and Kasten 2005).

Sulfide distribution in sediments is chiefly controlled by sulfate-reducing bacteria activity (Vairavamurthy et al. 1995; Bianchi 2007). The intensity of bacterial activity is attributable to the variation in quantity and quality of organic matter, sulfate-reducing bacteria abundance, temperature, and sulfate availability (Kristensen et al. 1992; Zhang et al. 2013). The reliance of the sulfate reduction rate on sulfate availability was demonstrated in the vertical profiles of sulfate reduction rates in marine sediments: the sulfate reduction rate decreases downward where sulfate is limited (Leloup et al. 2007). Sulfate reduction rate in low-salinity sediments (i.e., estuary sediments) could be as high as that in high-salinity sediments, despite low sulfate availability and a smaller sulfate-reducing bacteria density, because of the availability of labile organic matter (Pallud and Van Cappellen 2006).

In Patos Estuary, southern Brazil, recent studies revealed that the sulfate reduction process in salt marsh sediments is strongly controlled by the local irregular hydrological regime (Mirlean and Costa 2017) and by biological disturbances caused by burrow crabs and native vegetation roots (Mirlean and Costa 2017; L. Costa et al. 2019). The hydrological regime of this estuary is controlled by winds and by river discharge (Moller *et al*. 2001). Southwest winds, which blow during the rainy season, promote the entrance of marine waters into the estuary, whereas northeast winds, which blow during the dry

season, enhance the river discharge (Moller *et al*. 1996). The irregular hydrological regime of Patos estuary enable prolonged residence times of brackish water during summer/fall and fresh water during winter/spring (Moller et al. 1996; Moller et al. 2001). Windom et al. (1999) demonstrated that the dissolved oxygen (DO) rates in the water column from Patos Estuary vary from saturated during winter/spring (i.e. fresh water period) to supersaturated during summer/fall (i.e. brackish water period). Furthermore, the water level from Patos Estuary is also altered by its irregular hydrological regime. The hydrologic pattern shows marked variations from high water levels during the fresh water period to low water levels during the brackish water period (Costa et al. 2003; Vaz et al. 2006; Möller et al. 2009).

Assuming the premise that variations in the hydrological regime influence water level (low at the dry season and high during the rainy season) and the DO availability in the estuary, causing subsequent changes in the redox conditions of the bottom sediments from shallow areas and from salt marshes within Patos Estuary. The objetive of the present work is to study sulfate reduction effects over Hg distribution in Patos Estuary sediments from a non vegetated shallow area and from a highly vegetated salt marsh during two distinct hydrological regimes (i.e., fresh water dominated and brackish water dominated).

Study area

Patos Estuary is the largest estuary of the south of Brazil with a surface area of approximately 900 km^2 (Kjerfve 1994), and receives contaminated effluents from Rio Grande city since the eighteenth century (Quintana and Mirlean 2019). Moreover, Patos Estuary harbors the second largest port in Brazil (i.e., the port of Rio Grande) with regards to amounts of cargo handled (Fig. 1). Patos Estuary is a microtidal system (i.e., < 0.5 m tidal range) with seasonal salinity variations whereby low salinities (maximum of 5 gL^{-1} of dissolved salts) dominate the system during the winter/spring (i.e., rainy season) and high salinities (20–30 gL^{-1} of dissolved salts) dominate during the summer/fall (i.e., dry season; Moller et al. 1996).

The southern Patos Estuary has over 7000 ha of salt marshes where *Spartina alterniflora* and *S. densiflora* constitute the dominant native vegetation (Costa et al.

2003). The Burrow crab (*Neohelice granulata*) is the main animal species that inhabit the salt marshes from Polvora Island (i.e., a small island located within Patos Estuary). The activities of these crustaceans promote significant alterations on physical and chemical aspects of the sediments (Costa et al. 2019). The burrow crabs excavate semi-permanent burrows, removing and redistributing considerable amounts of sediment during feeding and burrow maintenance (Iribarne et al. 2000).

Hg enriched urban effluents from Rio Grande city (i.e., a 200,000 inhabitants city located in the right bank of the estuary; Fig 1) contaminate the Patos Estuary bottom sediments (Mirlean *et al.* 2003). Urban soils from modern and ancient landfills used to build new land for the city growth are strongly contaminated by Hg (Mirlean and Oliveira 2006). High concentrations of Hg (i.e., up to 27 mg kg^{-1}) occur in both the oldest part of the city, occupied since the eighteenth century, and in more recently embanked areas, occupied since the nineteenth and twentieth centuries (Fragomeni et al. 2010; Quintana and Mirlean 2018). Hg contamination also was revealed in urban groundwater (Quintana and Mirlean 2018). Recently, a study proved that the onset of Hg contamination in Rio Grande can be dated to the eighteenth century (Quintana and Mirlean 2019).

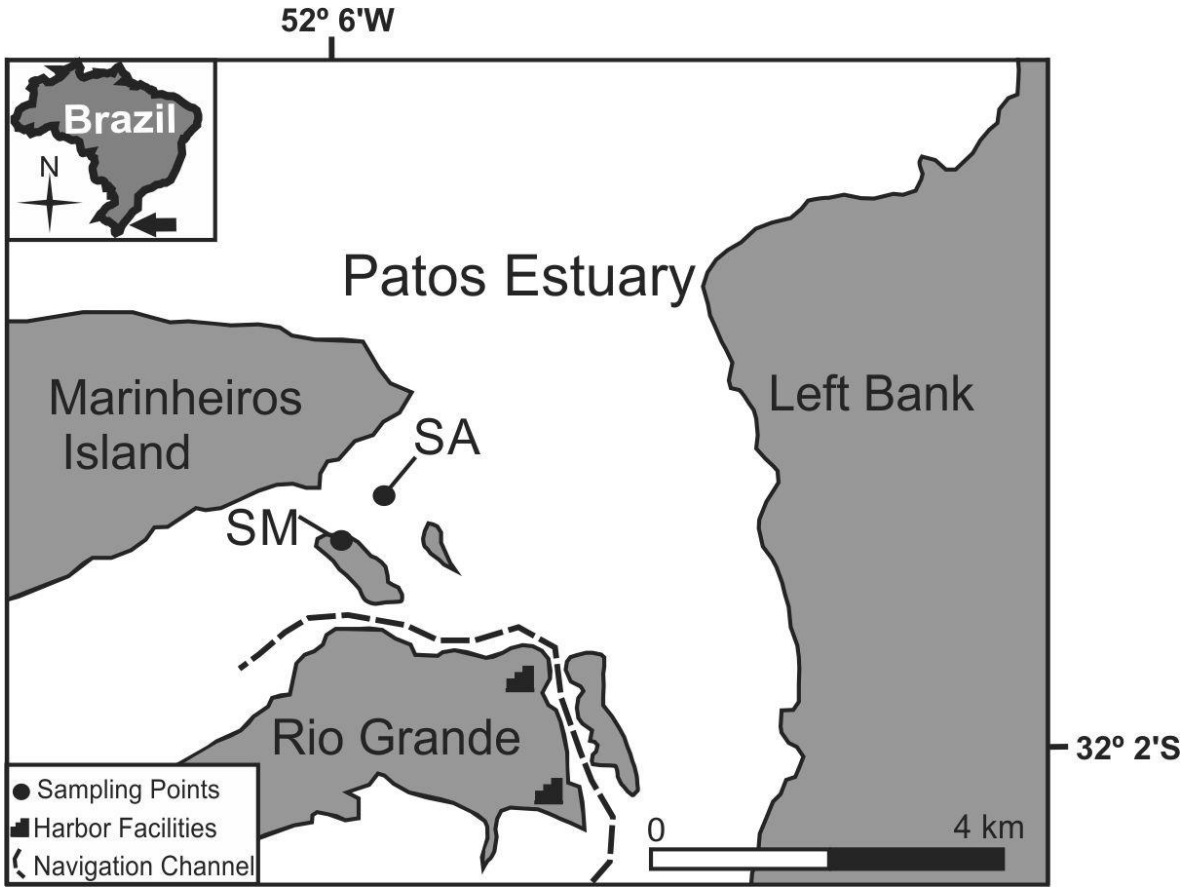

Figure 1. Sampling points location (SA and SM).

Materials and methods

Two sediment cores were collected in two different hydrological regimes (i.e., fresh water period and brackish water period) from two sampling points (i.e., open shallow area and salt marsh) located in the central portion of Patos Estuary (Fig. 1). In total, four sediment cores were collected. In September 2016, when the estuary was dominated by river discharge (i.e., fresh water period), the first two cores were collected respectively in an open shallow area (SA) close to Marinheiros Island and in a salt marsh (SM) within Polvora Island (Fig. 1). In April 2017, corresponding to marine waters entrance period (i.e., brackish water period), two sediment cores were collected in the same locations.

Pre-cleaned acrylic tubes (8 cm in diameter and 53 cm length) were used for sampling. Then, each core was hermetically sealed, transported to the laboratory and stored cold (4°C) for 12 hours before physicochemical measurements and subsamples separation. The cores were opened and split longitudinally into two halves followed by sectioning at 2 cm intervals along the length of each half of the four cores. The various subsamples were subsequently measured for redox potential (Eh), pH and free dissolved sulfide (i.e., ΣS^{-II}) concentrations in the pore waters (e.g., Costa et al., 2019). Separate aliquots of each 2 cm sediment subsample were then analyzed for Hg, Fe, and organic carbon (OC) contents.

Eh was measured on the freshly exposed surface of the sediment cores using a naked Pt-electrode (Analion®). The pH was measured in filtered (0.45 µm Milipore® membrane) interstitial pore waters extracted from the sediment subsamples by centrifugation (3000 rpm). The determination of ΣS^{-II} in the interstitial pore water was performed using a silver/sulfide combination ion selective electrode (model Hanna® 9616 BNC) coupled to an Orion™ ISE/pH/mV/Eh/temperature meter (model 209a; Brooks 2001). A basic antioxidant solution for sulfides (Sulfide Antioxidant Buffer - SAOB, Hanna Intruments®) and a sulfide standard ($Na_2S.9H_2O$) were previously made and used for calibration of the ion selective electrode. The electrode was calibrated after every 12 readings from a three-point calibration curve (100, 1000, 10000 µmol L^{-1}). The

fine grain sediments (<63 μm), composed of silt and clay according to Wentworth's classification, were recovered from subsamples using standard sieve methods (ASTM C136/C136M).

The acid digestion of homogenized sediment subsamples was carried out according to EPA method 7471 for Hg determination (USEPA 1998). A cold vapor system, coupled to an AAS GBS 932, was used for Hg measurements. Each sample was analyzed in triplicate; RSD of the three measurements of Hg did not exceed 5%. A certified reference material, MESS-3 sample (NRCC 2004), was included with the analyzed samples for quality control measurement. The recovery of reference samples was in the 91% confidence limits for the CRM.

Fe was extracted from the samples following the EPA method 3050B (USEPA 1996). The extracted solutions were diluted by a factor of 1:400 (v/v) and measured by UV/VIS spectrophotometry using a DR 2800 Spectrophotometer from Hach Company®, method 8008 – FerroVer® Method (HACH, 2007). Spiked duplicate samples were processed on a routine basis (5% of each sampling point), with RSD < 5%. The quality control of Fe analysis was ensured by the extraction and quantification of certified reference material MESS-4. The precision of the reference samples was always within 5% of the suggested values for Fe. Reported concentrations for the samples were blank subtracted.

Organic carbon (OC) content of the sediment samples was determined on dried sediments samples (30 mg) by using a TOC - VCPH, model SSM - 5000A, Shimadzu® with combustion detector. OC results are presented in percentage of organic carbon in dried sediment, and RSD was < 5 % for triplicate analyses.

Taking into consideration the short time between the sampling periods, OC, fine grain sediment, Hg and Fe contents found during the fresh water period were considered conservative for both sampling periods. Data were compared by statistical analysis (principal component analysis and Spearman correlation coefficient).

Results

Shallow area

Mean Eh values in SA during the fresh water period were -189 ± 115 mV and -177 ± 120 mV during the brackish water period, furthermore the Eh vertical distribution was similar in both sampling periods (Fig. 2), presenting a clear downward decrease trend, reaching -350 mV (51 cm of depth) during brackish water period and -366 mV (51 cm of depth) during fresh water period (Table 1). Mean conductivity was much higher for the brackish water period (36.4 ± 5.7) in comparison to that of the fresh water period (15.9 ± 3.9 mS cm^{-1}; Table 1). The pH values were relatively stable considering both sampling periods, ranging from 6.9 to 8.2 during the fresh water period and 7.3 to 7.8 during the brackish water period (Table 1).

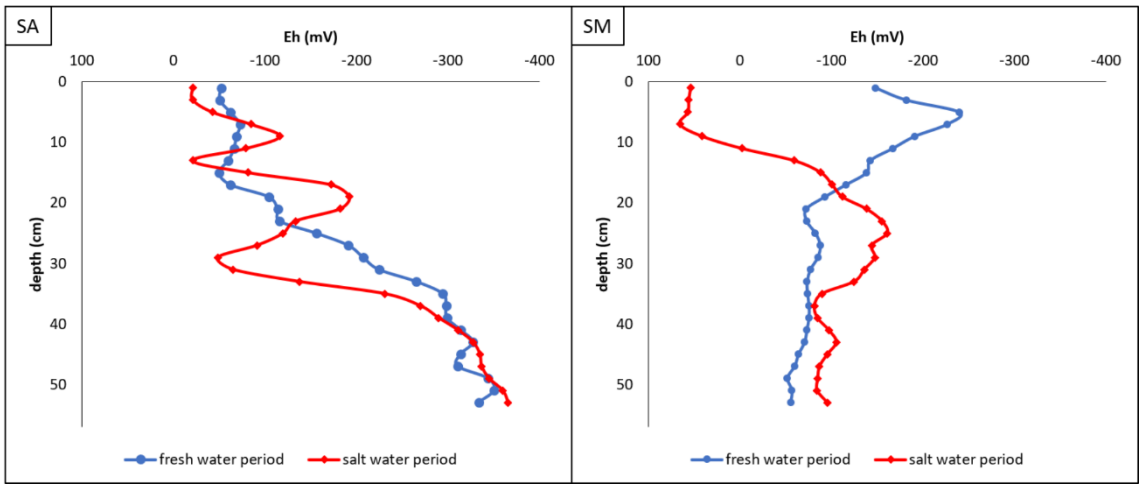

Figure 2. Redox potential (Eh) vertical distribution for sites SA and SM.

Table 1. Geochemical parameters for samples location, SA and SM, during both hydrological regimes (i.e., fresh water period and brackish water period). The upper numbers are the concentration range, and the mean ± SD for the entire core is presented within parentheses.

Parameter	SA (fresh water)	SA (brackish water)	SM (brackish water)	SM (salt water)
Eh (mV)	- 350 – -50 (-189 ± 115)	- 366 – -21 (-177 ± 120)	- 240 – -51 (-105 ± 54)	- 161 – 65 (-74 ± 70)
Conductivity (mS cm^{-1})	10.3 – 21.2 (15.9 ± 3.9)	29.9 – 51.9 (36.4 ± 5.7)	8.6 – 20.4 (14.5 ± 3.5)	24.7 – 28.6 (26.6 ± 1)
pH	6.8 – 8.2 (7.7 ± 0.4)	7.3 – 7.8 (7.6 ± 0.1)	7 – 8 (7.6 ± 0.3)	6.1 – 7.6 (7 ± 0.4)

OC (%)	0.26 – 1.1 (0.51 ± 0.29)	*	0.26 – 4.85 (1.12 ± 1.26)	*
<63 µm (%)	13 – 50.6 (28 ± 13.8)	*	14.7 – 56.3 (33.7 ± 12.9)	*
Hg (µg kg^{-1})	7.6 – 36.6 (19.6 ± 10.8)	*	2.8 – 23 (14 ± 7)	*
Fe (%)	1.35 – 2.82 (1.92 ± 0.45)	*	1.23 – 2.37 (1.76 ± 0.33)	*
ΣS^{-II} (µmol L^{-1})	11.2 – 703.6 (240.1 ± 255.4)	7.3 – 405.7 (135.5 ± 122.6)	7.3 – 45.6 (19.4 ± 11.8)	6.1 – 15.7 (9.8 ± 2.5)

*conservative measurements (values from fresh water period)

The vertical distribution for OC and <63 µm particles (Fig. 3) was similar and statistically correlated ($r^2 = 0.83$, $p < 0.01$, $n = 54$), most probably due to organic coating of fine grain sediments (Winfrey 1988). In general, the higher contents of OC and <63 µm particles occurred in deep sedimentary layers, beneath 30 cm depth (Fig. 3). Mean contents for both parameters were 0.51 ± 29 % for OC and 28 ± 13.8 % for <63 µm particles (Table 1). Metals (Hg and Fe) and ΣS^{-II} vertical distribution were similar ($r^2 = 0.85$, $p < 0.01$, $n = 54$ for Hg and ΣS^{-II}; $r^2 = 0.69$, $p < 0.01$, $n = 54$ for Fe and ΣS^{-II}) presenting a concentration increase downward in the sediment profile in both sampling periods (Fig. 4 and 5). The same trend was observed for OC and <63 µm sediment, suggesting a probable association between these parameters (Hg, Fe, ΣS^{-II} and OC). Hg concentrations found in SA were similar to background levels for Patos Estuary (10 - 40 µg kg^{-1}, according to Quintana and Mirlean 2019) and rather inferior to Hg contents revealed previously in superficial sediments of the navigation channel of the port of Rio Grande (5 mg kg^{-1}; Mirlean et al 2001) during an environmental disaster occurred in 1998, when a massive sulfuric acid leaking contaminated the estuary. Mean contents of ΣS^{-II} were superior during the fresh water period (240.1 ± 255.4 µmol L^{-1}) in comparison to the brackish water period (135.5 ± 122.6 µmol L^{-1}), indicating that the sulfate reduction process was more intense during the fresh water period (specially below 30 cm of depth).

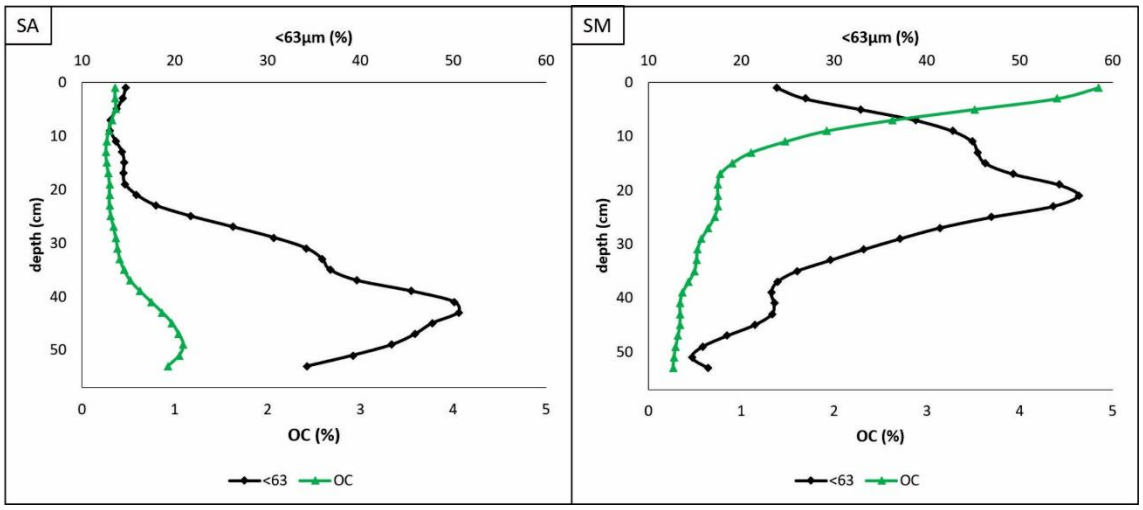

Figure 3. OC and fine grain (<63µm) vertical distribution for sites SA and SM.

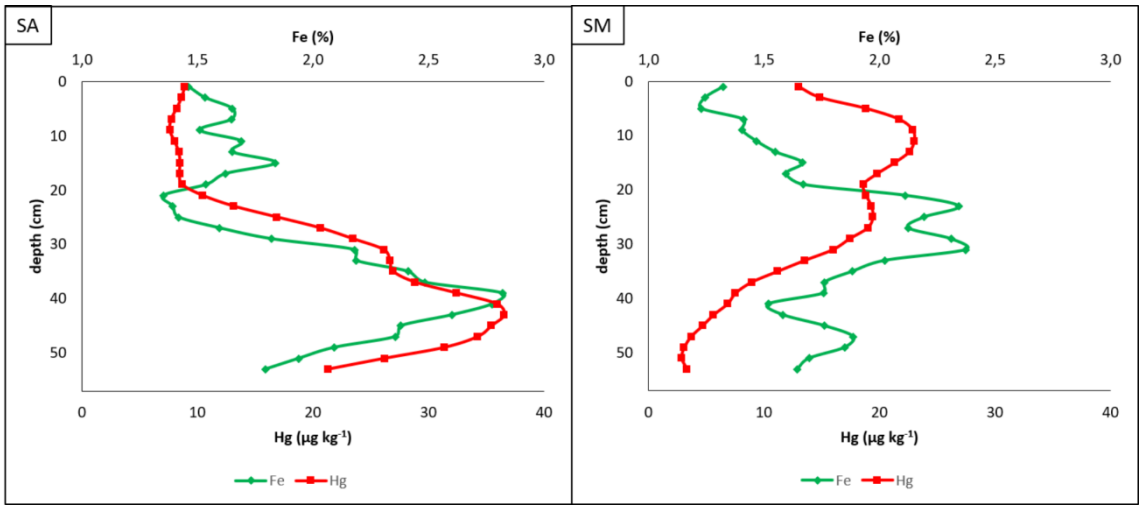

Figure 4. Hg and Fe vertical distribution for sites SA and SM.

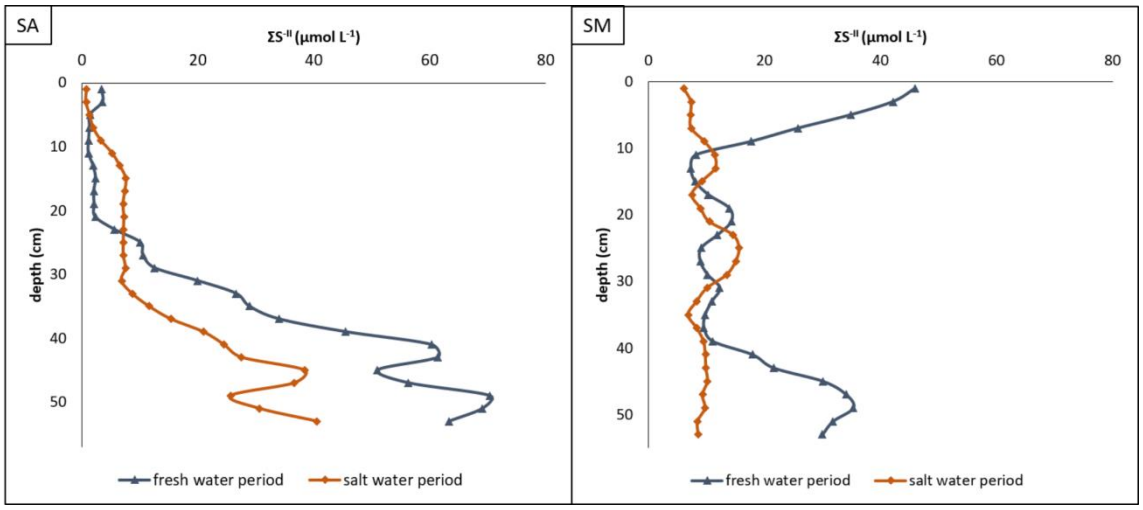

Figure 5. ΣS^{-II} vertical distribution for sites SA and SM.

Salt marsh

Mean Eh values in SM were -105 ± 54 mV during the fresh water period and -74 ± 70 mV during the brackish water period (Table 1). However, the most significant Eh variations were observed in the first 20 cm (Fig. 2) of the profile for both sampling periods; below this depth measurements were relatively stable. As well as was observed for SA, the mean conductivity in SM pore water was much higher during the brackish water period (26.6 ± 1 mS cm^{-1}) in comparison to that of the the fresh water period (14.5 ± 3.5 mS cm^{-1}; Table 1), corroborating the irregular regime of Patos Estuary. In general, pH values in pore water during the brackish water period (6.1 to 7.6) were lower than those found during the fresh water period (7 to 8; Table 1), furthermore, pH vertical distribution was different during both sampling periods, especially in the first 20 cm (Fig. 6). During the brackish water period the pH varied from 6.1 to 7 in the most superficial interstitial waters (1 to 15 cm), below, the pH was relatively stable, ranging from 7 to 7.6. A different vertical distribution occurred during the fresh water period with pH measurements ranging from 7 to 7.6 in the first 15 cm (Fig. 6) and, below, an oscillatory distribution was observed ranging from 7.4 to 8.

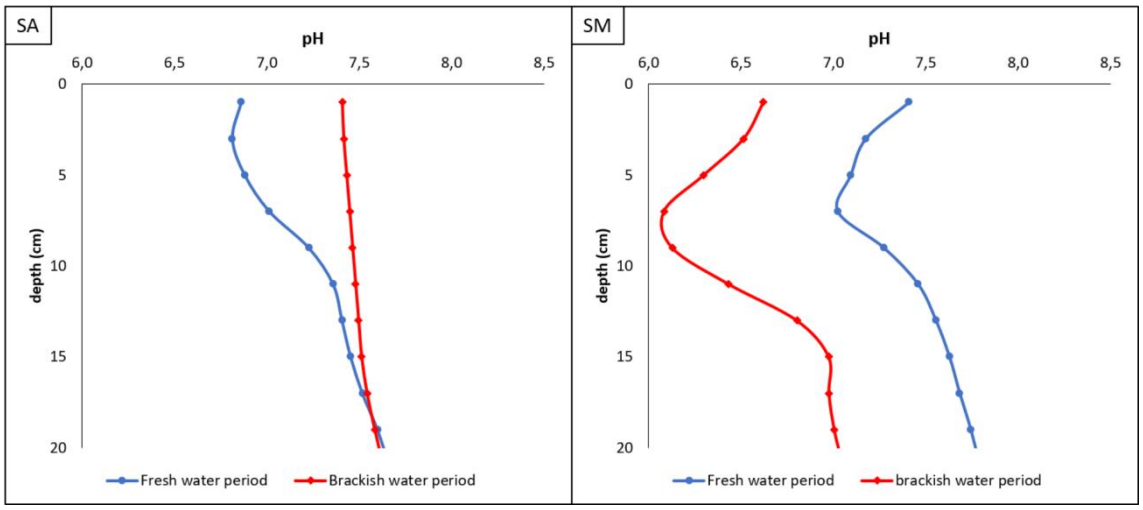

Figure 6. pH vertical distribution for sites SA and SM.

There was a decrease trend of OC contents downward up to 53 cm (Fig. 3) and the mean concentrations were 1.12 ± 1.26 % (Table 1), much superior than those found for SA sediments. The vertical distribution of <63 μm particles was different, showing an increase trend down to 21 cm of the profile, and, below, a decrease trend downward (Fig. 4). Vertical distribution of Hg and <63 μm particles (Fig. 3 and 4) were very similar (r^2 = 0.87, $p < 0.01$, n = 54), indicating the grain size control over the Hg distribution. In comparison, Fe distribution was rather different (Fig. 4), suggesting that Hg and Fe distribution were controlled by different geochemical processes. Mean concentrations for Hg and Fe were 14 ± 7 μg kg^{-1} and 1.76 ± 0.33 %, respectively. These contents were slightly inferior to those found for SA sediments (Table 1). The ΣS^{-II} vertical distribution was rather different for both sampling periods (Fig. 5) and very inferior to those found in SA pore water (Table 1). Furthermore, the mean contents of ΣS^{-II} were superior during the fresh water period (19.4 ± 11.8 μmol L^{-1}) in comparison to those of the brackish water period (9.8 ± 2.5 μmol L^{-1}; Table 1), suggesting that the sulfate reduction process intensity was different during both sampling periods.

Principal component analysis

The multivariate statistics of principal component analysis (PCA) was used to better understand relationships among metals (Hg and Fe), ΣS^{-II}, fine grain sediments (<63 μm), and OC contents of the sediment cores. Considering both sampling periods for

SA (n = 54, the PCA enabled us to distinguish two groups of variables based on two principal components that, together, explained 97.72% of the total variance of the data. Principal component 1 represented 85.85% of the data variance and was represented by all variables used for the PCA analysis (Hg, Fe, ΣS^{-II}, fine sediments and OC; Fig. 7; Table 2). This component is clearly related to the grain size control over the distribution of the studied variables. Principal component 2 explained 10.87% of the data variance and probably represents secondary mechanisms of metals immobilization in the sediments of SA.

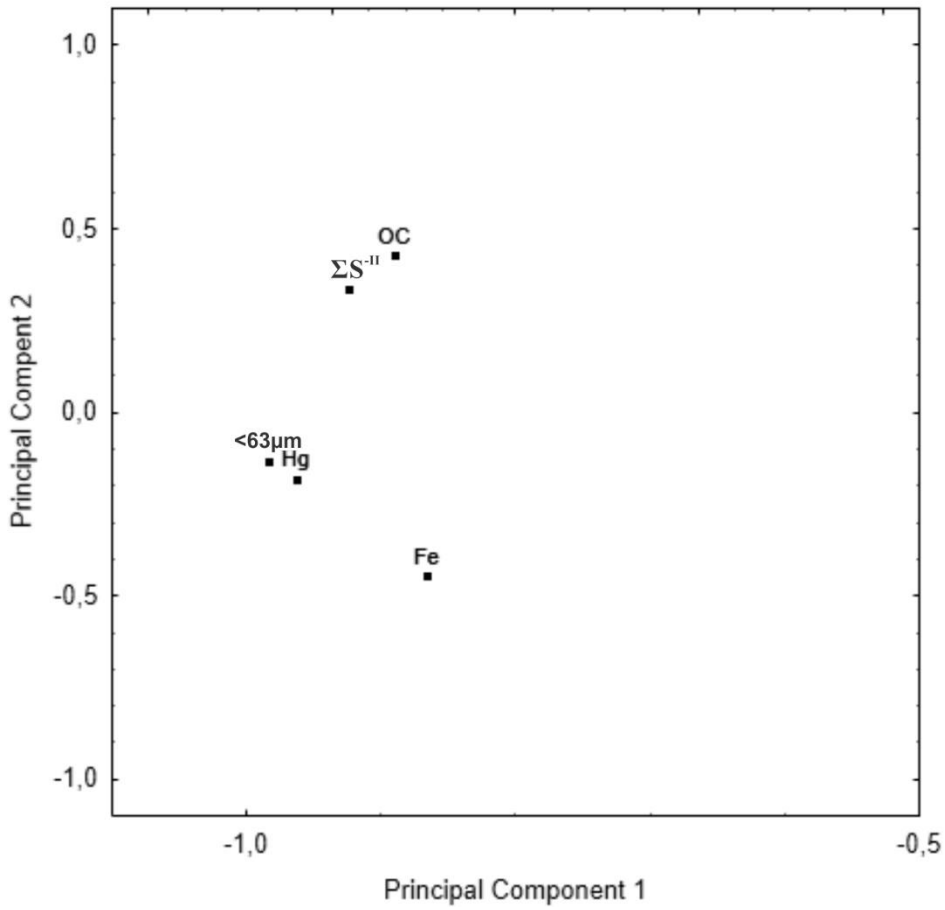

Figure 7. PCA plots (SA sampling point) for the two first principal components (self-staggered data), using Hg, Fe, TRIS, ΣS^{-II}, fine grain sediments (<63µm) and OC

Table 2. Variable loads for the two first principal components (self-staggered data), using OC, <63 µm, Hg, Fe and FS results from SA.

Variable	OC	<63 µm	Hg	Fe	ΣS^{-II}
Principal Component 1	-0,89	-0,98	-0,96	-0,86	-0,92
Principal Component 2	0,43	-0,13	-0,18	-0,45	0,33

Considering both sampling periods for SM (n = 54), two groups of variables were distinguish based on two principal components that explained 72.3% of the total variance of the data. Principal component 1 represented 39.66% of the data variance and was better represented by Hg and <63 µm particles (Fig. 8; Table 3), suggesting that fine sediments are controlling the distribution of Hg in SM sediments. Principal component 2 represented 32.64% of the data variance and was better represented by OC (positive load) and Fe (negative load), indicating that there are important secondary processes responsible for Fe immobilization and OC vertical distribution in SM sediments (Fig. 8; Table 3).

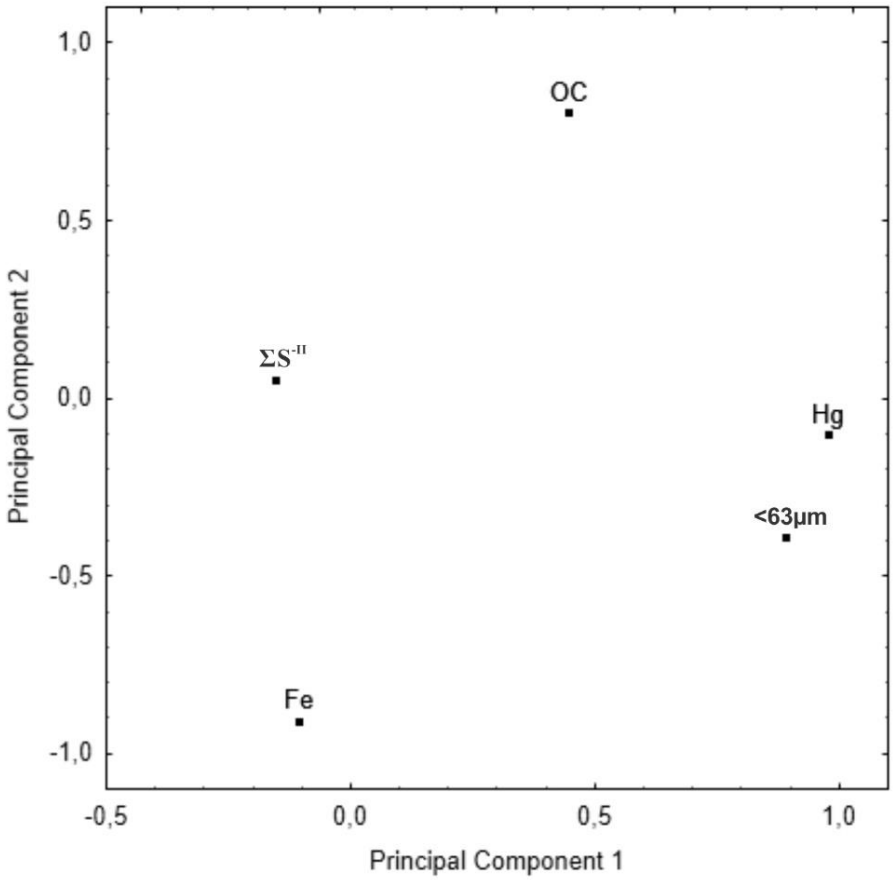

Figure 8. PCA plots (SM sampling point) for the two first principal components (self-staggered data), using Hg, Fe, TRIS, ΣS^{-II}, fine grain sediments (<63µm) and OC

Table 3. Variable loads for the two first principal components (self-staggered data), using OC, <63 µm, Hg, Fe and FS results from SM.

Variable	OC	<63 µm	Hg	Fe	ΣS^{-II}
Principal Component 1	0,45	0,89	0,98	-0,11	-0,15
Principal Component 2	0,80	-0,39	-0,10	-0,91	0,05

Discussion

pH and conductivity

The conductivity of pore water from SA directly reflected the irregular regime of Patos Estuary, since the values from this sampling point were much superior during the brackish water period (Table 1). Strong pH variations of pore water occurred in the first 20 cm depth of the profile. During the fresh water period, the pH of superficial pore water (i.e., 0 – 10 cm) was inferior to that found during the brackish water period (Fig. 6). It was a probable consequence of alkaline marine water diffusion to the sediments during the brackish water period and, in contrast, the diffusion of fresh water of continental origin leaded to a decrease of the pH of superficial pore water during the fresh water period.

Mean conductivity in SM pore water was inferior to that found at SA, especially during the brackish water period (Table 1), which is a probable consequence of the hypsometric level of these sampling points. The salt marsh from Polvora Island can be eventually exposed to subaerial conditions during the brackish water periods (i.e., dry season) since it is located on an intertidal mudflat 15 - 25 cm below the mean water level of Patos Estuary, preventing the continuous diffusion of brackish water to the sediments and enabling the diffusion of air to the sediments (Mirlean and Costa 2017). The salt marsh superficial sediment can also be exposed to rain water during subaerial exposition periods, contributing to the lower conductivity found in this sampling point.

The pH vertical distribution on porewater was similar in SM during both sampling periods, showing a strong decrease in the first 15 cm of the profile; however the mean pH

measurements were considerably inferior during the brackish water period (Table 1; Fig. 6). The acidification of superficial pore waters from Polvora Island was related to oxidation of insoluble iron sulfides due to brackish water diffusion to sediment, to biological disturbances and/or exposition to subaerial conditions eventually, liberating dissolved sulfides to pore water and enabling the subsequent formation of sulfuric acid (Mirlean and Costa 2017). Similar acidification was described for salt marsh sediments as a consequence of the oxidation of both iron sulfides and amines, enabling the formation of sulfuric and nitric acids, respectively (Liu et al. 2008). Such processes are probably responsible for the acidification of superficial pore waters at SM, especially during the brackish water period (Fig. 6).

Redox Potential of SA and SM sediments

Previous studies (Windom et al. 1999) proved that dissolved oxygen in Patos Estuary water column varies from saturated conditions at low salinity to supersaturated at high salinity, which explains, in part, the most oxidizing conditions presented in SA during the brackish water period (Table 1), mainly in the most superficial layers of the profile (Fig. 2). The most reducing conditions occurred in fine sediment horizons within SA profile (Fig. 2 and 3). Moreover, distributions of OC and <63 μm particles were very similar in SA sediments (Fig. 3), supporting the correlation of these parameters (Fig. 7 Table 2).

Eh vertical distribution in SM was rather different than that observed in SA, especially in the most superficial sediment layers, most probably because of the bioturbation caused by burrow crabs (i.e., *Neohelice granulata)* and native vegetation (i.e., *Spartina densiflora and Spartina alterniflora)* roots. Mean Eh values in SM were considerably superior to those of SA sediments (Table 1). Bioturbation caused by burrow crabs and roots of the vegetation were pointed as important oxidizing mechanisms for the sediments from these salt marshes (Costa et al. 2017; Mirlean and Costa 2017; L. Costa et al. 2019). Furthermore, SM is located in higher ground (15 - 25 cm below the mean water level of Patos Estuary) in comparison to SA (100 – 150 cm below the mean water of the estuary), therefore its superficial sediments can be eventually exposed to subaerial conditions, especially during brackish water periods, when the water level is lower due

the dry season period (Mirlean and Costa 2017), contributing to the elevated Eh values mainly in superficial sediment layers (0 - 20 cm; Fig. 2).

Organic Carbon and fine sediment distribution

The PCA analysis proved the statistical correlation of OC and fine grain sediments in SA (Fig. 7; Table2), which is consistent with the general trend of occurrence of high contents of organic matter in fine grain sediments due to organic coating of fine particles. Silt and clay size particles are known to have larger specific surface areas in comparison to sandy sediments, since the area/volume ratio of fine grain sediments is larger than that of these coarser grain materials. The surface of fine grain sediment particles tends to be coated by a film of organic material (Winfrey 1988; Rojas and Silva 2005; Álvarez-Iglesias and Rubio 2012). The organic matter film present in fine sediments serves as a substrate for bacterial activity, promoting oxygen consumption and subsequent sulfate ion consumption, lowering the redox potential, and enhancing the concomitant production of dissolved sulfide ions (Berner 1984; Jørgensen and Kasten 2005; Bianchi 2007). Therefore, the statistical correlation between ΣS^{-II}, OC and fine grain sediments observed in SA (Fig. 7; Table 2) is a clear evidence of the grain size control over organic matter vertical distribution and the sulfate reduction process in SA sediments.

Fine grain distribution in SM was probably influenced by the remobilization of sediment promoted by *Neohelice Granulata*. These crabs constantly disturb and redistribute the sediment to construct vertical burrows of about 10 cm diameter and 1 m depth (Angeletti and Cervellini 2015) and its population density varies from 15 to 77 per m^2 in estuaries of southwestern Atlantic (Alberti et al. 2007; Martinetto et al. 2016). The redistribution of sediment provoked by such crabs has probably changed the natural stratigraphy of SM profile; besides, *Spartina Densiflora* patches are natural physical traps for suspended particles, promoting organic matter and sediments accumulation in salt marshes (Castillo et al. 2003). OC vertical distribution was also influenced by bioturbation. The highest contents of OC were found within *Spartina*'s rhizosphere (i.e., 0 – 15 cm of depth; Mirlean and Costa 2017), indicating that the main source of organic matter for SM sediments is the native vegetation itself. The decrease of OC contents downward (Fig. 3) is a probable consequence of organic matter consumption by bacteria.

Metals and free dissolved sulfide distribution

Metals (Hg and Fe) distributions in SA sediments were also statistically correlated with <63 µm particles, OC and ΣS^{-II} (Fig. 7; Table 2.). Fe present in porewater tends to react with dissolved S^{-2}, forming mainly pyrite, which is the most abundant metal sulfide in estuarine sediments (Winfrey 1988; Jørgensen and Kasten 2005; Rickard and Luther 2007). The similar distributions of Fe, <63 µm particles, OC and ΣS^{-II} allowed us to presume that the formation of iron sulfide occurred in fine grain sediment horizons, where sulfate reduction is more intense. Moreover, mercury can also be adsorbed or coprecipitated with iron sulfide particles (Morse and Luther 1999; Jeong *et al*. 2007). Furthermore, Hg can be complexed with reduced sulfur groups present in sediment organic matter (Winfrey 1988). Thus, in undisturbed estuarine sediments where iron sulfides like mackinawite and pyrite are actively forming, similar distributions of Hg and Fe can be expected (Fig. 4).

Contrarily to SA, Fe vertical distribution in SM was not statistically related to fine grain sediments contents or to ΣS^{-II} (Fig. 8; Table 3). Previous studies revealed that Fe distribution in salt marshes sediments of Patos Estuary was associated with ferruginous incrustations and Fe oxyhydroxides nodules formation (Costa et al. 2017; Costa et al. 2019). Biological disturbances caused by vegetation and burrow crabs facilitate the penetration of oxygen to 25 – 35 cm depth in the sediment column of salt marshes from Polvora Island, creating propitious redox conditions to the formation of ferruginous incrustations (commonly formed in crab burrows walls) and nodules mainly composed by Fe and Mn oxyhydroxides (Costa et al. 2017; Costa et al. 2019). Nonetheless, bioturbation influence over redox conditions in SM sediments was not favorable for sulfate reduction process, since ΣS^{-II} concentrations were inferior to those found in SA porewater, especially during the brackish water period (Fig. 5; Table 1). Moreover, the lower availability of ΣS^{-II} in porewater hampers Fe sulfide formation. Therefore, there was no statistical correlation between Fe and ΣS^{-II} in SM sediments (Fig. 8; Table 3), suggesting that ferruginous incrustations and nodules of Fe and Mn oxyhydroxides are the main geochemical traps for Fe in the salt marshes from Polvora Island.

Hg vertical distribution in SM was statistically correlated to fine grain sediment contents, similarly to SA sampling point (Fig. 8; Table 3), indicating that the main Hg immobilization mechanisms are related to organic coating of fine sediments and/or

adsorption to reactive surface of <63 μm particles (Winfrey 1988). Furthermore, there is no correlation among Hg and ΣS^{-II} or Fe (Fig. 8; Table 3), suggesting that adsorption/incorporation of Hg into iron sulfide is of minor importance in SM sediments. No Hg contamination was revealed in SM and SA sediments, since their contents were comparable to background values (i.e., 10 - 40 μg kg^{-1}) previously reported (Quintana and Mirlean 2019).

Conclusion

The results obtained for shallow area sediments within Patos Estuary during both hydrological regimes (i.e., fresh water period and brackish water period) allow us to conclude that Hg distribution is controlled by fine grain sediments distribution. Mercury (hg), iron (Fe), organic carbon (OC), and soluble sulfides (ΣS^{-II}) were statistically correlated to <63 μm particles of sediments. Silt and clay presented elevated contents of OC, Fe, and Hg in comparison to coarser sediments, which likely reflects the predominance of the organic coating on the reactive surfaces of the fine-grained sediments. In turn, the organic matter served as substrate for oxygen and sulfate respiring bacteria, leading to an increase in the availability of ΣS^{-II} in the porewater, and, likely, the subsequent formation of iron sulfides. Thus, the immobilization of Hg in shallow area sediments, likely, is a consequence of adsorption on fine particles coated with organic matter as well as incorporation and/or adsorption on iron sulfide.

Salt marsh sediment from Polvora Island are subject to intense biological disturbances during both hydrological regimes. Such bioturbation provoked oxidizing redox conditions in the most superficial sediment layers. Burrow crabs (*Neohelice granulata*) and native vegetation (*Spartina densiflora* and *Spartina alterniflora*) roots enable the penetration of oxygen into superficial sediments, creating propitious conditions for the formation of ferruginous incrustations and Fe oxyhydroxides nodules in crab's burrows walls and in the rhizosphere zone. Such oxidizing conditions affect the sulfate reduction process, probably hamping the formation of iron sulfides. Therefore, it is probable that Fe accumulation in salt marsh sediments is controlled by ferruginous incrustations and Fe oxyhydroxides nodules formation. Furthermore, such oxidizing conditions likely favored the acidification of pore waters associated with the superficial

sediment due to oxidation of iron sulfide and subsequent sulfuric acid formation specially during the brackish water period (i.e., dry season).

OC distribution is also severely influenced by the native vegetation, which constitutes the main source of organic matter to the salt marsh sediments. Hg distribution is statistically correlated with fine grain sediment contents and OC, indicating that the immobilization of Hg likely reflects the adsorption on fine particles coated with organic matter. Despite the Hg contamination reported in the city of Rio Grande and in the sediments of the navigation channel of the local port, besides the presence of port-industrial facilities along the right bank of the estuary, no evidence that related anthropogenic activities have impacted the Hg content of the studied sediments is observed.

Acknowledgments

We are grateful to the coordination of improvement of higher level personnel of the Brazilian government (CAPES) by the grant of scholarship.

6. Considerações finais e conclusões

Concluímos que tanto a cobertura de solos quanto as águas subterrâneas da cidade de Rio Grande servem como fonte passiva de Hg para o estuário da Lagoa dos Patos. A contaminação das águas subterrâneas e dos solos urbanos por Hg teve como provável fonte primária os resíduos gerados pela fabricação de feltro. Apesar de as concentrações elevadas de mercúrio dissolvido encontradas nas águas subterrâneas, os limites legais para Hg na água potável não foram excedidos. É provável que solos, entulhos, lixo urbano e lama retirados de áreas contaminadas no século XVIII foram usados para construir aterros urbanos durante os séculos XIX e XX.

O presente estudo revelou que a contaminação por Hg na área de estudo iniciou no período colonial do sul do Brasil (1770 ± 6 anos). No entanto, não existem evidências documentadas sobre a fonte original de Hg. Considerando que o nitrato de mercúrio era amplamente utilizado na fabricação de feltro neste período, acredita-se que a fonte de contaminação mais provável foram os resíduos do processo químico de tratamento de peles chamado *carroting*. Este procedimento continuou a ser utilizado na produção industrial em Rio Grande durante o século XIX até a sua proibição na década de 60 do século XX. Contudo, é provável que a dispersão de resíduos contaminados por Hg ocorreu no século XVIII, quando a atividade era realizada de maneira artesanal.

A imobilização de Hg nos sedimentos de áreas rasas da margem esquerda do estuário da Lagoa dos Patos ocorre como consequência de processos geoquímicos controlados principalmente pela distribuição de sedimentos finos. É provável que a formação de sulfetos metálicos tenha ocorrido majoritariamente em camadas sedimentares com maior conteúdo de grão finos. Estes sedimentos exibiram teores elevados de carbono orgânico, Fe e Hg em comparação aos sedimentos grosseiros (areias), provavelmente devido ao revestimento orgânico da superfície dos grãos finos. Por sua vez, é provável que a matéria orgânica tenha servido como substrato para bactérias redutoras de sulfato levando a um aumento na disponibilidade de sulfetos dissolvidos nas águas intersticiais dos sedimentos e a subsequente formação de sulfetos metálicos. A imobilização de Hg nos sedimentos provavelmente se deve à combinação de adsorção em partículas finas, bem como a incorporação a sulfetos metálicos precipitados, como a pirita. As obras portuárias realizadas no canal de navegação principal provavelmente alteraram a hidrodinâmica natural do estuário, causando

mudanças na granulometria dos sedimentos. Consequentemente, tais mudanças podem ter influenciado na distribuição do Hg e nos processos de sulfato redução e de formação de sulfetos metálicos.

Os sedimentos das marismas da ilha da Polvora estão sujeitos à bioturbação durante os dois regimes hidrológicos dominantes no estuário. Tais perturbações levam a condições redox oxidantes nas camadas mais superficiais dos sedimentos. As tocas do caranguejo catanhão (*Neohelice granulata*) e as raízes da vegetação nativa (*Spartina densiflora* e *Spartina alterniflora*) facilitam a penetração de oxigênio em sedimentos superficiais, criando condições propícias para a formação de incrustações ferruginosas e nódulos de oxihidróxidos de Fe e Mn nas paredes dos túneis de caranguejos e na rizosfera. É provável que essas condições oxidantes afetem o processo de redução de sulfato, dificultando a formação de sulfetos metálicos. A oxidação de sulfetos metálicos e a subsequente formação de ácido sulfúrico, especialmente durante o período de domínio da água salobra, causou a acidificação das águas intersticiais superficiais nas marismas. A distribuição de carbono orgânico nas marismas também é severamente influenciada pela vegetação nativa, que constitui a principal fonte de matéria orgânica para os sedimentos. A distribuição de Hg nos sedimentos das marismas é controlada principalmente pelo conteúdo de siltes, argilas e carbono orgânico, indicando que a imobilização de Hg provavelmente corre através da adsorção em partículas finas revestidas com matéria orgânica.

Apesar da presença de instalações industriais portuárias ao longo da margem direita do estuário da Lagoa dos Patos, não existem evidências óbvias de que as atividades antropogênicas tenham impactado o teor de Hg nos sedimentos da margem esquerda do estuário (tanto nas áreas rasas quanto nas marismas). É provável que o canal de navegação artificial do porto local atue como uma barreira hidrodinâmica, limitando o transporte de sedimentos contaminados da cidade de Rio Grande, na margem direita, para a margem esquerda mais "protegida" do estuário. Sendo assim, a hipótese levantada, de que tanto processos geoquímicos naturais quanto contaminação antrópica seriam responsáveis por anomalias de concentração de mercúrio nos sedimentos do estuário da Lagoa dos Patos foi rejeitada.

Todos os objetivos traçados para o presente estudo foram alcançados: as principais fontes de mercúrio para o estuário foram determinadas, o período inicial do processo de contaminação por este metal na região foi descoberto, a distribuição do mercúrio nos

sedimentos do estuário foi caracterizada e a importância dos processos formação de sulfetos metálicos em zonas de redução de sulfato na sua imobilização foi revelada e, por fim, os efeitos do regime hidrológico sobre a distribuição de mercúrio em áreas rasas e em marismas no estuário foram caracterizados. Contudo, ainda restam perguntas sem resposta acerca dos riscos por contaminação de mercúrio na cidade de Rio Grande. É necessário investigar a possível intoxicação das pessoas por mercúrio gasoso, que pode exsudar do solo urbano contaminado na forma de metil-mercúrio ou mercúrio elementar. Também é preciso estudar a contaminação das águas pluviais por mercúrio, tendo em vista que a poeira suspensa na atmosfera é rica em partículas de solo suspensas pela ação dos ventos. Por fim, trabalhos acerca da especiação do mercúrio nos solos e nas águas superficiais e subterrâneas também se fazem necessários, visto que as formas organometálicas deste metal são as mais perigosas para a biota.

7. Referências Bibliográficas

Adler Miserendino, Rebecca, Jean Remy Davée Guimarães, Gary Schudel, Sanghamitra Ghosh, José Marcus Godoy, Ellen K. Silbergeld, Peter S.J. Lees, and Bridget A. Bergquist. 2018. Mercury Pollution in Amapá, Brazil: Mercury Amalgamation in Artisanal and Small-Scale Gold Mining or Land-Cover and Land-Use Changes? *ACS Earth and Space Chemistry* 2: 441–450. doi:10.1021/acsearthspacechem.7b00089.

Alberti, Juan, Mauricio Escapa, Pedro Daleo, Oscar Iribarne, Brian Silliman, and Mark Bertness. 2007. Local and geographic variation in grazing intensity by herbivorous crabs in SW Atlantic salt marshes. *Marine Ecology Progress Series* 349: 235–243. doi:10.3354/meps07089.

Álvarez-Iglesias, P., and B. Rubio. 2012. Early diagenesis of organic-matter-rich sediments in a ría environment: Organic matter sources, pyrites morphology and limitation of pyritization at depth. *Estuarine, Coastal and Shelf Science* 100. Elsevier Ltd: 113–123. doi:10.1016/j.ecss.2012.01.005.

Angeletti, Sabrina, and Patricia M. Cervellini. 2015. Estructura poblacional del cangrejo cavador Neohelice granulata (Brachyura, Varunidae) en una marisma del Atlántico

sudoccidental. *Latin American Journal of Aquatic Research* 43: 539–547. doi:10.3856/vol43-issue3-fulltext-15.

Anne, Kimberly, Daniel Hryhorczuk, Giovanni Saffirio, Thomas Sinks, Daniel C Paschal, Edwin H Chen, and Kimberly Anne Sing. 2003. Organic Mercury Levels among the Yanomama 32: 434–439.

Antiqueira, J., and L. Calliari. 2005a. Características sedimentares da desembocadura da Laguna dos Patos. *Gravel* 25: 39–46.

Antiqueira, J, and L Calliari. 2005b. Características sedimentares da desembocadura da Laguna dos Patos. *Gravel* 3: 39–46.

Assis, C, and L F Veríssimo. 1997. *Uma história de realizações: Empresas Petróleo Ipiranga 60 anos*. 1st ed. São Paulo: Premio.

Barkay, Tamar, Susan M. Miller, and Anne O. Summers. 2003. Bacterial mercury resistance from atoms to ecosystems. *FEMS Microbiology Reviews* 27: 355–384. doi:10.1016/S0168-6445(03)00046-9.

Barnett, Mark O., Ralph R. Turner, and Philip C. Singer. 2001. Oxidative dissolution of metacinnabar (β-HgS) by dissolved oxygen. *Applied Geochemistry* 16: 1499–1512. doi:10.1016/S0883-2927(01)00026-9.

Van Bemmelen, J.M. 1886. Bijdragen tot de kennis van den alluvialen bodem in Nederland. *Verhandelingen der Akademie van Wetenschappen, Amsterdam* 25: 33–105.

Benoit, J. M., C. C. Gilmour, R. P. Mason, G. S. Riedel, and G. F. Riedel. 1998. Behavior of mercury in the Patuxent river estuary. *Biogeochemistry* 40: 249–265. doi:10.1023/A:1005905700864.

Berner, R. A. 1984. Sedimentary pyrite formation. *American Journal of Science* 268: 1–23. doi:10.2475/ajs.268.1.1.

Bianchi, T.S. 2007. *Biogeochemistry of Estuaries*. 1 st. New York, USA: Oxford University Press.

Bonnissel-Gissinger, Pascale, Marc Alnot, Jean Paul Lickes, Jean Jacques Ehrhardt, and Philippe Behra. 1999. Modeling the adsorption of mercury(II) on (hydr)oxides II:

α-FeOOH (goethite) and amorphous silica. *Journal of Colloid and Interface Science* 215: 313–322. doi:10.1006/jcis.1999.6263.

Brasil, Decreto 97.507/1989, de 13 de fevereiro de 1989. Dispõe sobre licenciamento de atividade mineral, o uso do mercúrio metálico e docianeto em áreas de extração de ouro, e dá outras providências.

Brasil, Lei 12.305/2010, de 2 de agosto de 2010. Estabelece a Política Nacional de Resíduos Sólidos (PNRS).

Brasil, Lei 9.976/2000, de 3 de julho de 2000. Dispõe sobre a produção de cloro e da outras providências.

Brito, Saturnino. 1918. *Saneamento do Rio Grande*. 1st ed. Porto Alegre: Officinas Graphicas do Instituto de Eletro-Technica da Escola de Engenharia de Porto Alegre.

Brooks, K.M. 2001. *An evaluation of the relationship between salmon farm biomass, organic inputs to sediments, physicochemical changes associated with those inputs and the infaunal response – with emphasis on total sediment*. *Aquatic Environmental Sciences*. Washington, USA.

Brown, James R., G. Michael Bancroft, William S. Fyfe, and Ronald A.N. McLean. 1979. Mercury Removal from Water by Iron Sulfide Minerals. An Electron Spectroscopy for Chemical Analysis (ESCA) Study. *Environmental Science and Technology* 13: 1142–1144. doi:10.1021/es60157a013.

Brüchert, Volker, Bo Barker Jørgensen, Kirsten Neumann, Daniela Riechmann, Manfred Schlösser, and Heide Schulz. 2003. Regulation of bacterial sulfate reduction and hydrogen sulfide fluxes in the central Namibian coastal upwelling zone. *Geochimica et Cosmochimica Acta* 67: 4505–4518. doi:10.1016/S0016-7037(03)00275-8.

Bunsen, R. 1847. Ueber den innern Zusammenhang der pseudovulkanischen Erscheinungen Islands. *Ann. Chem. Pharm.*: 1–59.

Castillo, Jesús, M. Figueroa, Teresa Luque Palomo, Alfredo Rubio-Casal, and Francisco Jiménez Nieva. 2003. Intratussock tiller distribution and biomass of Spartina densiflora Brongn: in an invaded salt marsh. *Lagascalia* 23: 61–73.

CCME. 2003. *Canadian Water Quality Guidelines for the Protection of Aquatic Life: Guidance on the Site-Specific Application of Water Quality Guidelines in Canada: Procedures for Deriving Numerical Water Quality Objectives*. *Canadian Environmental Quality Guidelines*.

Cesar, Willy. 2015. *Rio Grande do big bang a 2015*. 1st ed. Rio de Janeiro: Topbooks.

CONAMA, 2005. Resolução nº 357. Dispõe sobre a classificação dos corpos de água e diretrizes ambientais para o seu enquadramento, bem como estabelece as condições e padrões de lançamento de efluentes, e dá outras providências. *Publicada no dou de 18/03/2005*. Conselho Nacional do Meio Ambiente – CONAMA. Ministério do Meio Ambiente.

CONAMA, 2008. Resolução nº 396. Dispõe sobre a classificação e diretrizes ambientais para o enquadramento das águas subterrâneas e dá outras providências. Publicada no dou de 07/04/2008.Conselho Nacional do Meio Ambiente - CONAMA Ministério do Meio Ambiente.

CONAMA, 2009. Resolução nº 420. Dispões sobre critérios e valores orientadores de qualidade do solo quanto à presença de substâncias químicas e estalece diretrizes para o gerenciamenteo ambiental de áreas contaminadas por essas substâncias em decorrência de atividades antrópicas. *Publicadas no dou 30/12/2009*. Conselho Nacional do Meio Ambiente – CONAMA. Ministério do Meio Ambiente.

CONAMA, 2012. Resolução nº 454. Estabelece as diretrizes gerais e os procedimentos referenciais para o gerenciamento do material a ser dragado em águas sobre jurisdição nacional 1 de novembro de 2012. *Publicada no dou de 01/11/12*. Conselho Nacional do Meio Ambiente – CONAMA. Ministério do Meio Ambiente.

Costa, Cesar, Juliano Marangon, and Adriana Azevedo. 2003. Plant zonation in irregularly flooded salt marshes: Relative importance of stress tolerance and biological interactions. *Journal of Ecology* 91: 951–965. doi:10.1046/j.1365-2745.2003.00821.x.

Costa, César S.B., Juliano C. Marangoni, and Adriana M.G. Azevedo. 2003. Plant zonation in irregularly flooded salt marshes: Relative importance of stress tolerance and biological interactions. *Journal of Ecology* 91: 951–965. doi:10.1046/j.1365-2745.2003.00821.x.

Costa, L., N. Mirlean, and F. Garcia. 2017. Arsenic Environmental Threshold Surpass in Estuarine Sediments: Effects of Bioturbation. *Bulletin of Environmental Contamination and Toxicology* 98. Springer US: 521–524. doi:10.1007/s00128-016-2024-z.

Costa, L., N. Mirlean, G. C. Quintana, S. Adebayo, and K. Johannesson. 2019. Distribution and Geochemistry of Arsenic in Sediments of the World ' s Largest Choked Estuary : the Patos Lagoon , Brazil. *Estuaries and Coasts*. Springer US. doi:https://doi.org/10.1007/s12237-019-00596-0.

Dorea, José G., Antonio C. Barbosa, Íris Ferrari, and Jurandir R. De Souza. 2003. Mercury in hair and in fish consumed by Riparian women of the Rio Negro, Amazon, Brazil. *International Journal of Environmental Health Research* 13: 239–248. doi:10.1080/0960312031000122398.

Dreys, N. 1827. *Nicolau Dreys Diaries*. Rio Grande.

Ehrhardt, Jean Jacques, Philippe Behra, Pascale Bonnissel-Gissinger, and Marc Alnot. 2000. XPS study of the sorption of Hg(II) onto pyrite FeS2. *Surface and Interface Analysis* 30: 269–272. doi:10.1002/1096-9918(200008)30:1<269::AID-SIA758>3.0.CO;2-N.

Forstner, Ulrich, and Wim Salomons. 1984. *Metals in the Hydrocycle*. 1 st. Berlin Heildelberg: Springer-Verlag. doi:10.1007/978-3-642-69325-0 e-1SBN-13:

Forstner, Ulrich, and G T W Wittmann. 1979. *Metal Pollution in the Aquatic Environment*. 1st ed. Berlin: Springer-Verlag.

Fossing, Henrik, and Bo Barker Jørgensen. 1989. Chromium Reduction Method of bacterial sulfate reduction in sediments : Measurement reduction of a single-step chromium method Evaluation. *Biogeochemistry* 8: 205–222.

Fragomeni, Luiz Paulo de Moura, Ari Roisenberg, and Nicolai Mirlean. 2010. Poluição por Mercúrio em Aterros Urbanos do Período Colonial no Extremosul do Brasil. *Quim. Nova* 33: 1631–1635.

Gripp, Mariana Luiza Ribeiro. 2012. Indicação Geoquímica de Desenvolvimento Urbanoindustrial em Cidade Portuária (Rio Grande - RS). Federal University of Rio Grande.

Hach, C. 2007. *DR 2800 Spectrophotometer User Manual*. USA. doi:10.3928/01477447-20101221-06.

Han, Seunghee, Anna Obraztsova, Patrizia Pretto, Dimitri D. Deheyn, Joris Gieskes, and Bradley M. Tebo. 2008. Sulfide and iron control on mercury speciation in anoxic estuarine sediment slurries. *Marine Chemistry* 111. Elsevier B.V.: 214–220. doi:10.1016/j.marchem.2008.05.002.

Hernández-Crespo, Carmen, and Miguel Martín. 2013. Mid-term variation of vertical distribution of acid volatile sulphide and simultaneously extracted metals in sediment cores from Lake Albufera (Valencia, Spain). *Archives of Environmental Contamination and Toxicology* 65: 654–664. doi:10.1007/s00244-013-9941-1.

Huerta-Diaz, M.A., and J.J. Reimer. 2010. Biogeochemistry of Sediments. In *Biogeochemistry and Pedogenetic Process in Saltmarsh and Mangrove Systems*, ed. X. L. O. Pérez and F. M. Vazquez, 1 st, 1–25. New York, USA: Nova Science.

Hyland, M. M., G. E. Jean, and G. M. Bancroft. 1990. XPS and AES studies of Hg(II) sorption and desorption reactions on sulphide minerals. *Geochimica et Cosmochimica Acta* 54: 1957–1967. doi:10.1016/0016-7037(90)90264-L.

Iribarne, Oscar, Florencia Botto, Paulina Martinetto, and Jorge L. Gutierrez. 2000. The role of burrows of the SW Atlantic intertidal crab Chasmagnathus granulata in trapping debris. *Marine Pollution Bulletin* 40: 1057–1062. doi:10.1016/S0025-326X(00)00058-8.

Jeong, Hoon Y., Bjorn Klaue, Joel D. Blum, and Kim F. Hayes. 2007. Sorption of mercuric ion by synthetic nanocrystalline mackinawite (FeS). *Environmental Science and Technology* 41: 7699–7705. doi:10.1021/es070289l.

Jørgensen, B.B., and S. Kasten. 2005. Sulfur Cycling and Methane Oxidation. In *Marine Geochemistry*, ed. H. D. Schulz and M. Zabel, 2 nd, 271–309. Berlin: Springer.

Justus, Cláudia Maria, Amarildo Pasini, Jaqueline Aparecida Raminelli, Leandro Simões Azeredo Gonçalves, and André Celligoi. 2020. Chemical elements in the water of the São Pedro river basin, Faxinal - Paraná. *Semina:Ciencias Agrarias* 41: 743–752. doi:10.5433/1679-0359.2020v41n3p743.

Kjerfve, B. 1994. Coastal lagoons. In *Coastal lagoon processes*, ed. B. Kjerfve, 1–8. Amsterdam, The Netherlands: Elsevier Oceanographic Series. doi:10.1016/0378-3839(95)90002-0.

Kristensen, Erik, Frede Østerguard Andersen, and Thomas Henry Blackburn. 1992. Effects of benthic macrofauna and temperature on degradation of macroalgal detritus: The fate of organic carbon. *Limnology and Oceanography* 37: 1404–1419. doi:10.4319/lo.1992.37.7.1404.

Kütter, V. T., N. Mirlean, P. R. Baisch, M. T. Kütter, and E. V. Silva-Filho. 2009. Mercury in freshwater, estuarine, and marine fishes from Southern Brazil and its ecological implication. *Environmental monitoring and assessment* 159: 35–42. doi:10.1007/s10661-008-0610-1.

Lacerda, Luiz Drude., and Olaf Malm. 2008. Contaminação por mercúrio em ecossistemas aquáticos : uma análise das áreas críticas. *Estudos Avançados* 22: 173–190.

Leivas, Florisbello. 1922. *Relatório Final da Comissão de Saneamento Municipal do Rio Grande*. 1st ed. Rio Grande: Livraria Rio-Grandense – R. Strauch.

Leloup, Julie, Alexander Loy, Nina J. Knab, Christian Borowski, Michael Wagner, and Bo Barker Jørgensen. 2007. Diversity and abundance of sulfate-reducing microorganisms in the sulfate and methane zones of a marine sediment, Black Sea. *Environmental Microbiology* 9: 131–142. doi:10.1111/j.1462-2920.2006.01122.x.

Lindberg, S. E., D. Wallschläger, E. M. Prestbo, N. S. Bloom, J. Price, and D. Reinhart. 2001. Methylated mercury species in municipal waste landfill gas sampled in Florida, USA. *Atmospheric Environment* 35: 4011–4015. doi:10.1016/S1352-2310(01)00176-5.

Liu, Zhanfei, Cindy Lee, and Robert C. Aller. 2008. Drying effects on decomposition of salt marsh sediment and on lysine sorption. *Journal of Marine Research* 66: 665–689. doi:10.1357/002224008787536781.

Long, E. R, D. D. McDonald, S. L. Smith, and F. D. Calder. 1995. Incidence of Adverse Biological Effects Within Ranges of Chemical Concentrations in Marine and Estuarine Sediments. *EnvironmentalManagemen* 19: 81–97. doi:https://doi.org/10.1007/BF02472006.

Machado, W, M Moscatelli, L G Rezende, and L D Lacerda. 2002. Mercury, zinc, and copper accumulation in mangrove sediments surrounding a large land ll in southeast Brazil. *Environmental Technology* 120: 455–461.

Malm, Olaf. 1998. Gold mining as a source of mercury exposure in the Brazilian Amazon. *Environmental Research* 77: 73–78. doi:10.1006/enrs.1998.3828.

Marins, Rozane V., Francisco José De Paula Filho, Saulo Robério Rodrigues Maia, Luiz Drude De Lacerda, and Wanessa Sousa Marques. 2004. Distribuição de mercúrio total como indicador de poluição urbana e industrial na costa Brasileira. *Quimica Nova* 27: 763–770. doi:10.1590/S0100-40422004000500016.

Martinetto, Paulina, Diana I. Montemayor, Juan Alberti, César S.B. Costa, and Oscar Iribarne. 2016. Crab bioturbation and herbivory may account for variability in carbon sequestration and stocks in south west atlantic salt marshes. *Frontiers in Marine Science* 3: 1–12. doi:10.3389/fmars.2016.00122.

Meysman, Filip J.R., and Jack J. Middelburg. 2005. Acid-volatile sulfide (AVS) - A comment. *Marine Chemistry* 97: 206–212. doi:10.1016/j.marchem.2005.08.005.

Miranda, José Fernando, Adilson Curi, and Hernani Mota de Lima. 2020. Estimation of mercury released from an abandoned gold mine in Minas Gerais, Brazil. *Revista Escola de Minas* 73: 109–117. doi:10.1590/0370-44672018730182.

Mirlean, Nicolai, Vlad E. Andrus, and Paulo Baisch. 2003. Mercury pollution sources in sediments of Patos Lagoon Estuary, Southern Brazil. *Marine Pollution Bulletin* 46: 331–334. doi:10.1016/S0025-326X(02)00404-6.

Mirlean, Nicolai, Besnik Baraj, Luis Felipe Niencheski, Paulo Baisch, and Daniel Robinson. 2001. The effect of accidental sulphuric acid leaking on metal distributions in estuarine sediment of patos lagoon. *Marine Pollution Bulletin* 42: 1114–1117. doi:10.1016/S0025-326X(01)00099-6.

Mirlean, Nicolai, Lauro Calliari, Paulo Baisch, Ester Loitzenbauer, and Evgueni Shumilin. 2009. Urban activity and mercury contamination in estuarine and marine sediments (Southern Brazil). *Environmental Monitoring and Assessment* 157: 583–589. doi:10.1007/s10661-008-0558-1.

Mirlean, Nicolai, and Cesar S.B. Costa. 2017. Geochemical factors promoting die-back

gap formation in colonizing patches of Spartina densiflora in an irregularly flooded marsh. *Estuarine, Coastal and Shelf Science* 189. Elsevier Ltd: 104–114. doi:10.1016/j.ecss.2017.03.006.

Mirlean, Nicolai, and Cristian Oliveira. 2006. Mercury in Coastal Reclamation Fills in Southernmost Brazil: Historical and Environmental Facets. *Journal of Coastal Research* 226: 1573–1576. doi:10.2112/04-0352.1.

Moller, Osmar O., Patrice Castaing, Jean-Claude Salomon, and Pascal Lazure. 2001. The Influence of Local and Non-Local Forcing Effects on the Subtidal Circulation of Patos Lagoon. *Estuaries* 24: 297. doi:10.2307/1352953.

Möller, Osmar O., Jorge Pablo Castello, and Ana Carolina Vaz. 2009. The effect of river discharge and winds on the interannual variability of the pink shrimp Farfantepenaeus paulensis production in Patos Lagoon. *Estuaries and Coasts* 32: 787–796. doi:10.1007/s12237-009-9168-6.

Moller, Osmar O., João A. Lorenzzentti, José L. Stech, and Mauricio M. Mata. 1996. The Patos Lagoon summertime circulation and dynamics. *Continental Shelf Research* 16: 335–351. doi:10.1016/0278-4343(95)00014-R.

Morse, J W, and G W Luther. 1999. Chemical influences on trace metal-sulfide interactions in anoxic sediments. *Geochim. Cosmochim. Acta* 63: 3373–3378.

Muccillo-Baisch, Ana Luiza, Nicolai Mirlean, Daniela Carrazzoni, Maria Cristina Flores Soares, Gianni Peraza Goulart, and Paulo Baisch. 2012. Health effects of ingestion of mercury-polluted urban soil: An animal experiment. *Environmental Geochemistry and Health* 34: 43–53. doi:10.1007/s10653-011-9389-z.

Nascimento, CA, R Staggemeier, E Bianchi, MT Rodrigues, R Fabres, MC Soliman, M Bortoluzzi, et al. 2015. Monitoring of metals, organic compounds and coliforms in water catchment points from the Sinos River basin. *Brazilian Journal of Biology* 75: 50–56. doi:10.1590/1519-6984.1613.

Niencheski, L. F., W. S. Moore, and H. L. Windom. 2014. History of human activity in coastal southern Brazil from sediment. *Marine Pollution Bulletin* 78. Elsevier Ltd: 209–212. doi:10.1016/j.marpolbul.2013.10.042.

Niencheski, L. F., H. L. Windom, B. Baraj, D. Wells, and R. Smith. 2001. Mercury in

fish from patos and Mirim Lagoons, Southern Brazil. *Marine Pollution Bulletin* 42: 1403–1406. doi:10.1016/S0025-326X(01)00219-3.

NRCC. 2004. *HISS-1, MESS-3, PACS-2 Marine Sediment Reference Material for Trace Metals and other Constituents*. Canada.

Otero, X. L., T. O. Ferreira, M. A. Huerta-Díaz, C. S.M. Partiti, V. Souza, P. Vidal-Torrado, and F. Macías. 2009. Geochemistry of iron and manganese in soils and sediments of a mangrove system, Island of Pai Matos (Cananeia - SP, Brazil). *Geoderma* 148. Elsevier B.V.: 318–335. doi:10.1016/j.geoderma.2008.10.016.

Pallud, Céline, and Philippe Van Cappellen. 2006. Kinetics of microbial sulfate reduction in estuarine sediments. *Geochimica et Cosmochimica Acta* 70: 1148–1162. doi:10.1016/j.gca.2005.11.002.

Perelman, A. 1967. *Geochemistry of Epigenesis Monographs in Geoscience*. 1 st. New York: Plenum Press. doi:10_1007/978-1-4684-7520-3.

Pesavento, Sandra. 1985. *História da Indústria Sul-Rio-Grandense*. 1st ed. Guaíba: Rio Grande Companhia de Celulose do Sul - RIOCELL.

Pestana, M. H.D., and M. L.L. Formoso. 2003. Mercury contamination in Lavras do Sul, south Brazil: A legacy from past and recent gold mining. *Science of the Total Environment* 307: 125–140. doi:10.1016/S0048-9697(02)00535-1.

Pestana, M. H.D., P. Lechler, M. L.L. Formoso, and J. Miller. 2000. Mercury in sediments from gold and copper exploitation areas in the Camaqua River Basin, Southern Brazil. *Journal of South American Earth Sciences* 13: 537–547. doi:10.1016/S0895-9811(00)00039-0.

Pimentel, F. 1944. *Aspectos Gerais do Município do Rio Grande*. 1 st. Porto Alegre: Gráfica Imprensa Oficial.

Queiroz, Maria Luiza Bertuline. 1987. *A vila do Rio Grandede São Pedro - 1737 - 1822*. 1 st. Rio Grande: Editora da Furg.

Quintana, G. C., and N. Mirlean. 2019. Record of Hg pollution around outset of colonization in Southern Brazil. *Environmental Monitoring and Assessment* 191. Environmental Monitoring and Assessment: 1–8. doi:10.1007/s10661-019-7404-5.

Quintana, G C, and N Mirlean. 2018. Groundwater Contamination by Mercury from the Aforetime Carroting Practice. *Bulletin of Environmental Contamination and Toxicology* 100. Springer US: 839–842. doi:10.1007/s00128-018-2333-5.

Rickard, David, and George W. Luther. 2007. *Chemistry of Iron Sulfides. Chemical Reviews*. Vol. 107. doi:10.1021/cr0503658.

Risher, J. F. 2003. Concise International Chemical Assessment Document 50: Elemental mercurcy and inorganic mercury compounds: Human health aspects. *IPCS Concise International Chemical Assessment Documents*.

Rojas, Nora, and Nelson Silva. 2005. Early diagenesis and vertical distribution of organic carbon and total nitrogen in recent sediments from southern Chilean fjords (Boca del Guafo to Pulluche Channel). *Investigaciones marinas* 33: 183–194. doi:10.4067/s0717-71782005000200005.

Saet, Yu E, Revich B A, and E P Yanin. 1990. *Geochemistry of the Environment*. Moscow: Nedra.

Saint-Hilaire, August. 1820. *August Saint-Hilaire Diaries*. Rio Grande.

Schnug, Ewald, and Bernd G. Lottermoser. 2013. Fertilizer-derived uranium and its threat to human health. *Environmental Science and Technology* 47: 2433–2434. doi:10.1021/es4002357.

Skyllberg, U.;, P.R.; Bloom, J.; Qian, C.M.; Lin, and W.F. Bleam. 2006. Complexation of mercury(II) in soil organic matter: EXAFS evidence for linear two-coordination with reduced sulfur groups. *Environmental Science and Technology* 40.

Svensson, Margareta, Anders Düker, and Bert Allard. 2006. Formation of cinnabar-estimation of favourable conditions in a proposed Swedish repository. *Journal of Hazardous Materials* 136: 830–836. doi:10.1016/j.jhazmat.2006.01.018.

Unep. 2002. *Chemicals: Global Mercury assessment*. Switzerland: United Nations Environment Program.

USEPA. 1996. *Method 3050B: Acid digestion of sediments, sludges, and soils. 1996*. Vol. 2. doi:10.1117/12.528651.

USEPA. 1998. *METHOD 7471B: Mercury in Solid or Semisolid Waste*.

USEPA. 2002. *Method 1631: Mercury in water by oxidation, purge and trap, and cold vapor atomic fluorescence spectrometry*. *EPA 821-R-96-012. US EPA, Office of Water, Washington, DC.*

Vairavamurthy, Murthy A., Wilson L. Orr, and Bernard Manowitz. 1995. *Geochemical Transformations of Sedimentary Sulfur: An Introduction*. doi:10.1021/bk-1995-0612.ch001.

Varekamp, J.C.a, B.b Kreulen, M.R.b Buchholtz Ten Brink, and E.L.b Mecray. 2003. Mercury contamination chronologies from Connecticut wetlands and Long Island Sound sediments. *Environmental Geology* 43: 268–282. doi:10.1007/s00254-002-0624-x.

Vaz, Ana Carolina, O. O. Möller jr, and Tabajara Lucas de Almeida. 2006. Análise quantitativa da descarga dos rios afluentes da Lagoa dos Patos. *Atlântica* 28: 13–23.

Wang, Qianrui, Daekeun Kim, Dionysios D. Dionysiou, George A. Sorial, and Dennis Timberlake. 2004. Sources and remediation for mercury contamination in aquatic systems - A literature review. *Environmental Pollution* 131: 323–336. doi:10.1016/j.envpol.2004.01.010.

WHO. 1989. *Mercury environmental health criteria 86*. Switzerland: World Healh Organization.

World Health Organization – WHO, **2020**. Disponível em <http://www.who.int/ipcs/assessment/public_health/mercury/en/> Acesso em Maio, 2020.

Windom, H. L., L. F. Niencheski, and R. G. Smith. 1999. Biogeochemistry of nutrients and trace metals in the estuarine region of the patos lagoon (Brazil). *Estuarine, Coastal and Shelf Science* 48: 113–123. doi:10.1006/ecss.1998.0410.

Winfrey, P.G.C.Campbell; A.G. Lewis; P.M. Chapamn; A.A. Crowder; W.K Fletcher; B. Imber; S.N. Luoma; P.M. Stokes; M. 1988. *Biologicaly Available Metals in Sediments*. Edited by National Reseach Concil of Canada. 1 st. Halifax: National Reseach Concil of Canada.

Wolfenden, S, J M Charnock, J Hilton, F R Livens, and D J Vaughan. 2005. Sulfide

Species as A Sink for. *Mercury in Lake Sediments. Environmental Science & Technology* 39: 6644–6648.

Yang, Yongqiang, Ling Zhang, Fanrong Chen, Mingliang Kang, Shijun Wu, and Jinsong Liu. 2014. Seasonal Variation of Acid Volatile Sulfide and Simultaneously Extracted Metals in Sediment Cores from the Pearl River Estuary. *Soil and Sediment Contamination* 23: 480–496. doi:10.1080/15320383.2014.838207.

Zhang, Lei, Qianjiahua Liao, Wei He, Jingge Shang, and Chengxin Fan. 2013. The effects of temperature on oxygen uptake and nutrient flux in sediment inhabited by molluscs. *Journal of Limnology* 72: 13–20. doi:10.4081/jlimnol.2013.e2.